THE UNIVERSITY OF ARIZONA
DEPT. OF ELECTRICAL AND COMPUTER ENGINEERING

MMW Millimeter Wave Circuits and Antennas Laboratory

Active Metamaterial: Gain and Stability, and Microfluidic Chip for THz Cell Spectroscopy

Qi Tang

Committee: Dr. Hao Xin (advisor),

Dr. Steven Dvorak, and Dr. Siyang Cao

12 / 16 / 2016
ECE 501

Outline

1. Active gain metamaterial

2. Non-Foster antenna matching

3. Sign choice of refractive index for active gain medium

4. Microfluidic device for THz Spectroscopy of live cells

Metamaterial (MTM)

- **Artificially engineered** composite material to achieve **unconventional** properties.
- In 1968, V. Veselago theoretically discovered medium **Negative Refractive Index Medium (NIM)** exists if both ϵ and $\mu < 0$.
- Push technology beyond conventional limits and produce vastly new opportunities beyond what nature can offer.

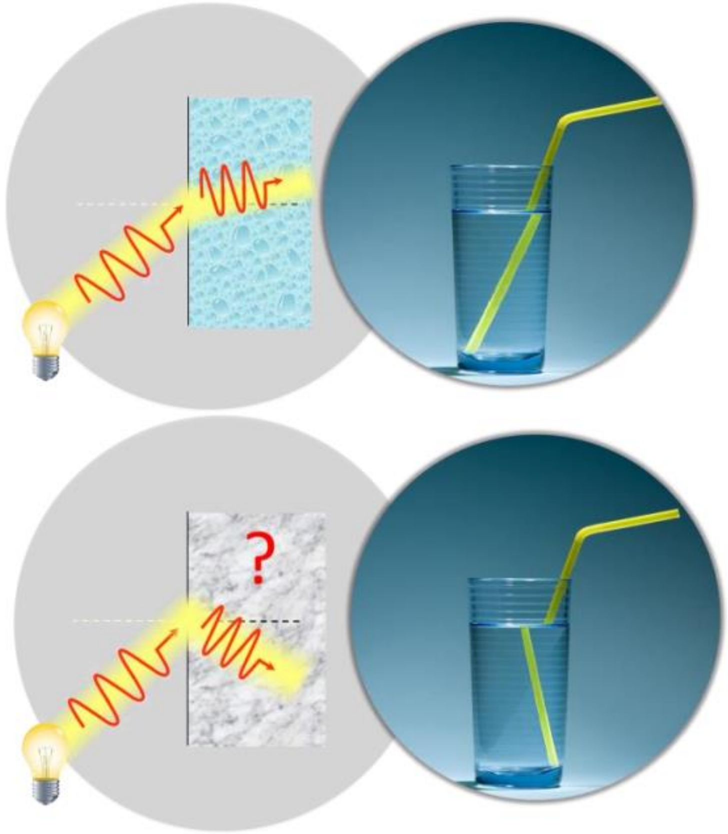

Positive (top) vs. negative (bottom) refraction

Applications: invisibility cloaking, perfect lens, novel antennas and microwave circuits, etc.

Practical implementations

Volumetric MTM

- metal wires (ε<0)
- Split ring resonators (SRRs) (μ<0)

1D Transmission Line (TL)

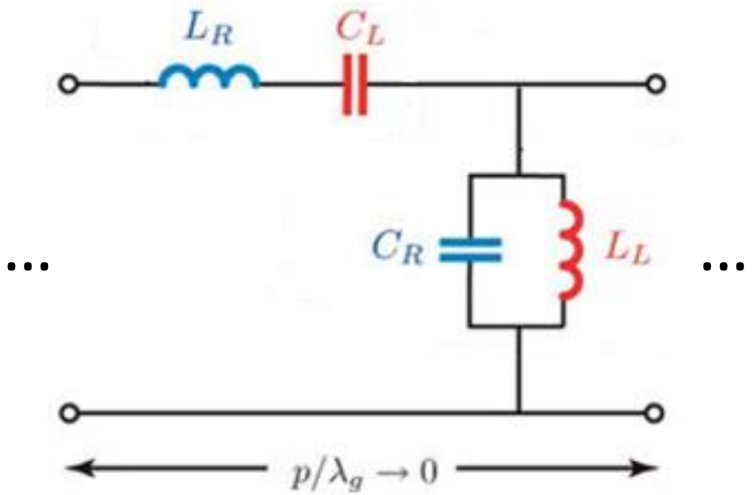

- Series capacitor (ε<0)
- Shunt inductor (μ<0)

Periodically arranged unit cells for which the physical size is much smaller than a wavelength (e.g. $< \lambda/4$).

R. A. Shelby, D. R. Smith, and S. Schultz, *Science*, 292, 5514, 77–9, Apr. 2001; C. Caloz and T. Itoh, *APS conf.*, 2002, 2, 412–415.

MTM applications and limits

Most applications require low loss and wideband MTMs.

1. Pendry's Perfect lens

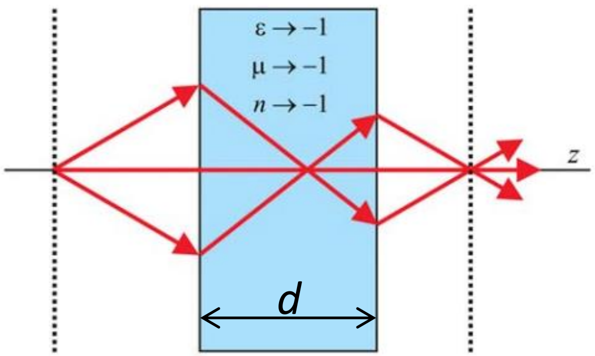

J. B. Pendry, Phys. Rev. Lett., 85, 2000.

Let ε= -1, μ = -1+δμ,

Resolution enhancement: $R = -\frac{1}{2\pi}\ln\left|\frac{\delta\mu}{2}\right|\frac{\lambda}{d}$

λ/d	R	$\delta\mu$
1.5	10	$< \sim 6 \times 10^{-19}$
10	10	0.002

2. Invisibility cloaking

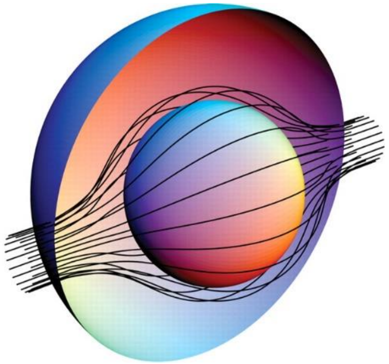

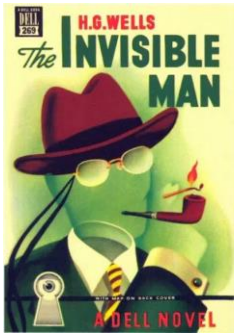

J.B. Pendry et al., *Science* 312.5781, 2006.

$$\frac{\mathrm{Im}\, n}{\mathrm{Re}\, n} \ll \frac{1}{4\pi}\frac{\lambda}{h+d}.$$

- ~10^{-8} for cloaking a human at visible light.

A typical low loss optical NIM reported in experiment has $\left|\frac{\mathrm{Im}\, n}{Re\, n}\right| = 0.28$.

J. Valentine, et al., *Nature*, 455, 376–379, 2008.

The bandwidth of passive NIM with negligible loss is fundamentally limited.

Introducing active MTMs

- By incorporating gain medium/ device into passive MTMs, we can
  - compensate loss / provide gain
  - potential to trade gain with bandwidth.
- The added design degree of freedom may enable new and rich physical phenomena and insights.
- Explore abnormal physical phenomena, e.g. superluminal group velocity, loss-free propagation, and unusual dispersions.
- Develop novel applications: novel antennas, spasers, optical data processing and quantum information applications.

Implementation of gain medium / device

At optical frequency:

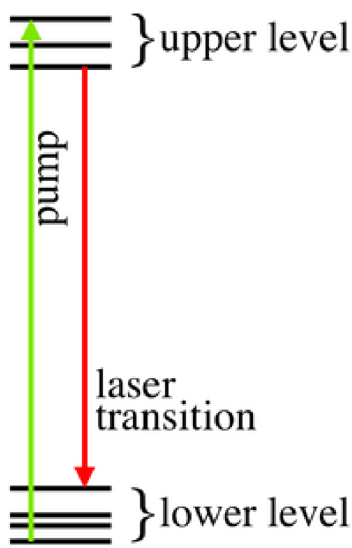

- **Mature in laser and optical amplifier devices**
- **Ion-doped crystals**
- **Semiconductor: quantum wells/dots**
- **Organic dye molecule solution, e.g. Rhodamine 800 (Rh800)**

At microwave frequency:

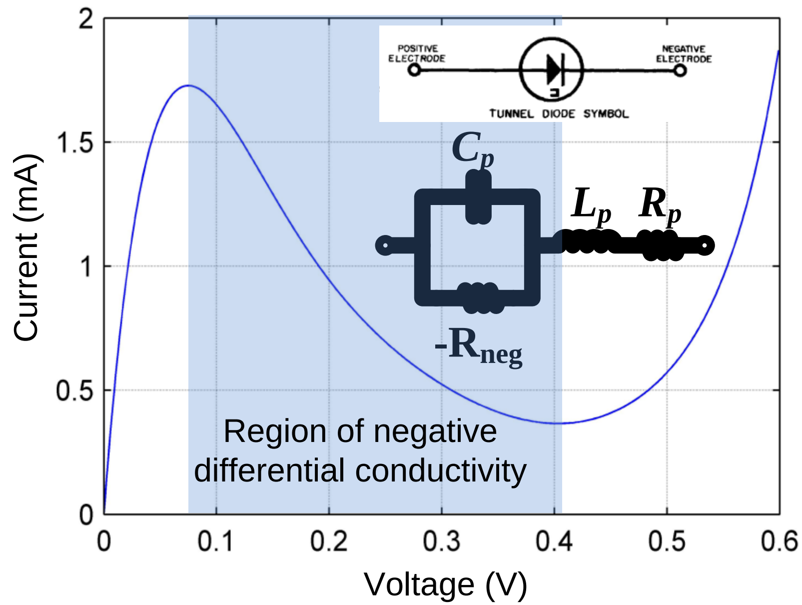

- **Many electronic devices, such as Tunnel diodes, transistor based -R circuits.**
- **Tunnel diodes (TDs) selected: One device, easier biasing and modeling.**

Basics of transmission line (TL) MTM

Passive Composite Left-/Right-handed (CLRH) TL

Series –R gain device

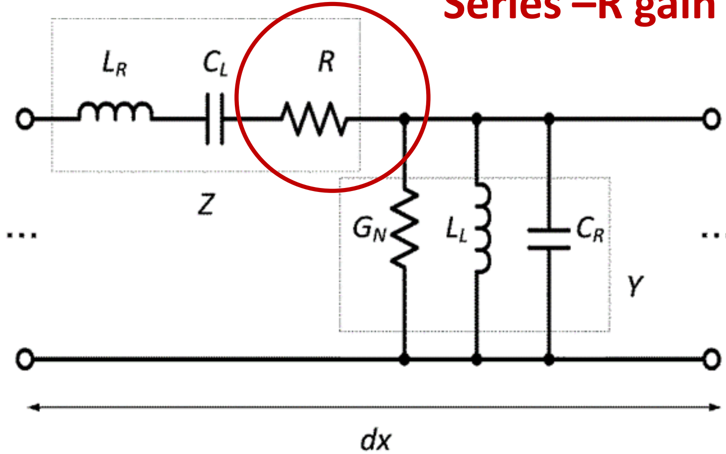

$$\beta = \frac{n\omega}{c}$$

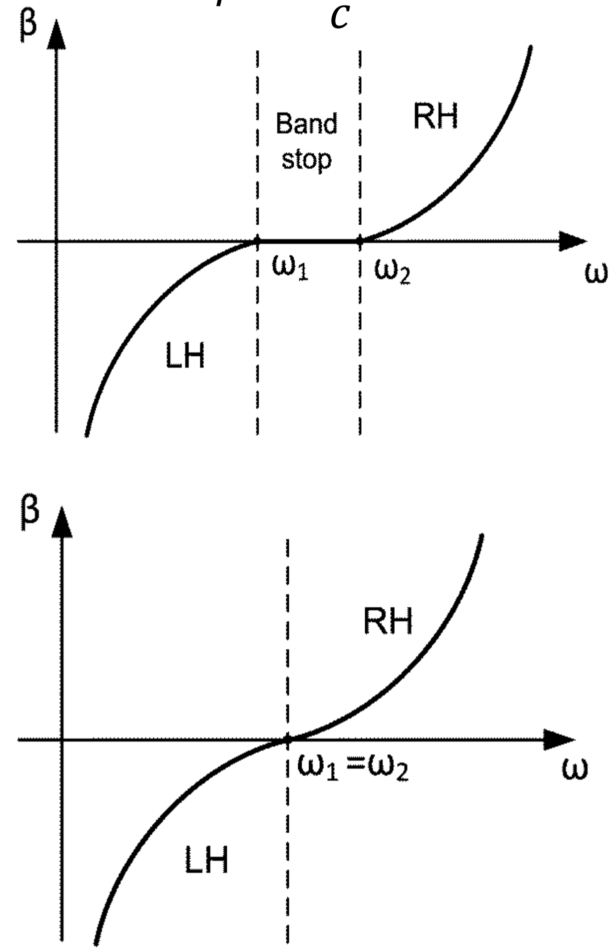

$$\epsilon(\omega) = Y/j\omega,$$

$$\mu(\omega) = Z/j\omega.$$

$$\gamma = \alpha + j\beta = \sqrt{ZY},$$

$$\eta = \sqrt{Z/Y}.$$

Practical design of active CLRH TL

Layout design

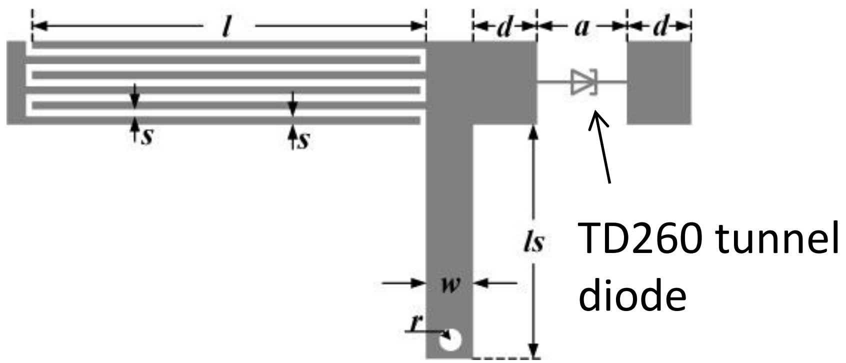

Equivalent circuit model

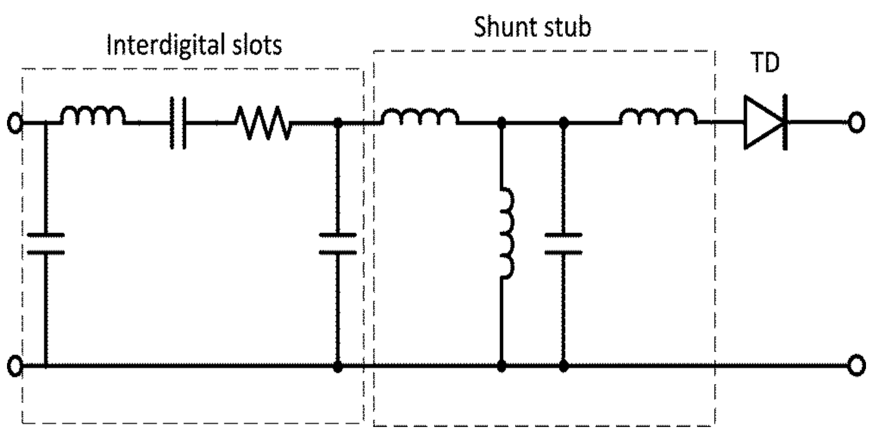

Photo of fabricated circuit

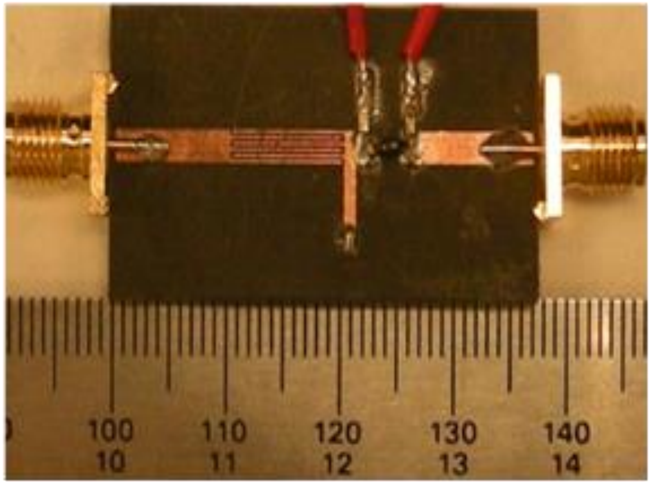

Simulated and measured S-parameters

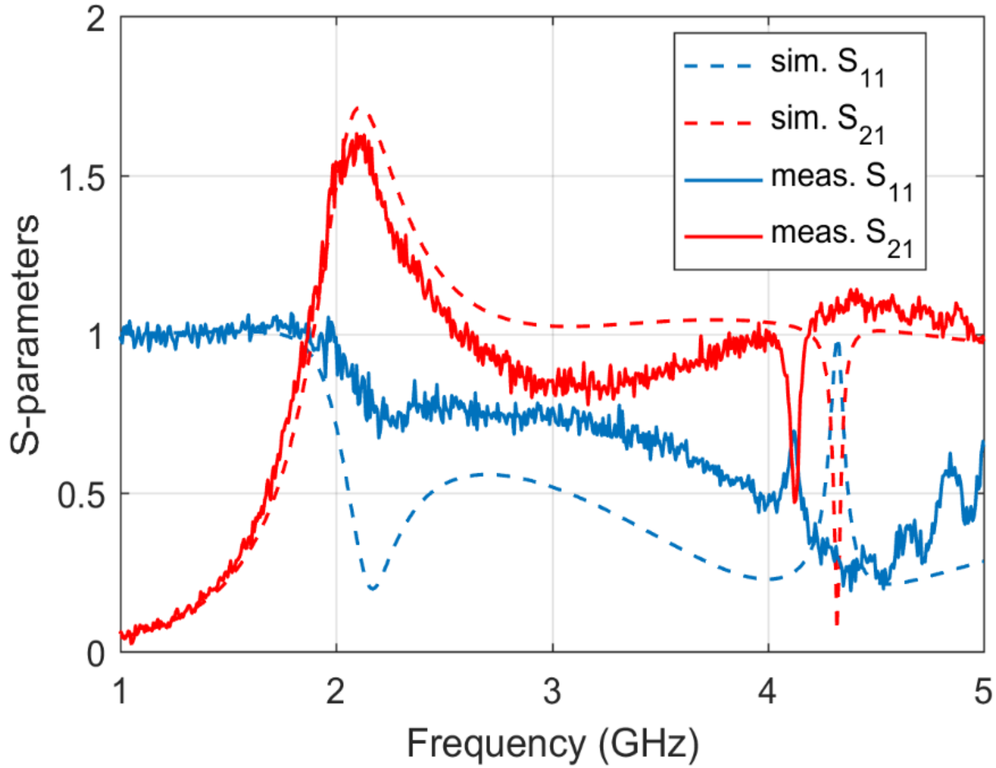

- S21 > 1 indicates gain
- Experimental result matches with simulation

Retrieved parameters from measurement

ARIZONA

Propagation constant

$\gamma = \alpha + j\beta$

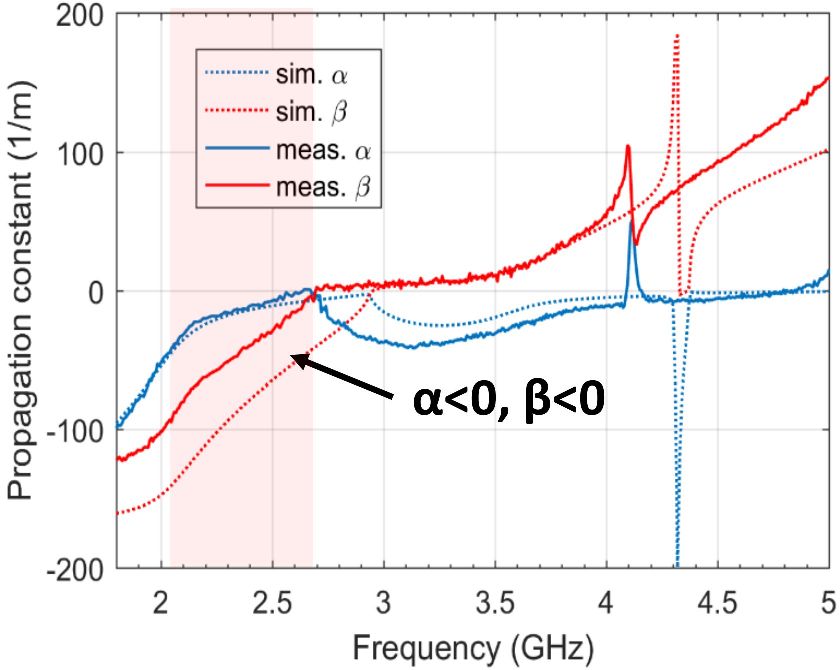

Refractive index

$n = n' - jn''$

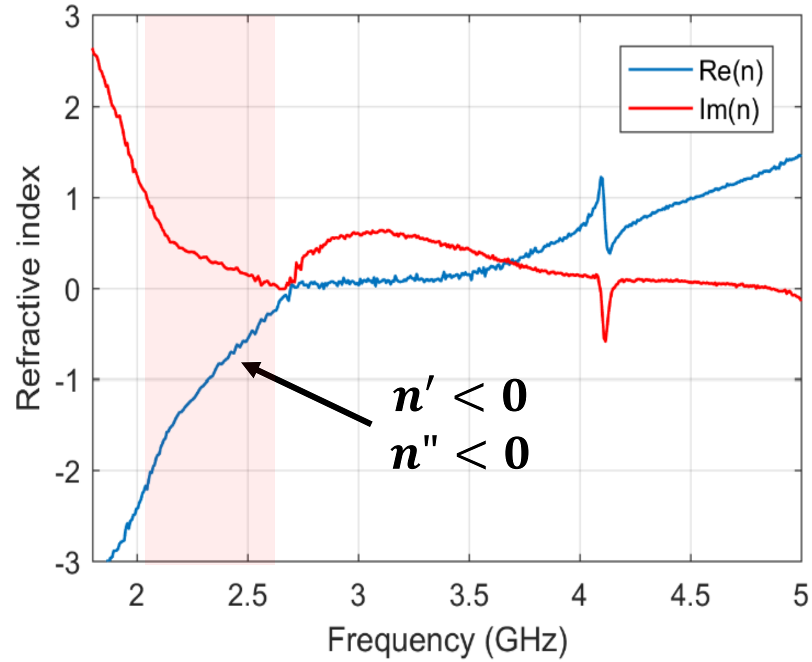

- **The first demonstrated CW gain TL MTM**
- **2, 3 unit cells are also measured and remain stable**

T. Jiang, et.al., Phys. Rev. Lett., 107, 20, 2011.

Tunable gain and nonlinearity

S_{21} for different DC bias

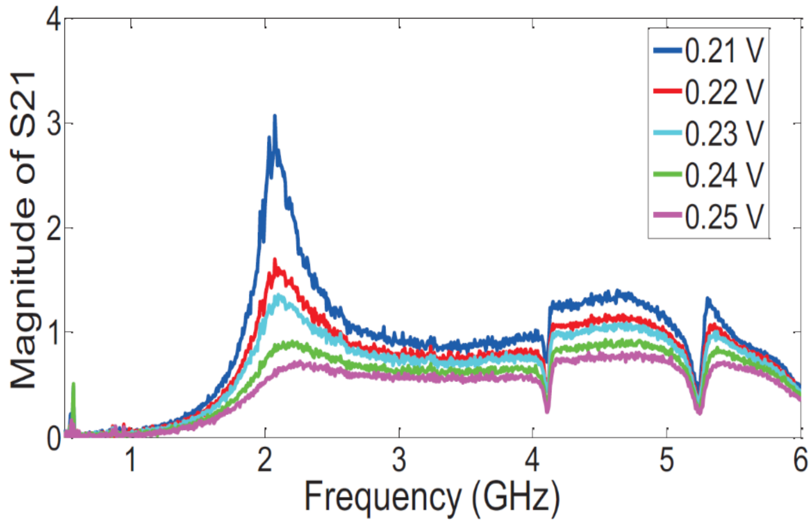

Tune the gain by sweeping DC bias voltage

Power @ Fund., 2^{nd}, 3^{rd} harmonic freq.

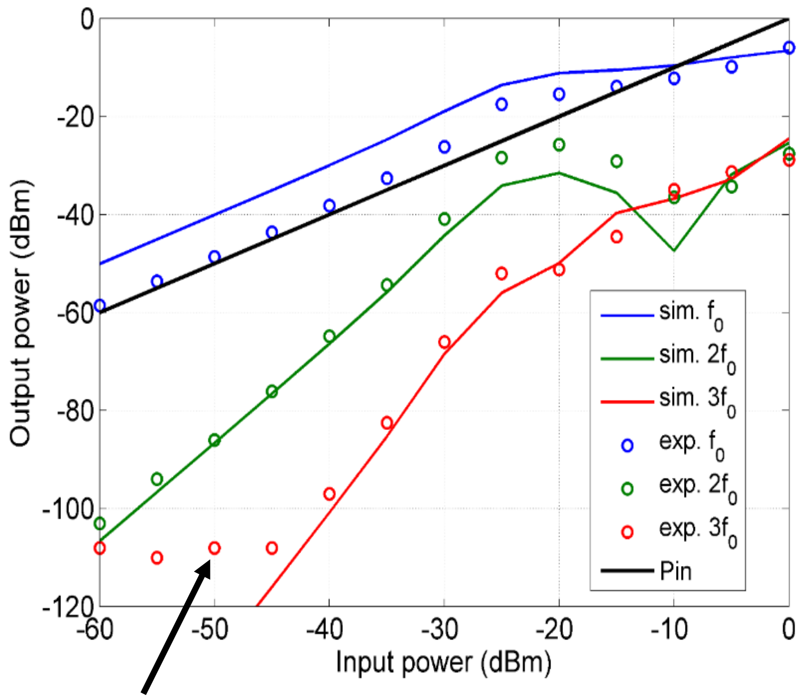

Noise floor of spectrum analyzer

Linear below -30 dBm input power

Active volumetric MTMs: modeling

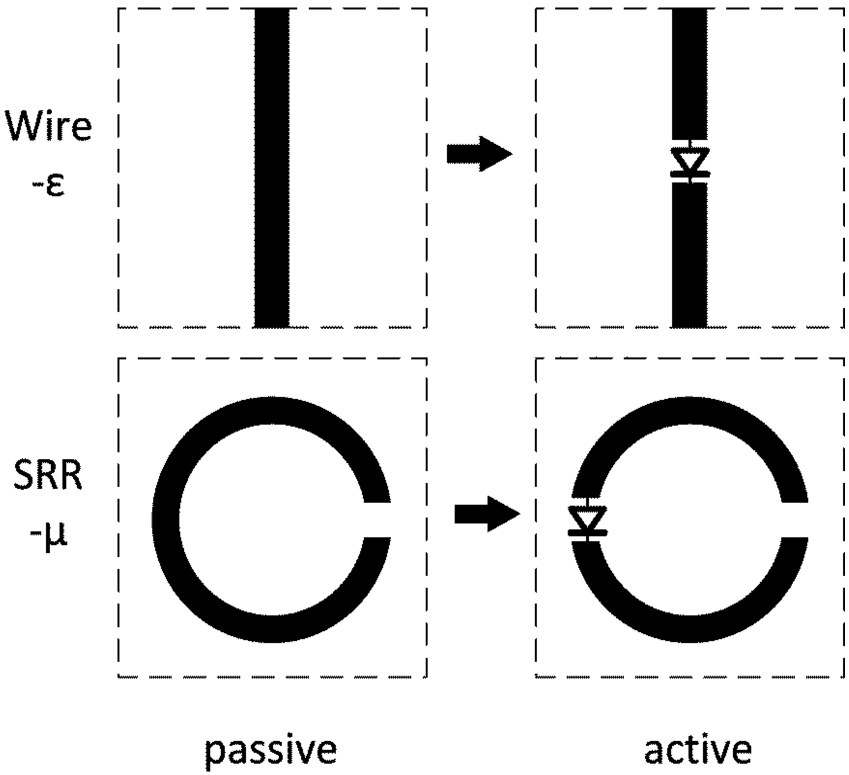

$$\epsilon_{eff} = 1 + \epsilon_c + \epsilon_d$$

$$\epsilon_c = -\frac{-[\omega^2 - 1/(LC)]/(dL\epsilon_0) - j\omega R/(dL^2\epsilon_0)}{[\omega^2 - 1/(LC)]^2 + [\omega(R - R_d)/L]^2}$$

$$\epsilon_d = -\frac{j\omega R_d/(dL^2\epsilon_0)}{[\omega^2 - 1/(LC)]^2 + [\omega(R - R_d)/L]^2}$$

$$\mu_{eff} = 1 + \mu_c + \mu_d = 1 - \frac{F}{\left(1 - \frac{1}{\omega^2 LC}\right) - \frac{jR}{\omega L} + \frac{jR_d}{\omega L}},$$

$$\mu_c = \frac{-F\left(1 - \frac{1}{\omega^2 LC}\right) - jFR/\omega L}{\left[\left(1 - \frac{1}{\omega^2 LC}\right)^2 + \left(\frac{R - R_d}{\omega L}\right)^2\right]},$$

$$\mu_d = \frac{jFR_d/\omega L}{\left[\left(1 - \frac{1}{\omega^2 LC}\right)^2 + \left(\frac{R - R_d}{\omega L}\right)^2\right]},$$

- Value of $-R_d$ controls the loss compensation level
- Control the loss/gain of ε and μ independently

Design and implementation

Tunnel diode

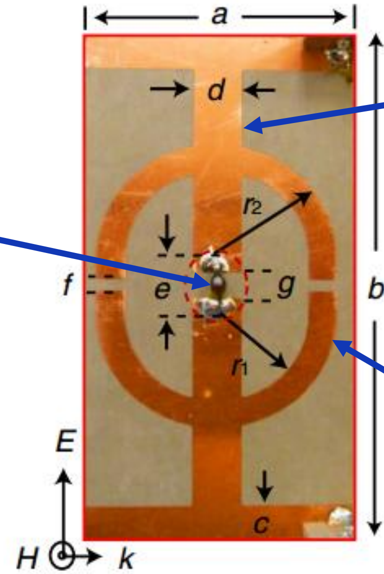

ε’<0
ε”<0

μ’ < 0
μ”> 0

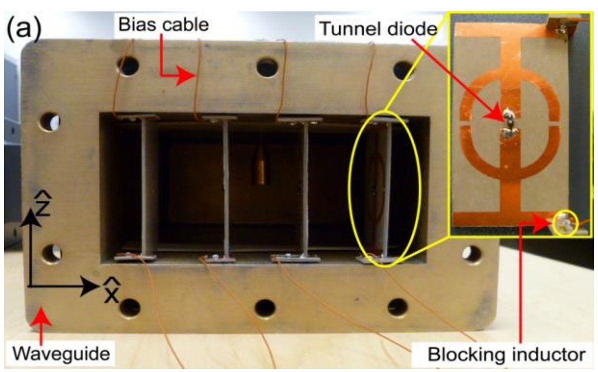

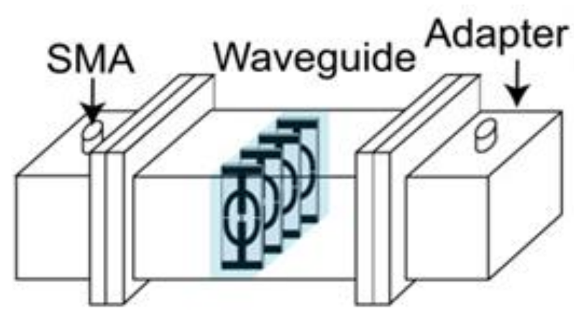

Measured S-parameters

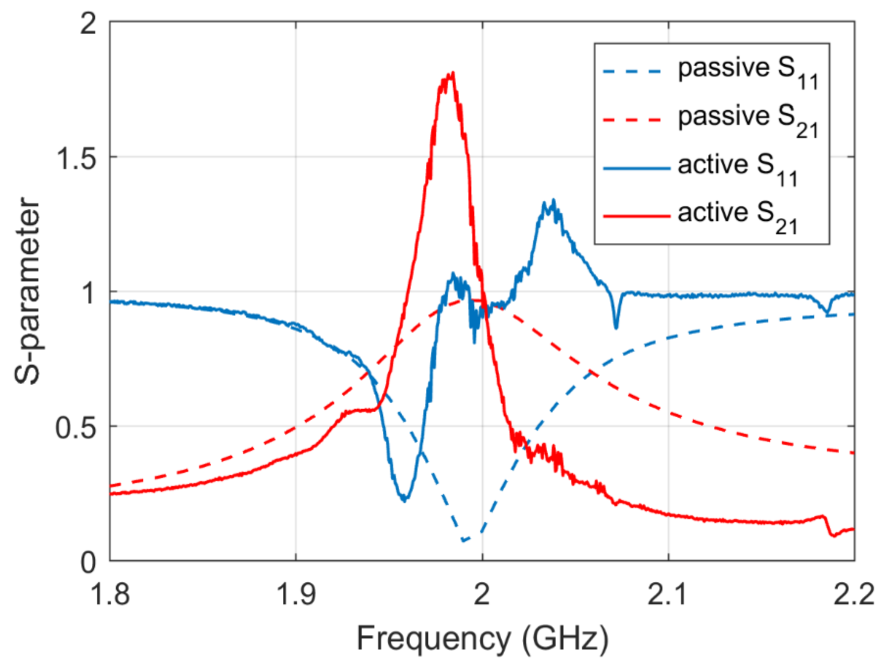

- Passive $S_{21} < 1$ indicates loss
- Active $S_{21} > 1$ indicates gain

Retrieved ε, μ and n

Retrieved ε, μ

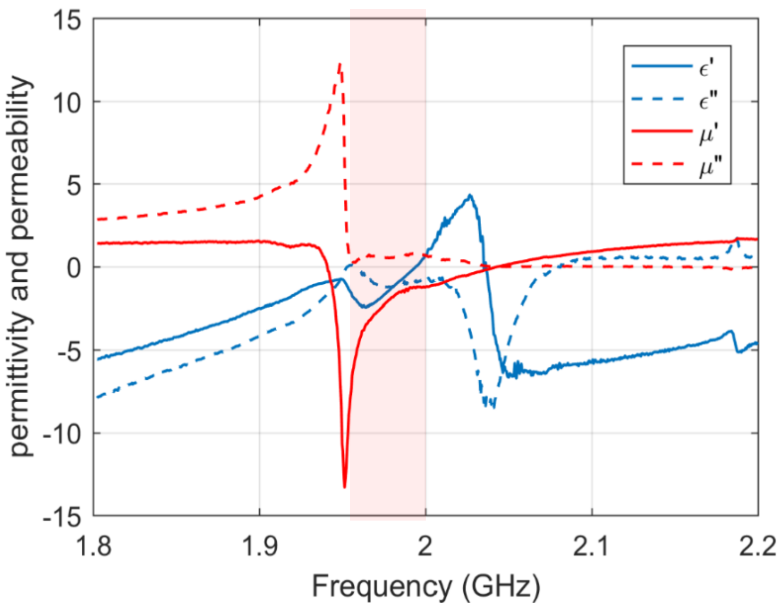

Retrieved n

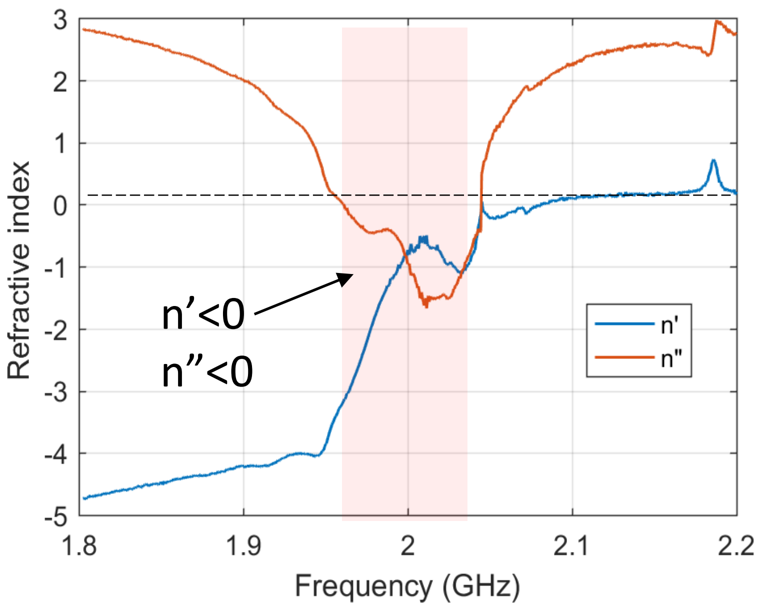

- **Near 2 GHz: ε', μ'<0, ε"<0, μ">0 , n' and n"<0**
- **The first demonstrated volumetric NIM with gain**

D. Ye, et. al., Nat. Commun., 5, Dec. 2014.

Summary

- **Conventional passive MTMs are lossy and dispersive.**
- **Gain device, such as tunnel diode, can be implemented into the passive MTM structure to compensate the loss or even provide the gain.**
- **An active gain CLRH TL MTM and a gain volumetric MTM are experimentally demonstrated.**

Outline

1. Active gain metamaterial

2. **Non-Foster antenna matching**

3. Sign choice of refractive index for active gain medium

4. Microfluidic device for THz Spectroscopy of live cells

Non-Foster element

Foster's reactance theorem: The reactance of a passive and lossless network always strictly monotonically increases with frequency.

Reactance
vs.
Frequency

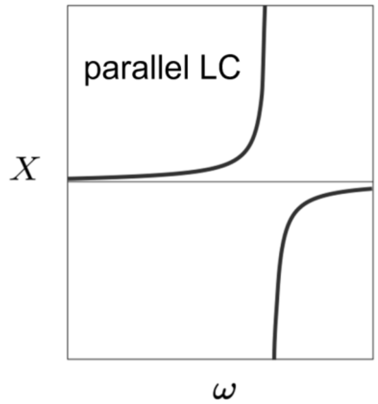

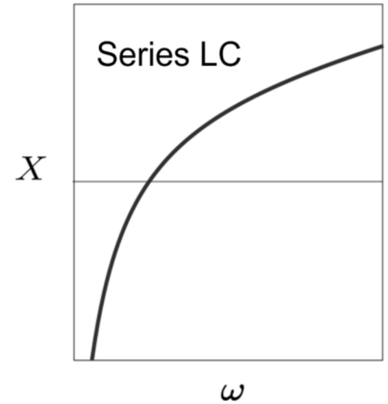

Only positive slope exists

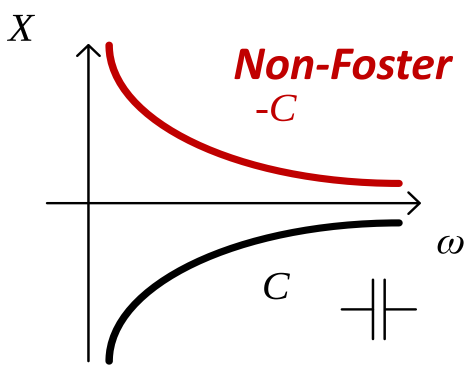

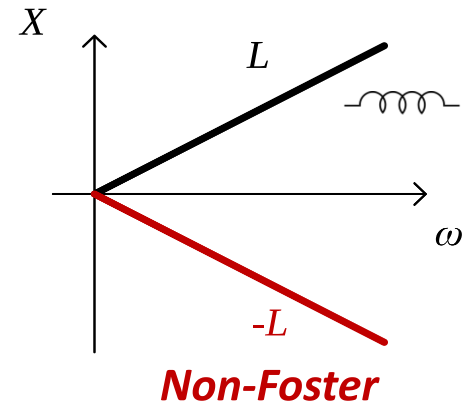

A lossless non-Foster element has to be active.

Bandwidth limit of electrically small antenna

- Define electrically small antenna $ka \ll 1, k = 2\pi/\lambda$
- **Chu's limit:** the radiation quality factor for a lossless electrically small antenna follows

$$Q_{chu} \geq \frac{1}{k^3a^3} + \frac{1}{ka}$$

$$BW_{3dB,\max} = \frac{k^3a^3}{1 + k^2a^2} \approx (ka)^3$$

Impedance of a 10 cm monopole antenna

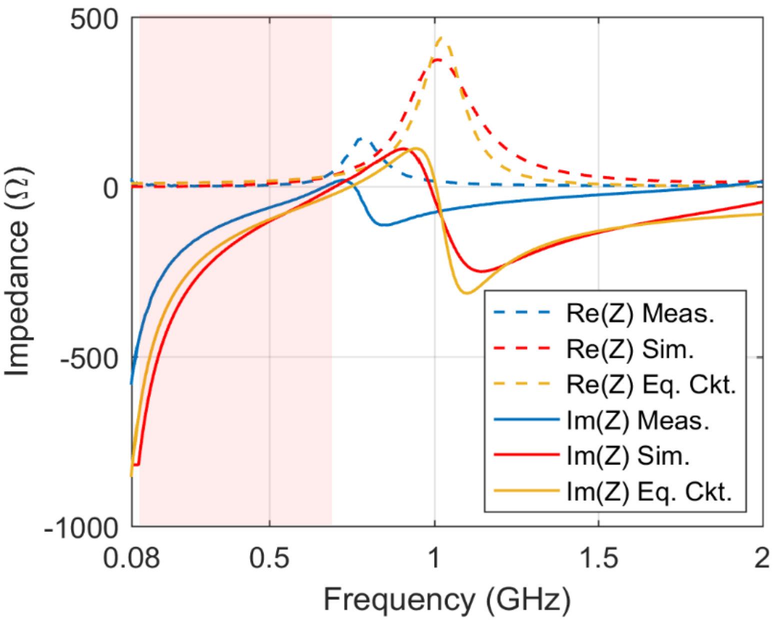

- **Large quality factor, thus suffers from limited bandwidth.**
- **Very low radiation efficiency due to small radiation resistance comparable to conductor resistance.**

Ideal non-Foster antenna matching circuit

Negative imaging modeling technique

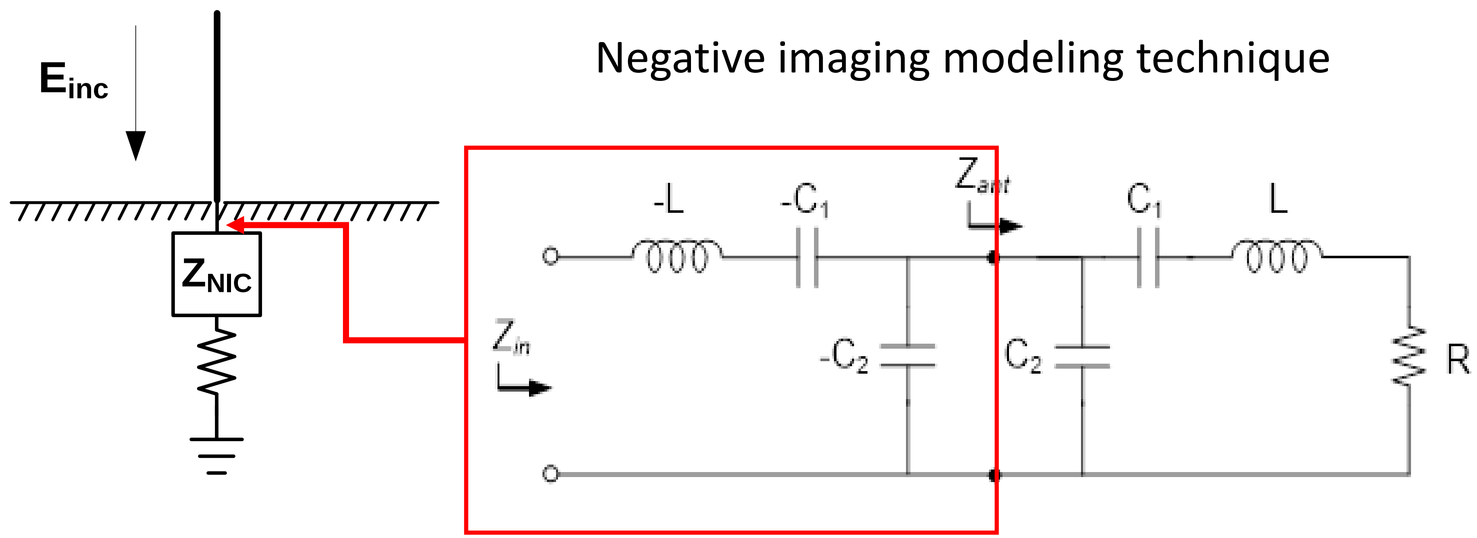

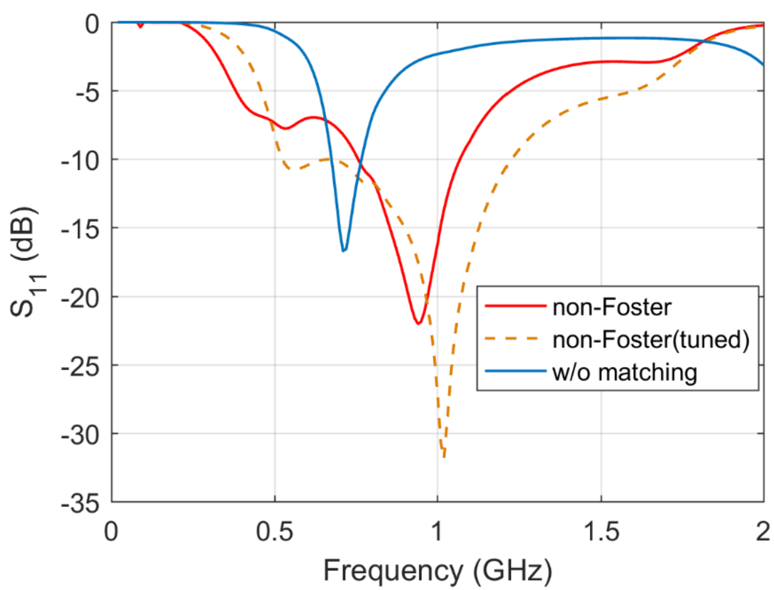

- 6 dB bandwidth: 170 MHz→780 MHz
- (Tuned) 10 dB bandwidth: 100 MHz→700 MHz
- Many practical problems need to consider, including the transistor selection, device parasitics, biasing, noise and most importantly stability.

Implementation methods of non-Foster Element

Cross-coupled transistor

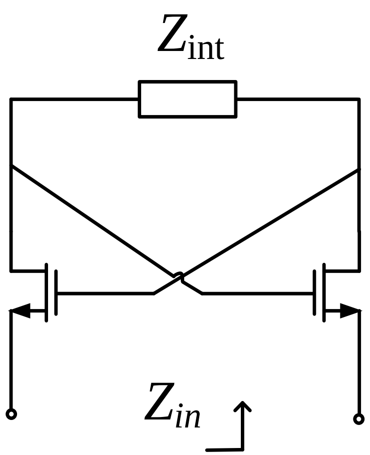

Operational amplifier

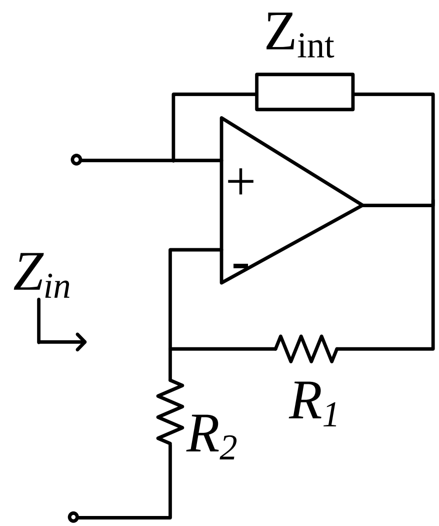

Negative resistor

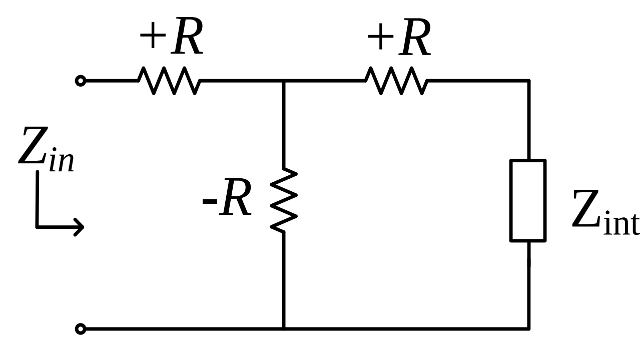

- **Convert or invert the positive impedance Z_{int} into negative impedance.**
- $Z_{in} \propto - Z_{\text{int}}$ **or** $Z_{in} \propto -1 / Z_{\text{int}}$.

Stability test methods

- **Time domain (Transient simulation):**
  - Inefficient for parametric study
  - Not predict degrees of stability, where instability comes from
- **Linear frequency domain:**
  - K-Δ factor, μ factor, Llewellen factors, etc. (Rollet’s proviso)
  - Return ratio, loop gain (easy implemented but not sufficient in more complicated case)
  - Return difference, Normalized Determinant Function (NDF) method (Complexity ⇔ Accuracy)

Procedure of NDF analysis

1. Obtain the circuit model of network, and find the admittance / impedance matrix
2. Calculate the determinant as Δ
3. Deactivate all active devices i.e. let g_m =0
4. Calculate its determinant as Δ_0.
5. $$NDF = \frac{\Delta}{\Delta_0} = \frac{(s-z_1)(s-z_2)(s-z_3)\cdots}{(s-p_1)(s-p_2)(s-p_3)\cdots},$$
6. No RHP zeros ➔ Stable.
   – Directly solve the roots.
   – Routh-Hurwitz criterion.
   – Nyquist plot.

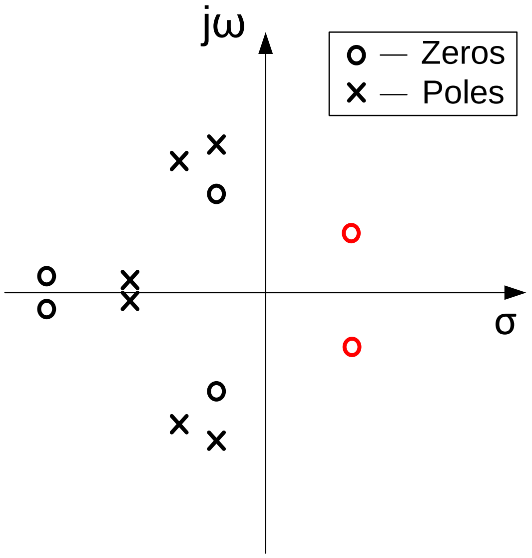

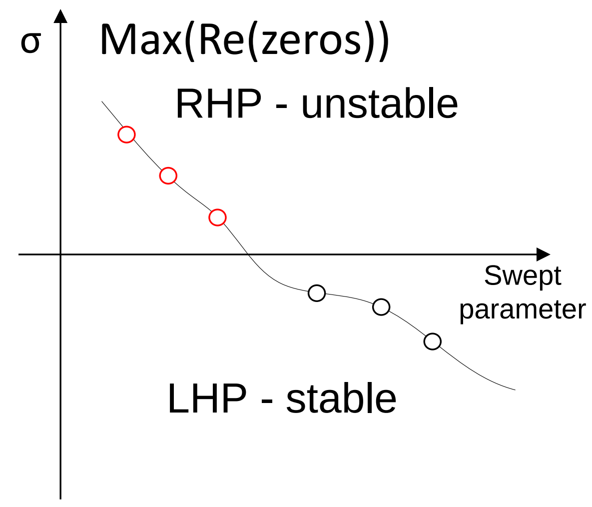

A simple example of NDF

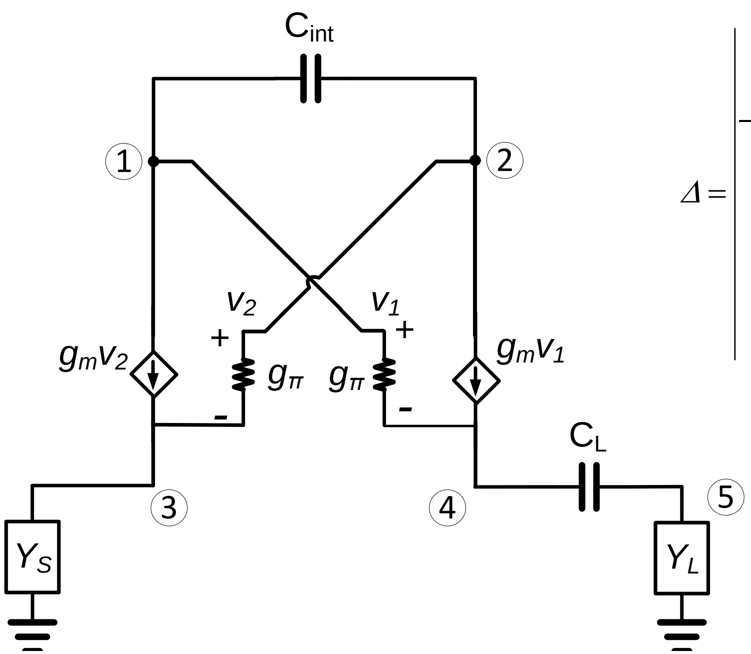

$$\Delta = \begin{vmatrix} sC_{\text{int}} + g_\pi & -sC_{\text{int}} + g_m & -g_m & -g_\pi & 0 \\ -sC_{\text{int}} + g_m & sC_{\text{int}} + g_\pi & -g_\pi & -g_m & 0 \\ 0 & -g_m - g_\pi & g_m + g_\pi + Y_s & 0 & 0 \\ -g_m - g_\pi & 0 & 0 & g_m + g_\pi + sC_L & -sC_L \\ 0 & 0 & 0 & -sC_L & sC_L + Y_L \end{vmatrix}$$

$$\Delta_0 = \begin{vmatrix} sC_{\text{int}} + g_\pi & -sC_{\text{int}} & 0 & -g_\pi & 0 \\ -sC_{\text{int}} & sC_{\text{int}} + g_\pi & -g_\pi & 0 & 0 \\ 0 & -g_\pi & g_\pi + Y_s & 0 & 0 \\ -g_\pi & 0 & 0 & g_\pi + sC_L & -sC_L \\ 0 & 0 & 0 & -sC_L & sC_L + Y_L \end{vmatrix}$$

$$z_1 = 0$$

$$z_2 = \frac{C_L - C_{\text{int}}}{C_{\text{int}} C_L (2/g_m + 1/Y_L + 1/Y_S)}$$

Stable condition is $C_{\text{int}} > C_L$

Practical factors have to taken into account for stability analysis.

The effect of device parasitics

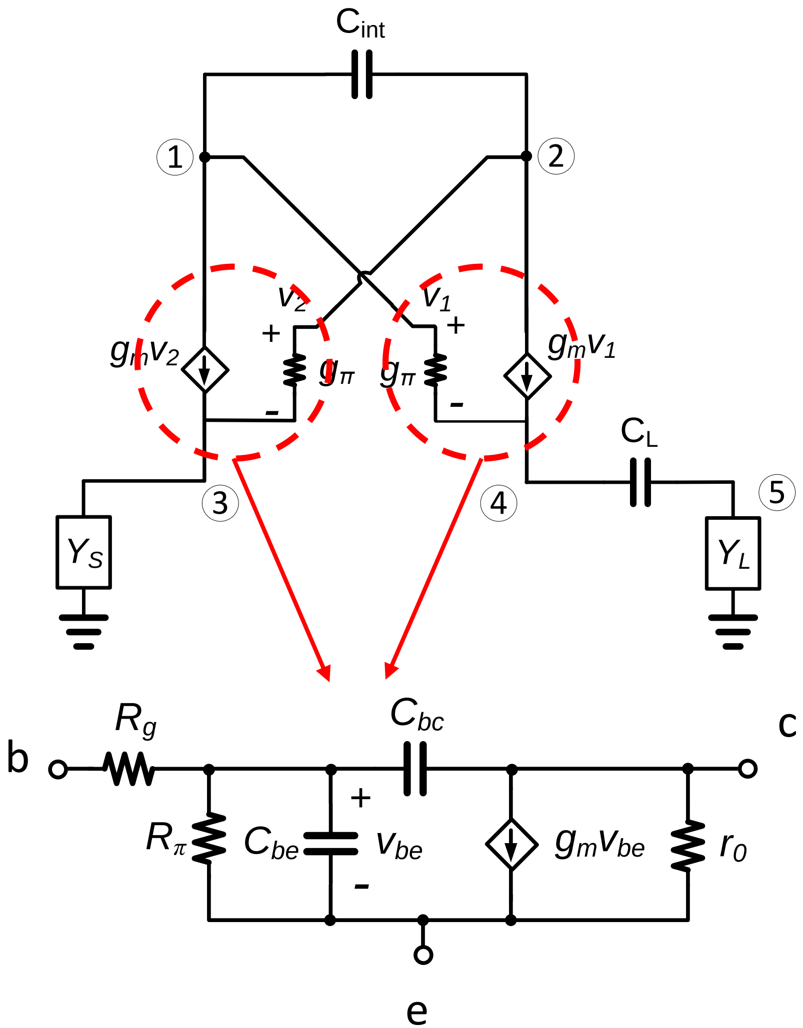

Max(Re(zeros)) vs. parameter C_{int}

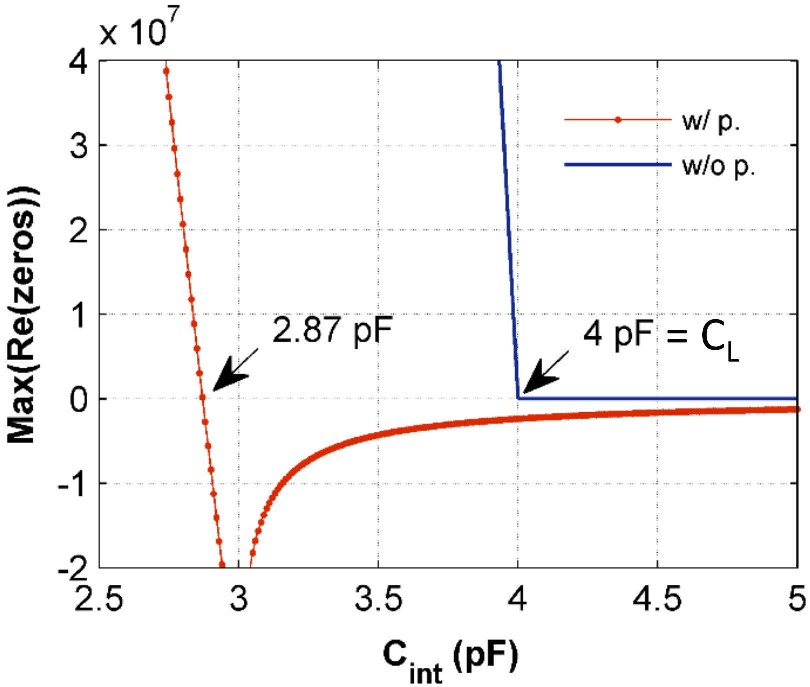

The stable condition of $C_{int} > C_L$ is shifted down by 1.13 pF when device parasitics are taken into account.

The effect of DC biasing network

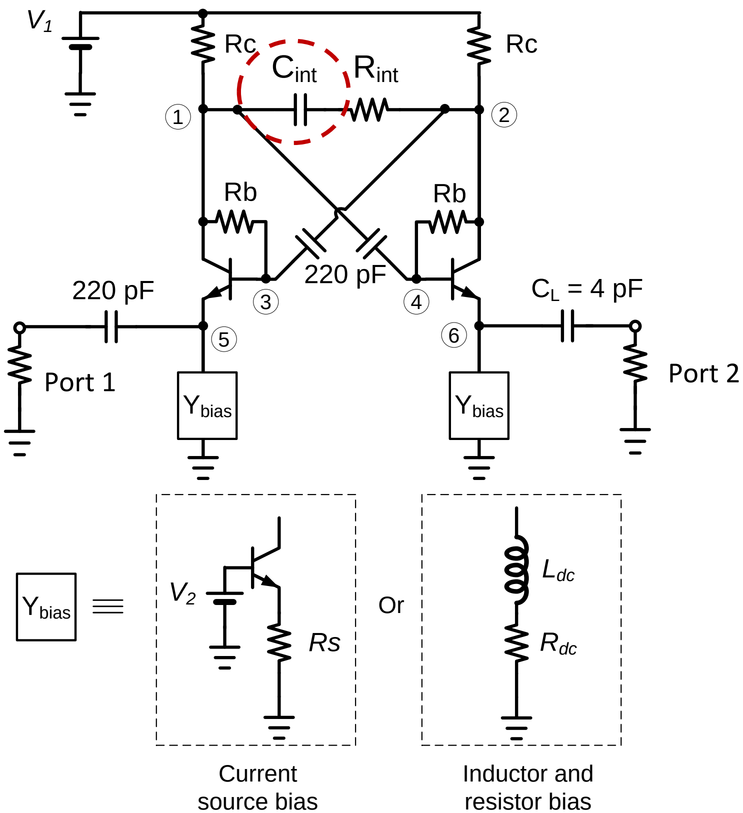

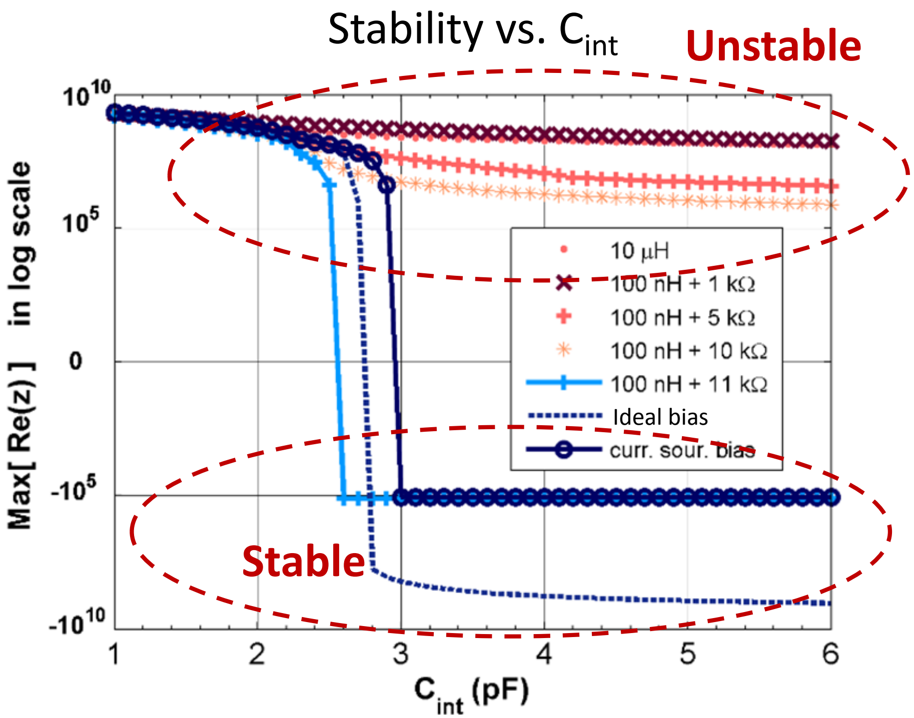

- **Always unstable for any values of C_{int} when an inductor-resistor bias is selected (up to 100 nH and 10 kΩ).**
- **A more practical choice of active current source bias is stable.**

The effect of TLs in layout

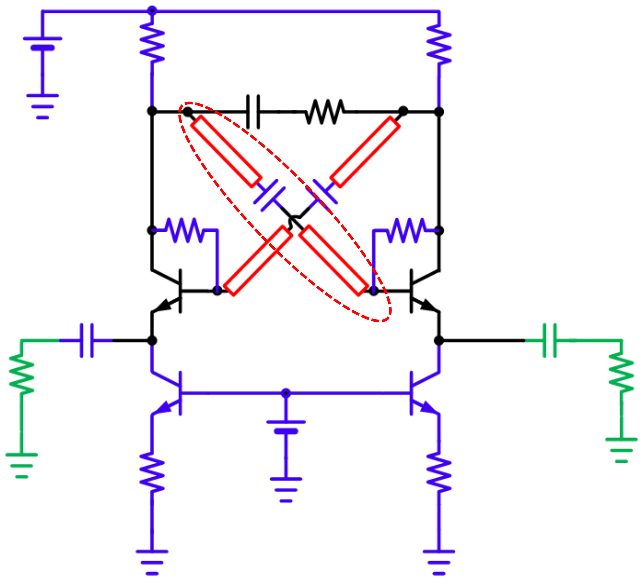

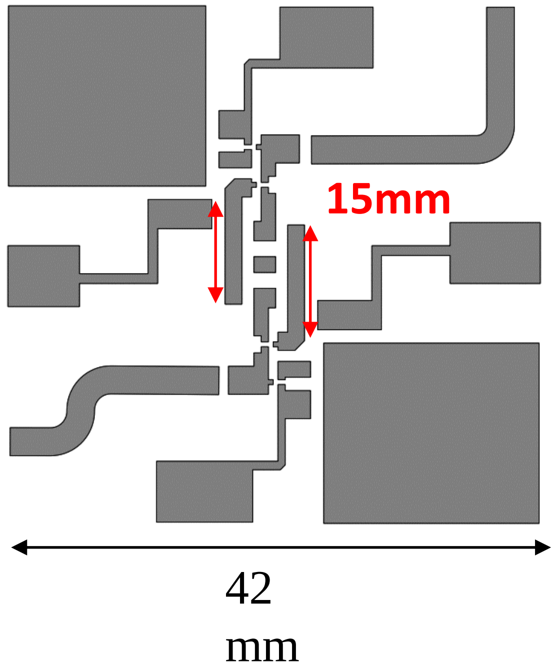

15 mm (~0.01 λ) transmission line in the loop

The effect of TLs in layout: Nyquist plot

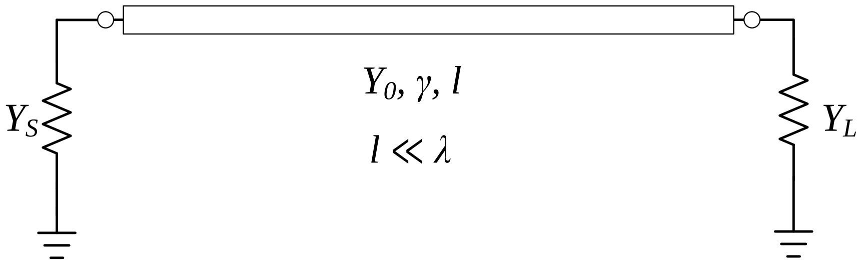

$$\mathbf{Y_{TL}} = \begin{bmatrix} Y_S + Y_0 \operatorname{ctgh}(\gamma l) & -Y_0 \operatorname{csch}(\gamma l) \\ -Y_0 \operatorname{csch}(\gamma l) & Y_L + Y_0 \operatorname{ctgh}(\gamma l) \end{bmatrix}$$

For example:

$$f(s) = \frac{s^2 - 4s + 3}{s^2 + 2s + 1}$$

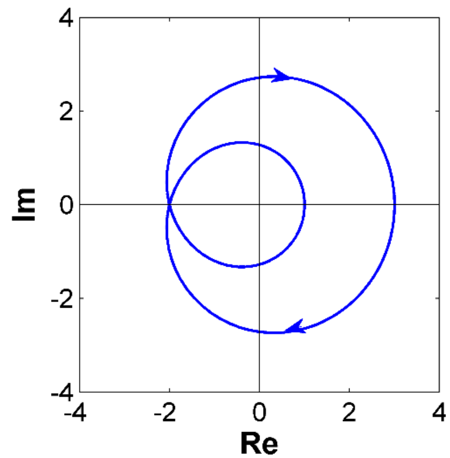

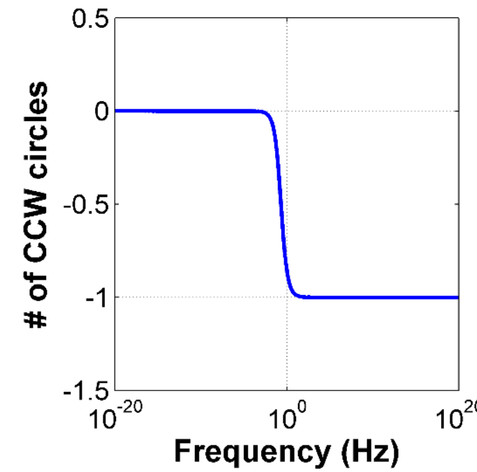

- **TLs can be modeled with Y matrix with hyperbolic functions.**
- **Nyquist plot to count the number of RHP zeros without directly solving the equation.**

Stability for different length of TL in feedback loop

Sweep the transconductance (g_m) of the transistor

(a) *l* = 0 mm

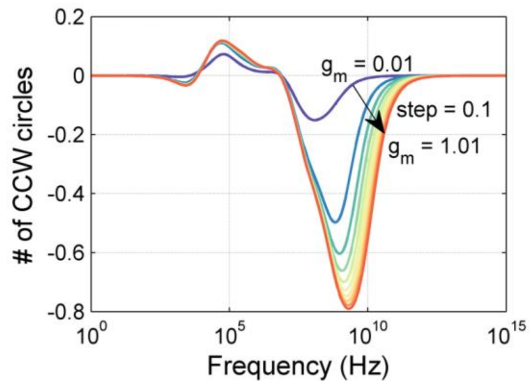

(b) *l* = 1 mm

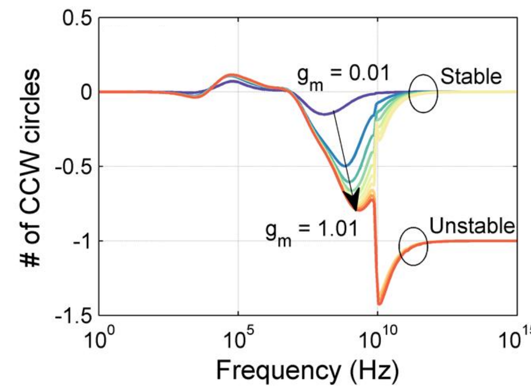

(c) *l* = 3 mm

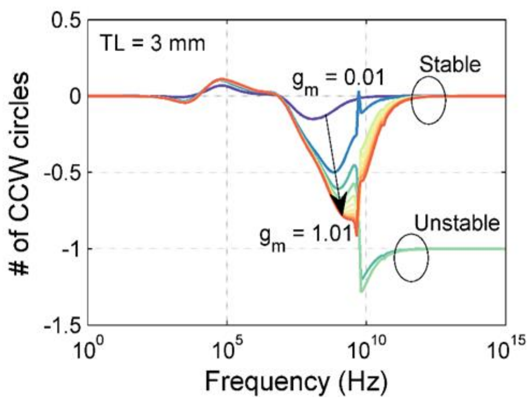

(d) *l* = 15 mm

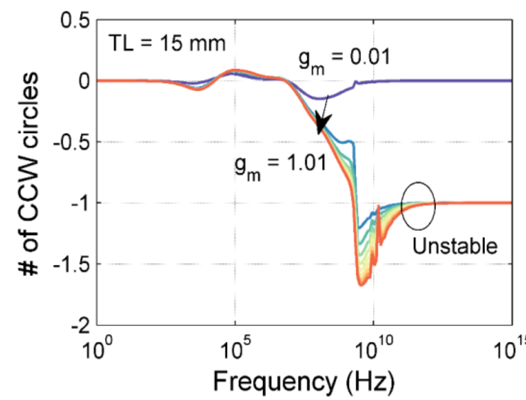

The short (~0.01λ_0 at 300 MHz) TL in the feedback loop has a large impact on the stability.

Adding stabilization resistors

Test I

Without R_{stb}

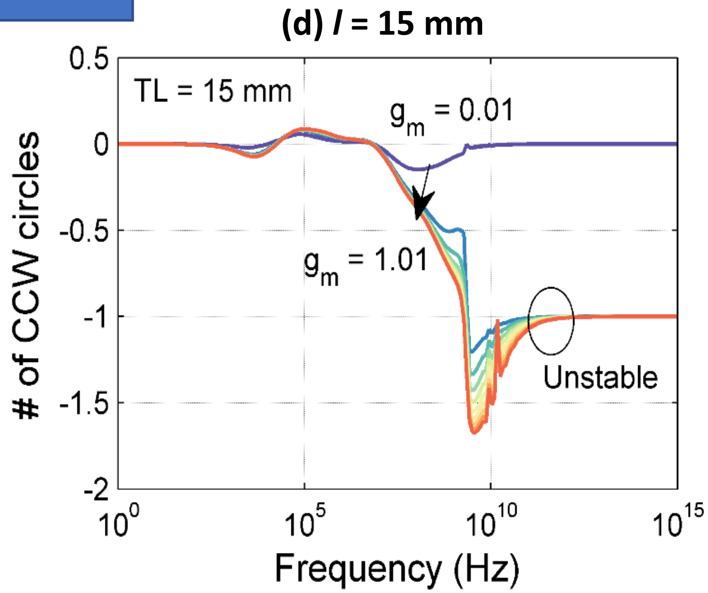

Unstable

Test II

Series R_{stb} = 50 Ω

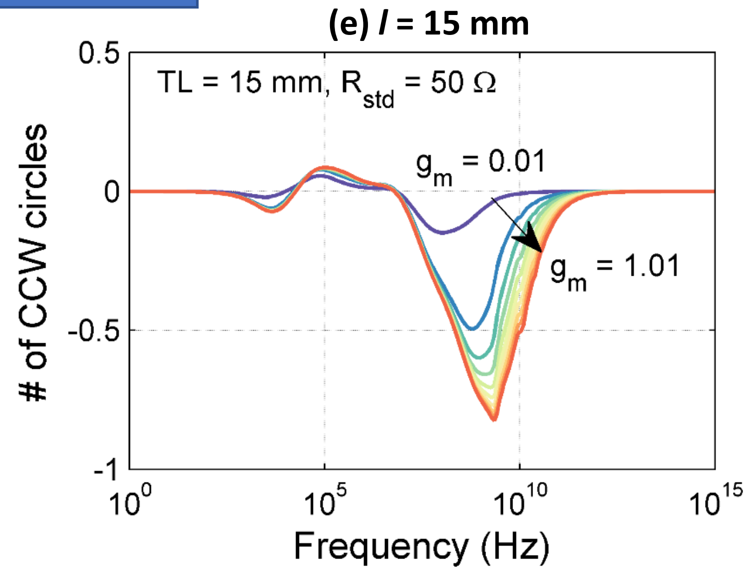

Stable

- The circuit becomes stable across all values of g_m.
- The efficiency of the matching circuit drops by 1.6 dB.

Experimental setup and fabrication

Experimental setup

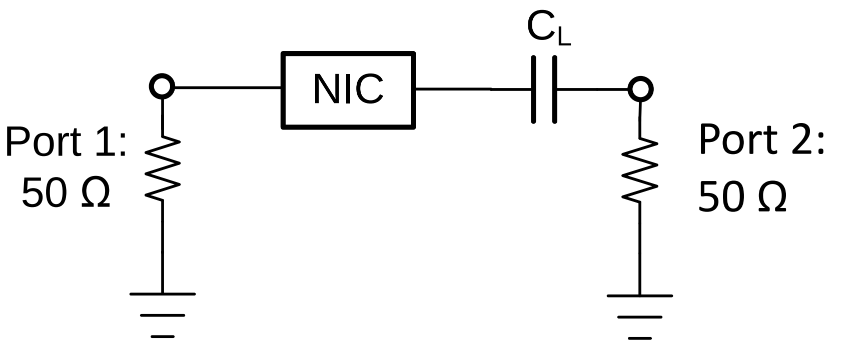

A photo of fabricated circuit

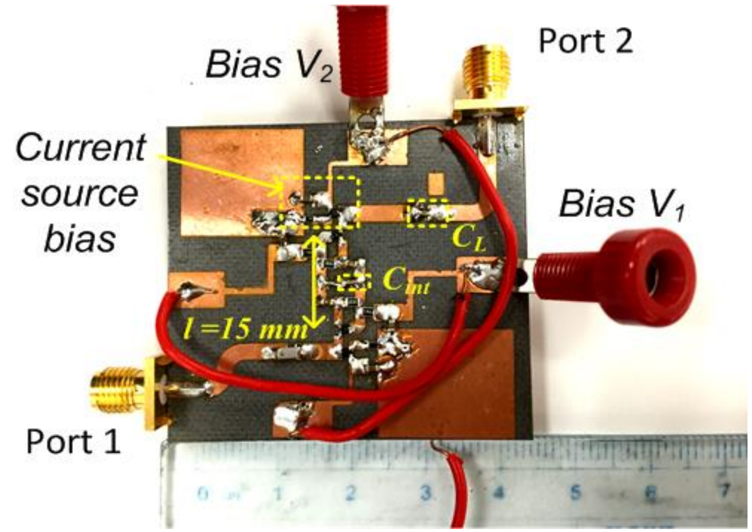

- Non-Foster circuit loaded with a positive capacitor.
- Test S_{11} and S_{21} to evaluate the performance of negative capacitor.
- Deembed C_L and microstrip line to extract the impedance of non-Foster circuit.

Experimental verification of NDF analysis

Test I

Without R_{stb}

No input signal

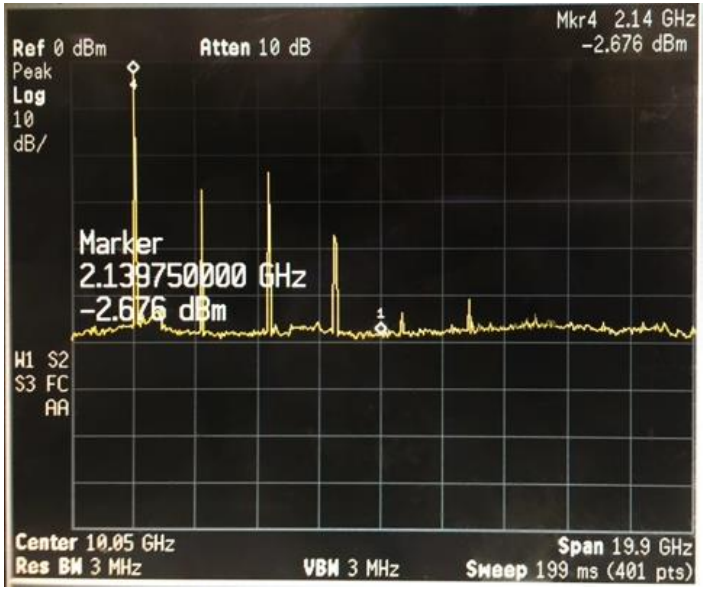

Self-oscillation @ 2.1 GHz

Test II

Series R_{stb} = 50 Ω

Input signal: -20 dBm @ 300 MHz

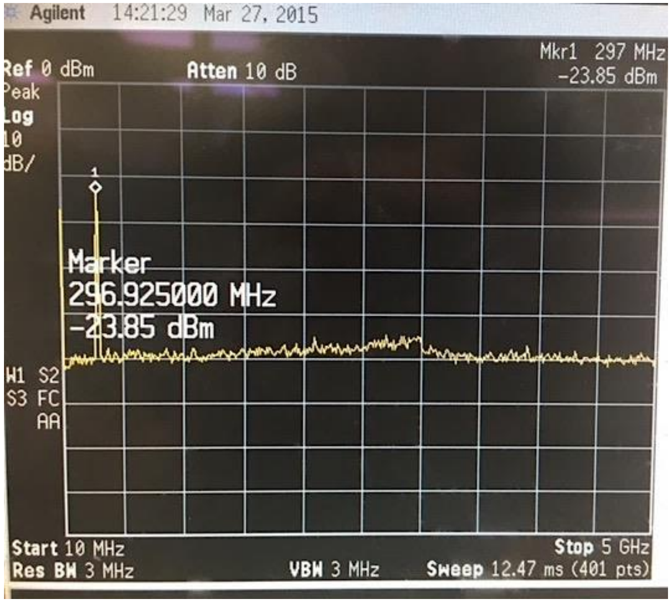

- **No oscillations observed.**
- **Loss of the non-Foster matching circuit is about -3.8 dB.**

HF helical antenna with non-Foster matching circuit

HF band: 3 to 30 MHz

2m

- **The helical antenna has the lowest self-resonant frequency at 24 MHz.**
- **A -40 pF negative capacitor is required to fully cancel the reactance of the helical antenna at HF band.**

Characterize the negative capacitance

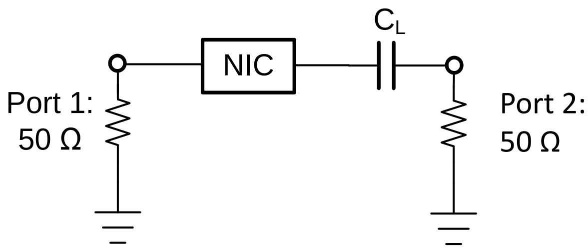

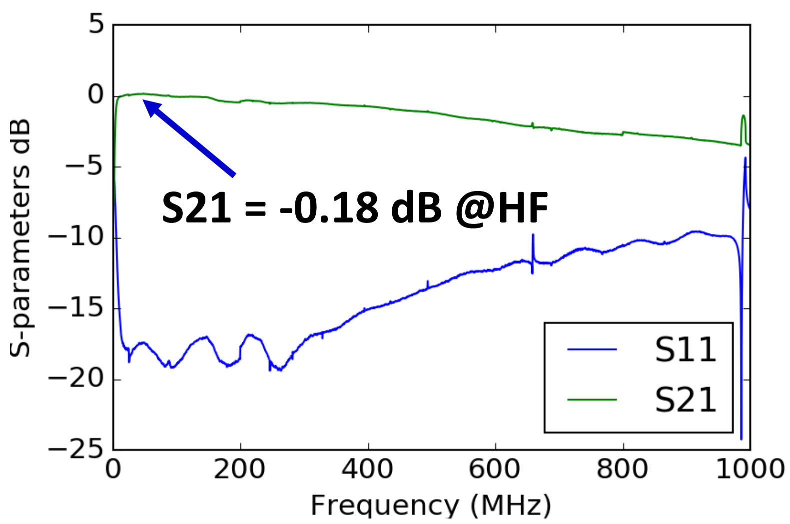

Extracted impedance and -C

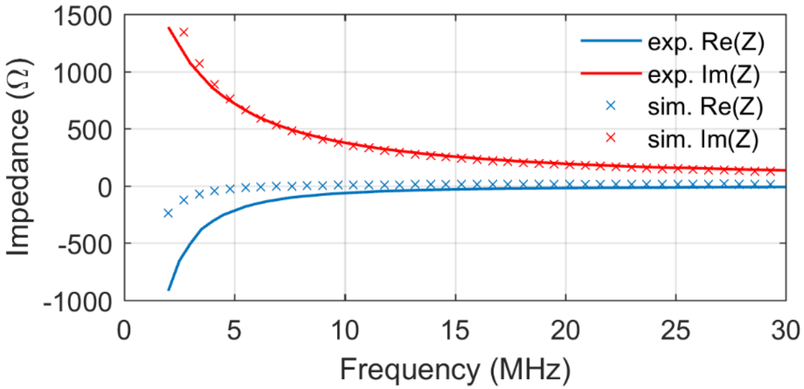

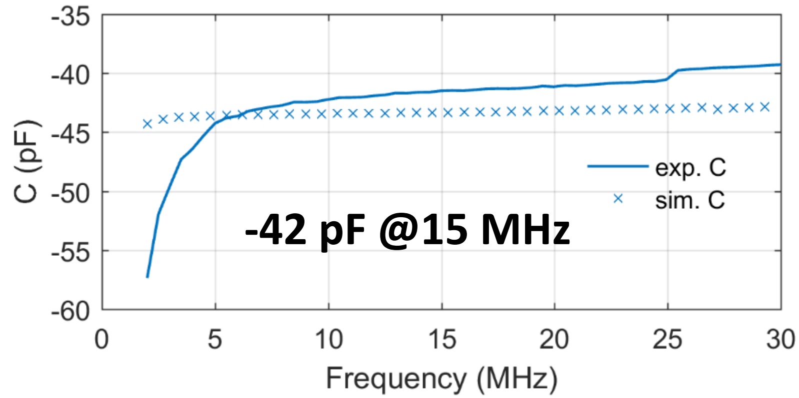

- The circuit loss is largely reduced due to the use of smaller value of R_{stb}.
- A -42 pF negative capacitor with low parasitic R is achieved at HF band.

S_{11} of non-Foster matched helical antenna

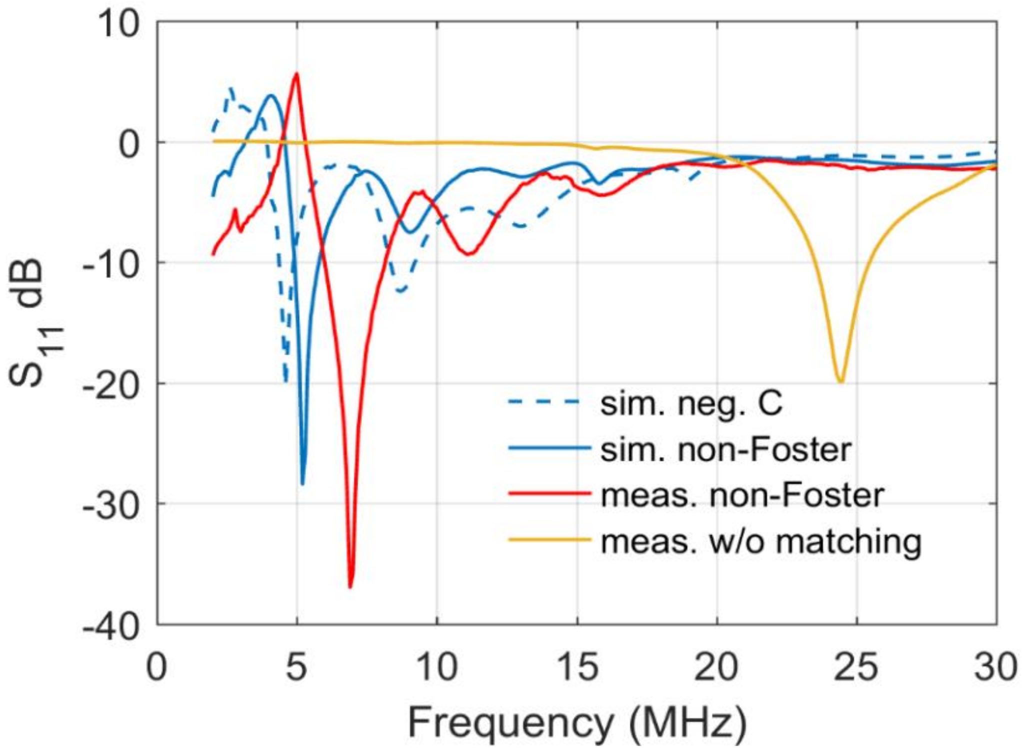

- Improvement of S_{11} near 7 MHz.
- Simulation and measurement results show good consistency.
- The improvement of return loss, however, does not guarantee the increase of the overall gain.
- A field test of gain / efficiency is necessary.

Field test environment

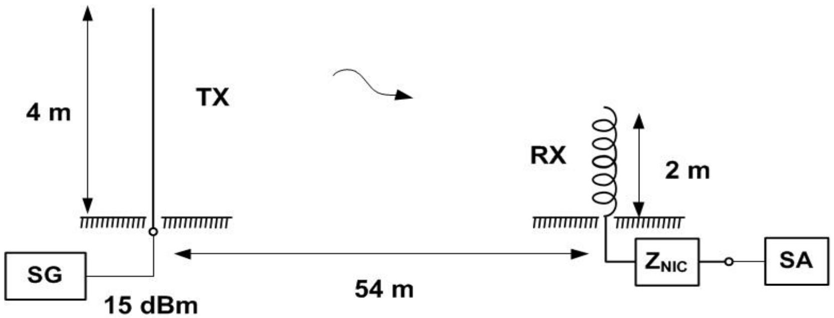

(a)

(b)

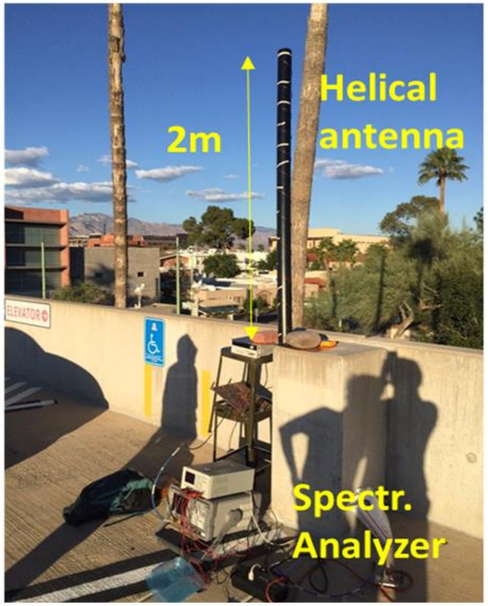

(c)

- The distance of the link is 54 meter (about 0.5 to 5 λ from 3 to 30 MHz).
- Testing cases: 1) helical antenna with non-Foster matching; 2) without matching; 3) a commercial well-matched 4-meter whip antenna.

Received signal enhancement by non-Foster matching circuit

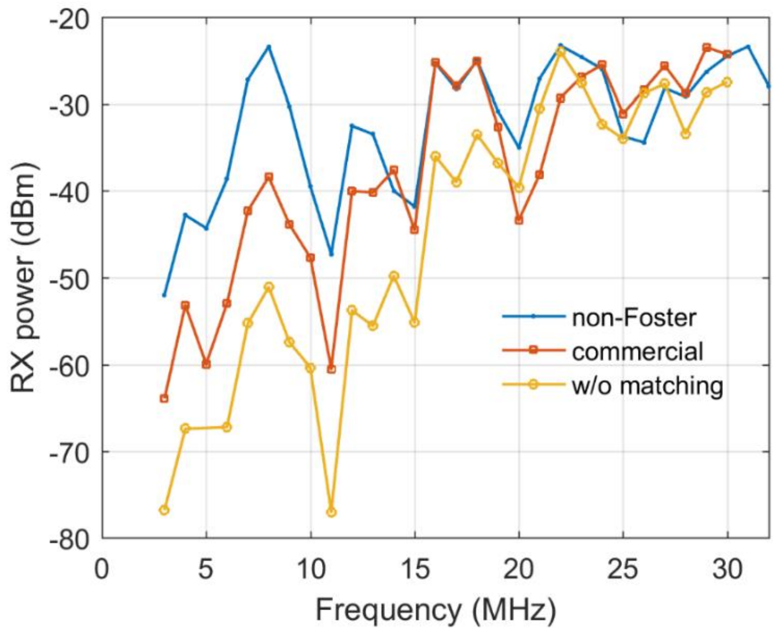

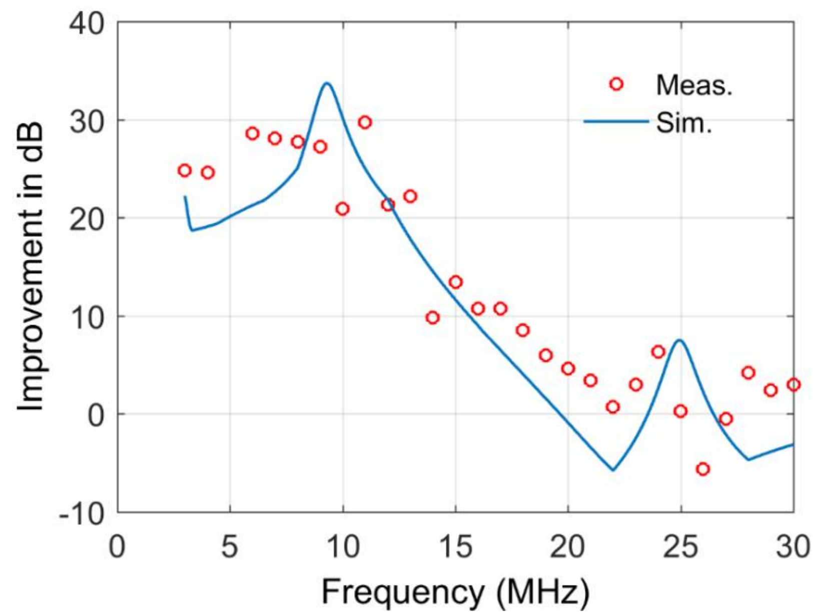

- **20-30 dB received signal power enhancement by non-Foster matching circuit at 3-13 MHz compared to without matching case.**
- **About 15 dB improvement compared to the commercial antenna.**

Summary

- We proposed NDF method to analyze the stability of the non-Foster circuit.
- Practical factors of influencing the stability are studied, including the device parasitics, biasing networks, TLs in the layout and antenna load impedance.
- The result of NDF analysis is experimentally verified.
- A stable negative capacitor is achieved.
- A helical antenna with non-Foster matching circuit is designed and tested.
- Non-Foster matching circuit can largely improve the received signal strength in a wide bandwidth.

Outline

1. Active gain metamaterial
2. Non-Foster antenna matching
3. **Sign choice of refractive index for active gain medium**
4. Microfluidic device for THz Spectroscopy of live cells

Sign choice of refractive index

$$\boldsymbol{n = \pm\sqrt{\epsilon\mu} = n' - jn"}$$

In 1968, V. Veselago theoretically discovered **n < 0 if both $\boldsymbol{\epsilon}$ and $\boldsymbol{\mu < 0}$**.

- **passive lossless case**
- **To resolve the sign of gain media is not trivial**

Average Poynting vector

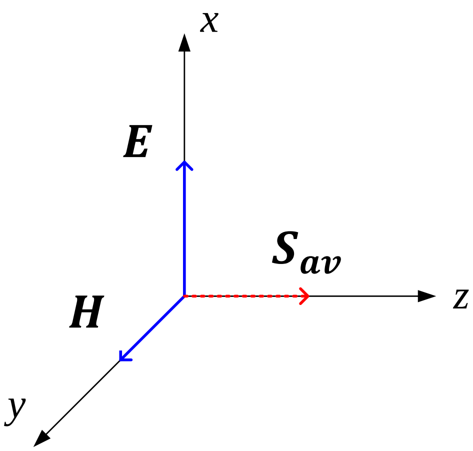

$$\boldsymbol{S_{av}} = \frac{1}{2} Re(\boldsymbol{E} \times \boldsymbol{H}^*) = \hat{z} \frac{\eta'}{2|\eta|^2} E_0^2 \mathrm{e}^{-2n'' k_0 z}$$

- η’ > 0/ η’ < 0 → positive/negative direction
- n” > 0/ n” < 0 → decay/amplify

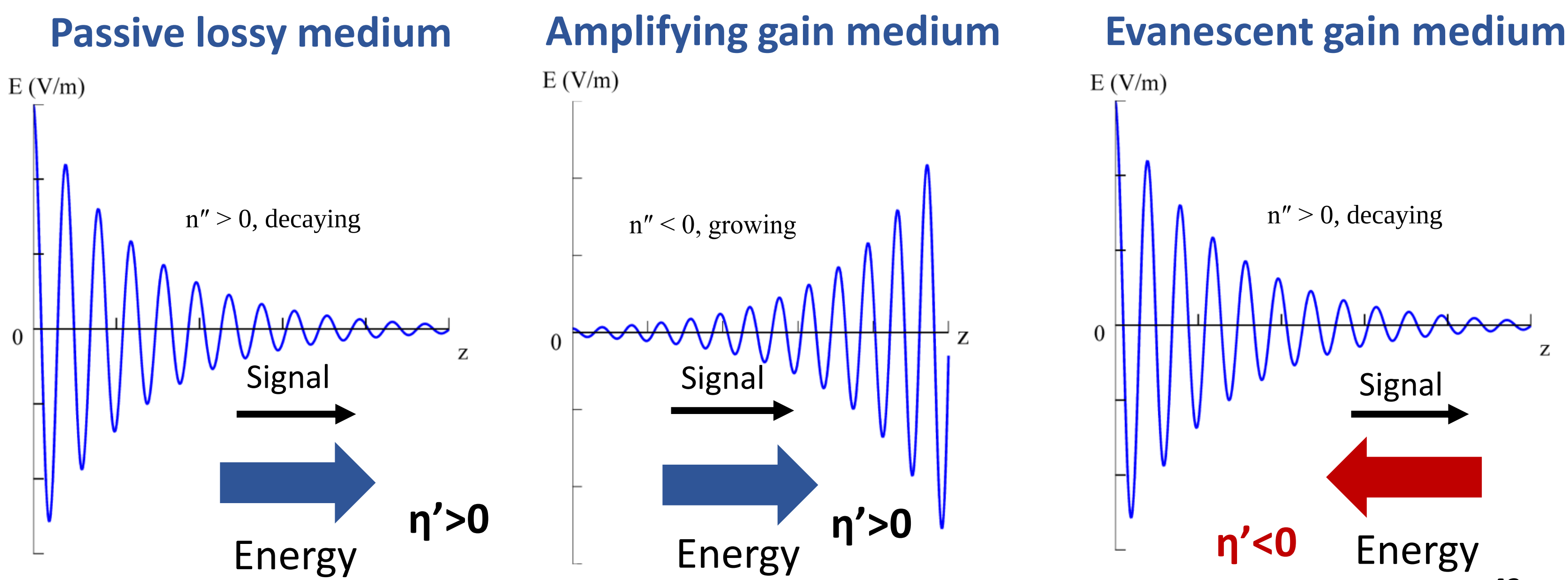

Sign choice for lossy or gain medium

Energy conservation theorem

$\eta^2 = \mu/\epsilon \, , \eta = n/(c\epsilon)$

1) Lossy medium $\Leftrightarrow$ $\frac{\epsilon''}{|\epsilon|} + \frac{\mu''}{|\mu|} > 0,$ $\Leftrightarrow$ $\eta' n'' > 0;$

2) Gain medium $\frac{\epsilon''}{|\epsilon|} + \frac{\mu''}{|\mu|} < 0,$ $\eta' n'' < 0.$

- **For lossy medium, energy only comes from the excitation, thus the sign can be unambiguously determined by n”>0 and/or η’>0.**
- **For gain medium, energy comes from both the excitation and medium itself, thus it is not clear the direction of average power flow.**
- **Gain medium: η’>0 and n”<0, or η’<0 and n”>0.**

Different sign choice methods

Method 1: let η'>0 ➔ n">0 for lossy medium, and n"<0 for gain medium.

$$n = +\sqrt{\epsilon\mu} \cdot \mathrm{sign}[-\mathrm{Im}(\sqrt{\epsilon\mu})] \cdot \mathrm{sign}(\epsilon''/|\epsilon| + \mu''/|\mu|)$$

Method 2: n follows analytical continuation

$$n(\omega) = +\sqrt{|\epsilon(\omega)||\mu(\omega)|}e^{j\frac{(\phi_\epsilon+\phi_\mu)}{2}}$$

- **Method 1 and 2 are consistent when η'>0**
- **Method 2 allows the sign choice of η'<0 in some special gain media**

- **If η'<0 existed, could it be stable?**
- **We will focus on the discussion on the relation between sign choice and stability of gain medium system.**

A gain slab system

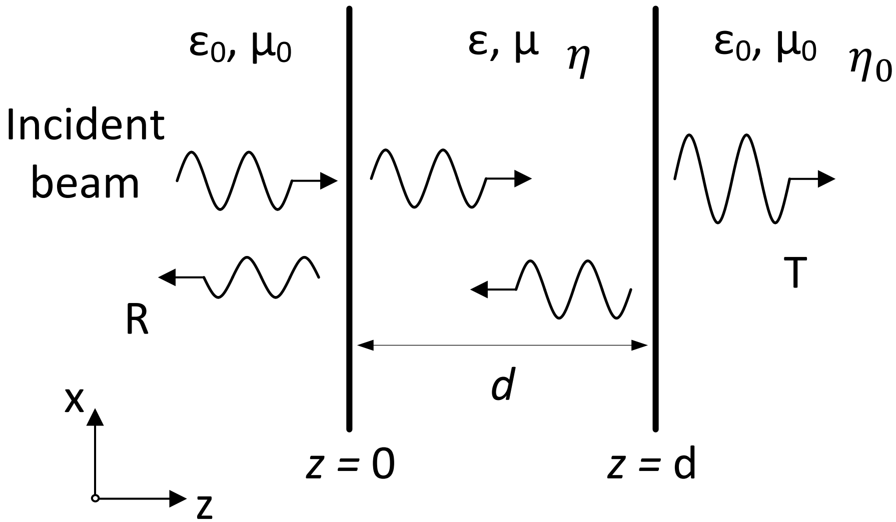

Reflection coefficient at the interface $\Gamma = \dfrac{\eta_0 - \eta}{\eta_0 + \eta}$

$$\boldsymbol{R = -\Gamma + (1-\Gamma^2)\Gamma e^{-2\gamma d} \sum_{m=0}^{\infty} \left(\Gamma^2 e^{-2\gamma d}\right)^m}$$

$$\boldsymbol{T = (1-\Gamma^2) e^{-\gamma d} \sum_{m=0}^{\infty} \left(\Gamma^2 e^{-2\gamma d}\right)^m}$$

- Define **Loop Gain** parameter: $LG = \Gamma^2 e^{-2\gamma d}$

Widely used in electronics and control system theory

- A sufficient convergence condition: if $|LG| < 1$, $\sum_{n=0}^{\infty} (LG)^n = \frac{1}{1-LG}$.
- Define **Critical Length** d_c, such that $|LG(d = dc)| = 1$.

$$d_c = \frac{c}{\omega n''} \ln\left|\frac{\eta - \eta_0}{\eta + \eta_0}\right|$$

- **For lossy medium, $d_c < 0$**
- **For gain medium, $d_c > 0$**

Monochromatic stability analysis

Assume $\epsilon = -1.18 + j0.23, \mu = -1.20 - j0.12$

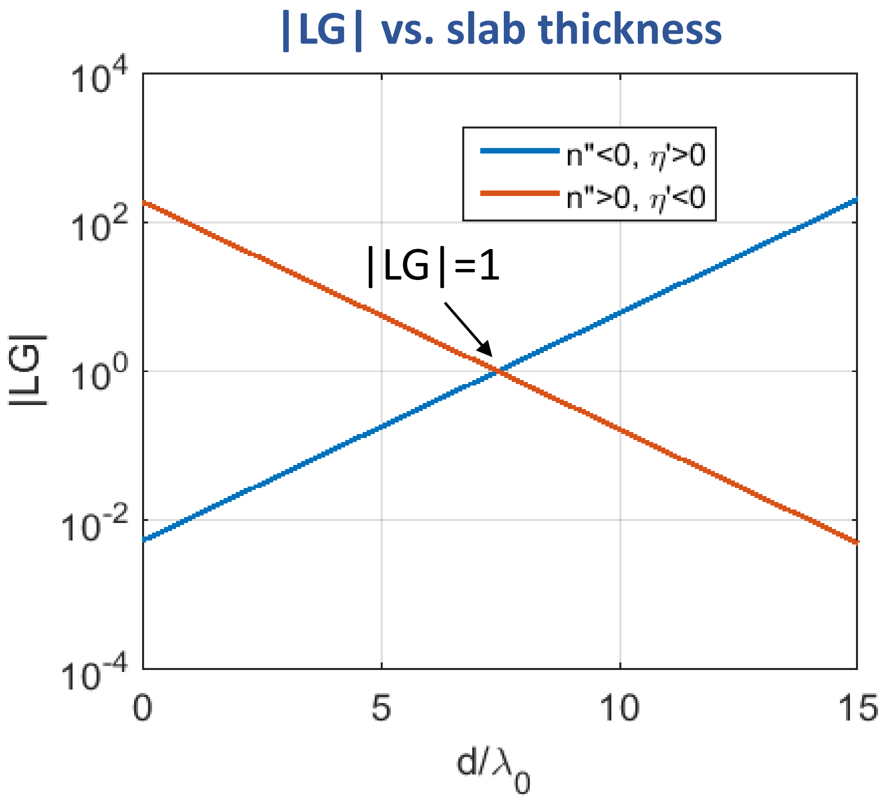

$$\frac{\epsilon''}{|\epsilon|} + \frac{\mu''}{|\mu|} = -0.0949 < 0$$

Gain medium, and $d_c = 7.45\lambda_0$

- For η'>0 and n"<0, the slab is stable for small thickness $d<d_c$.
- For η'<0 and n">0, the slab is stable for large thickness $d>d_c$.

- **The sign can be uniquely determined if we know:**
  1. **the size of the slab**
  2. **the slab is stable**

Example I: η’>0 gain medium

$$\epsilon(\omega) = 1 - \frac{F\omega_p^2}{\omega_p^2 - \omega^2 + j\kappa\omega} \quad F > 0 \text{ indicates gain. Let } \mu = 1$$

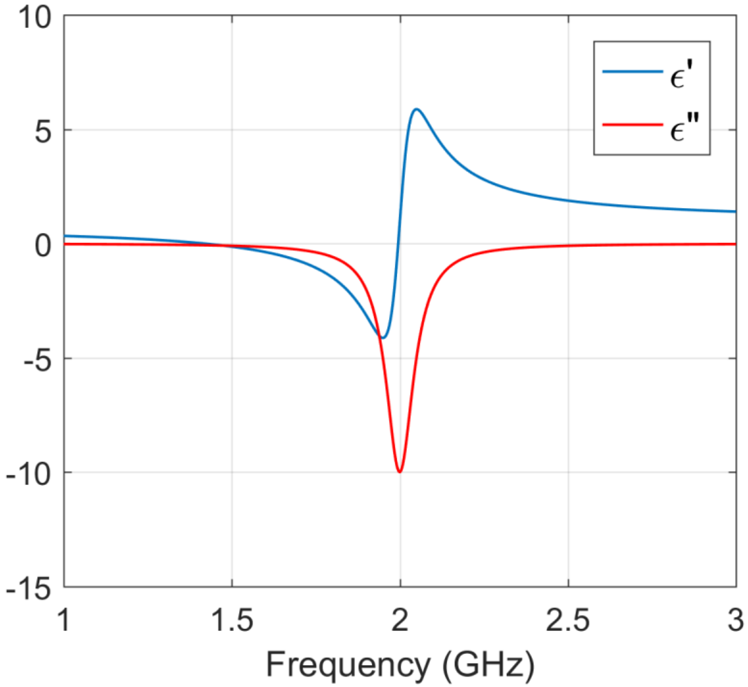

Both methods get same result

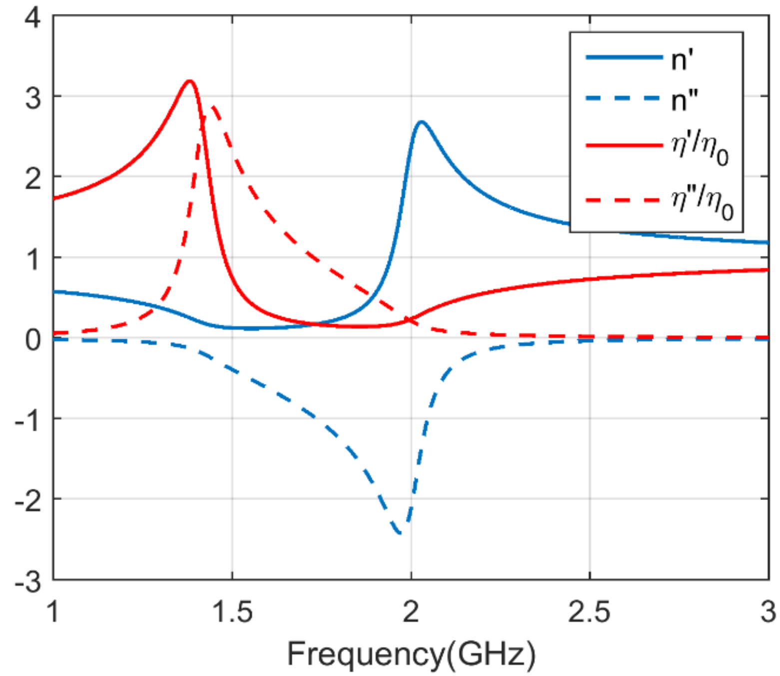

- **Method 1 and 2 have the same sign choice.**
- **$\eta' > 0$ and $n'' < 0$ for all frequencies.**

Example 1: stability analysis by Nyquist criterion

$$R = -\Gamma + (1-\Gamma^2)\Gamma e^{-2\gamma d}/(1-LG)$$

$$T = (1-\Gamma^2)e^{-\gamma d}/(1-LG)$$

Nyquist criterion analysis

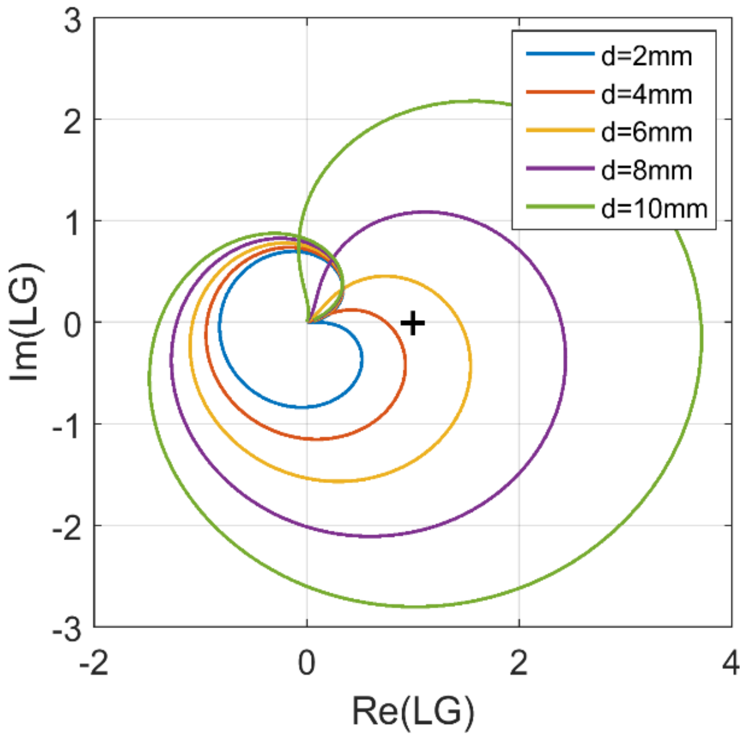

The stable region found by Nyquist criterion is d < 4.785 mm.

Monochromatic analysis

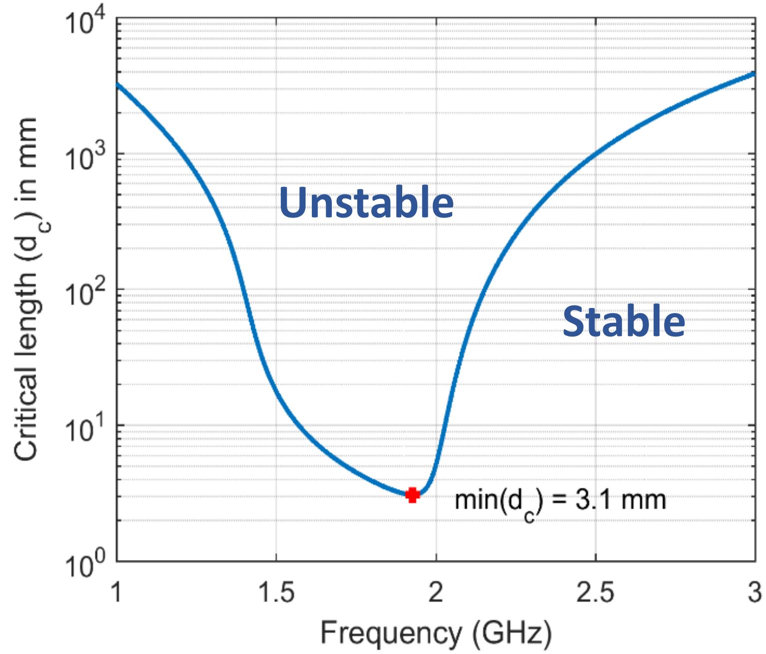

The stable region found by |LG|<1 is d<min(d_c) for η'>0, that is d < 3.1 mm.

Example II: η’<0 gain medium

$$\epsilon(\omega) = 1 + \frac{\alpha_1 \omega_1^2}{\omega_1^2 - (\omega - j\beta_1\omega_1)^2} + \frac{\alpha_2 \omega_2^2}{\omega_2^2 - (\omega - j\beta_2\omega_2)^2}. \quad \mu(\omega) = 1$$

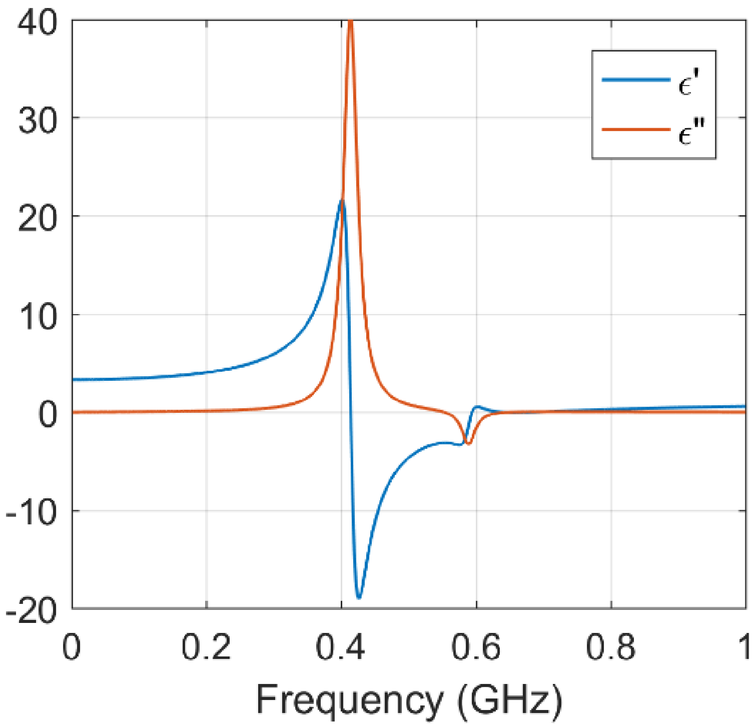

Zero and pole location

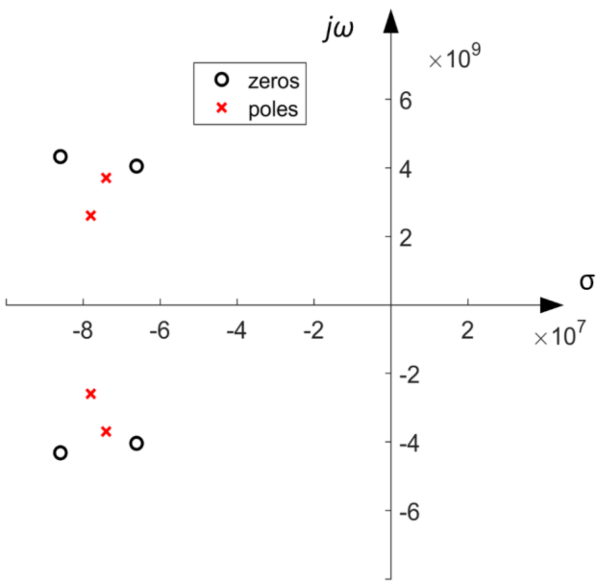

The double-resonant inverted Lorentzian model is a causal medium.

Example II: sign choice by two methods

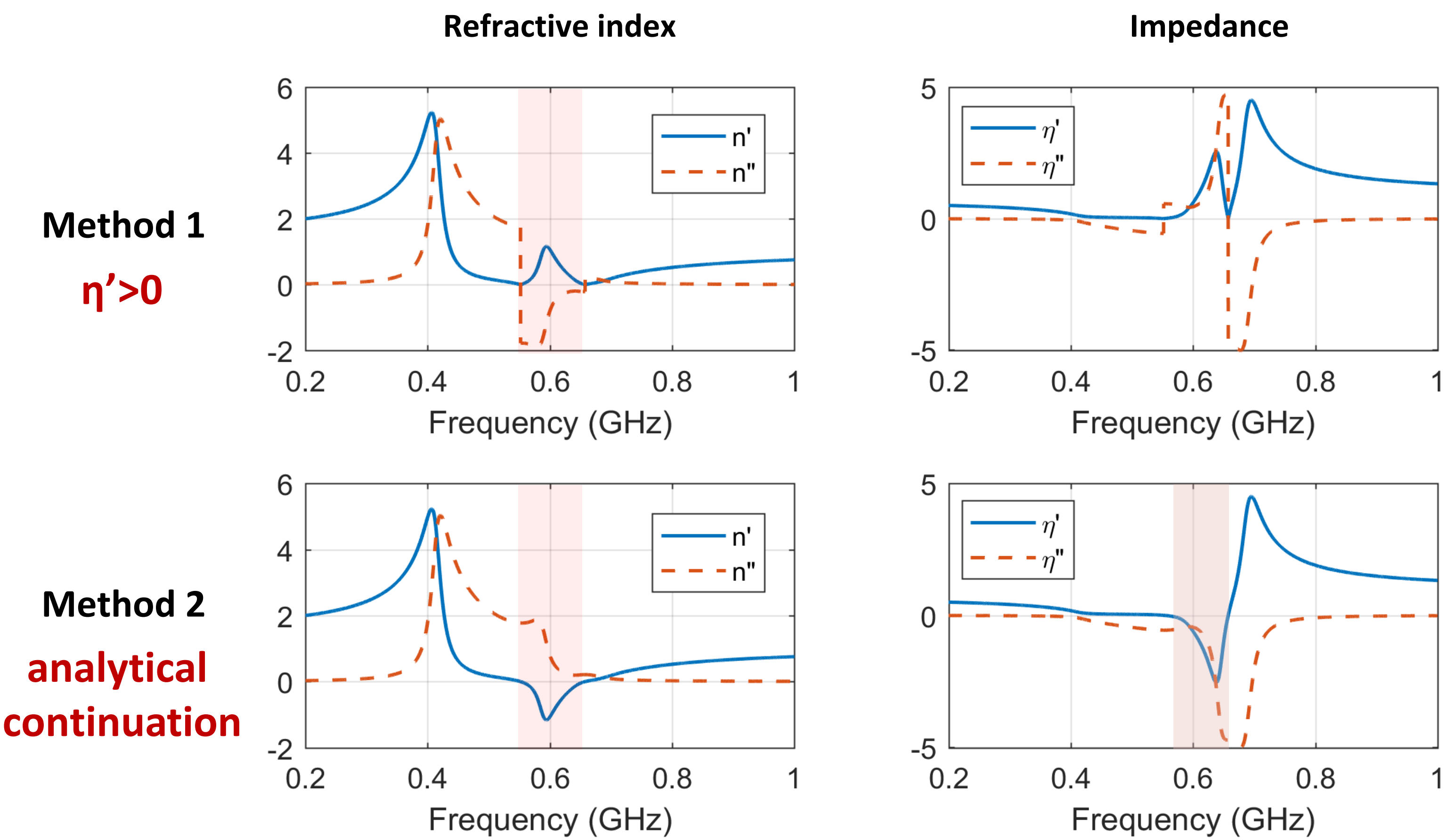

Method 1 and 2 are inconsistent in the frequency region of $\eta' < 0$.

Example II: stability analysis

Nyquist criterion analysis

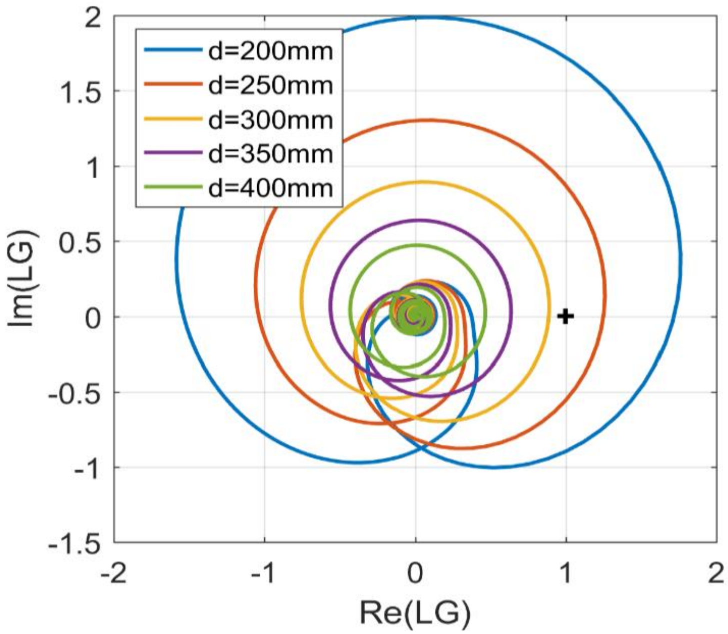

Nyquist criterion shows the stable region is d>283 mm

Monochromatic analysis

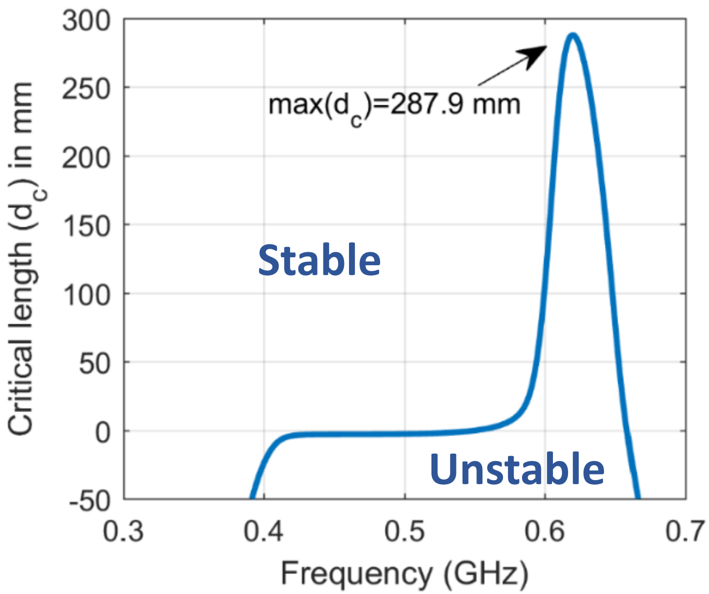

The stable region by |LG|<1 for $\eta' < 0$ is d > max(d_c), that is d>287.9 mm.

Summary

- Test the stability of a gain slab system by two criteria, i.e. a simple criterion $|LG|<1$ and the Nyquist criterion.
- Both criteria show $\eta' > 0$ ($\eta' < 0$) gain medium is stable when the slab thickness is small (large).
- A slight difference on the stability margin due to the $|LG|<1$ criterion is only a sufficient condition.

Outline

1. Active gain metamaterial
2. Non-Foster antenna matching
3. Sign choice of refractive index for active gain medium
4. **Microfluidic device for THz Spectroscopy of live cells**

Terahertz technology for biomedical applications

Terahertz (THz = 10^{12}Hz) technology has been rapidly developed for various biomedical applications:

1. Medical imaging for cancer diagnosis.
2. Body imaging for security checkpoint.
3. THz spectroscopy for cells or biomolecules, e.g, DNAs, RNAs, proteins, etc. (non-invasive and label-free)

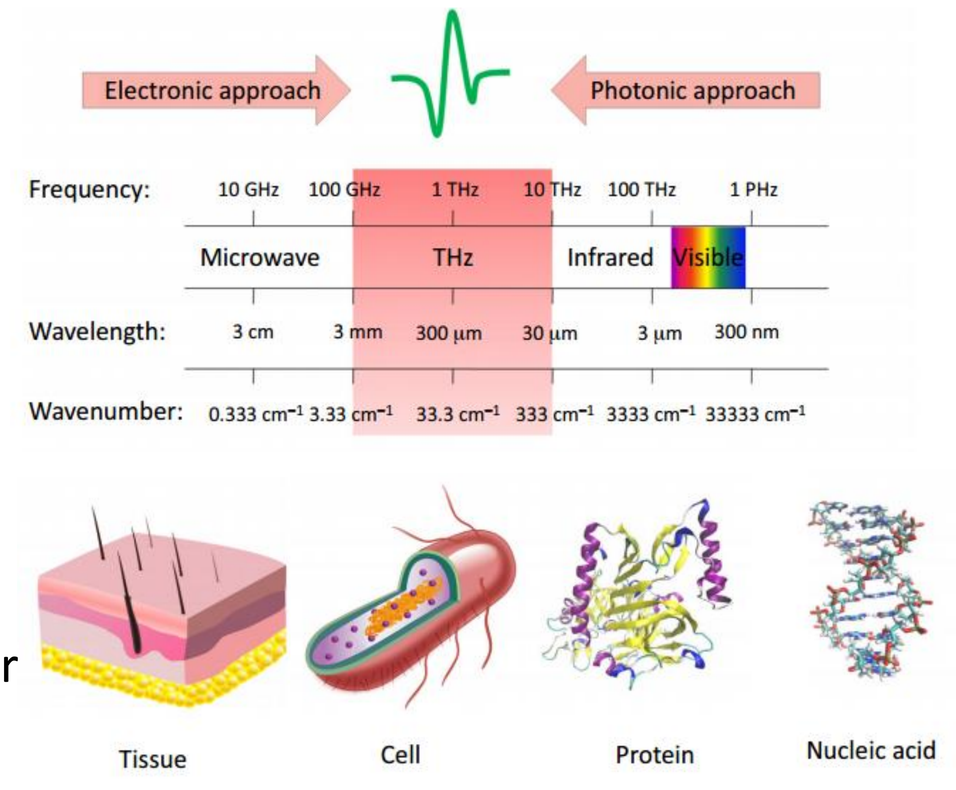

Yang, Xiang, et al. *Trends in biotechnology* (2016).

Motivation

- **Study THz spectral signatures of cells/biomolecules, which can be used for sensing, imaging and understanding the biological functions.**
- **Challenges:**
  - Large water absorption at THz frequencies. The water environment is important for live cells.
  - Dehydrated samples lead to poor reproducibility.
- **Developing convenient, cost effective microfluidic chip to hold the sample and improve the measurement reproducibility and efficiency**
  - Micro-dimensional features to avoid excessive THz absorption by aqueous media
  - Cell concentration or manipulation in chip
  - A steady temperature environment
  - Adequate SNR, bandwidth, and frequency resolution

Fabricated microfluidic device

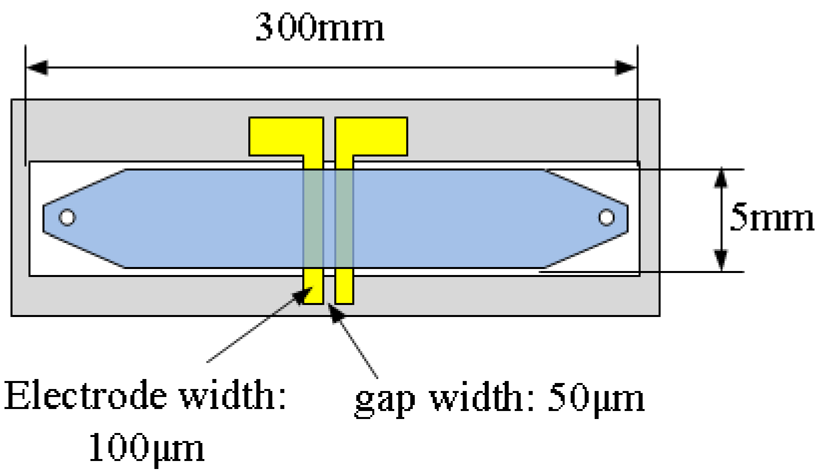

Channel fabrication procedure:

1. Use laser printer cutting acrylic to make a negative mold;
2. Use epoxy to make a reverse mold;
3. Pour PDMS on the mold;
4. Cure PDMS;
5. Peel away the PDMS channel;
6. Bond the PDMS channel to the glass substrate;

Channel Height – 300 μm

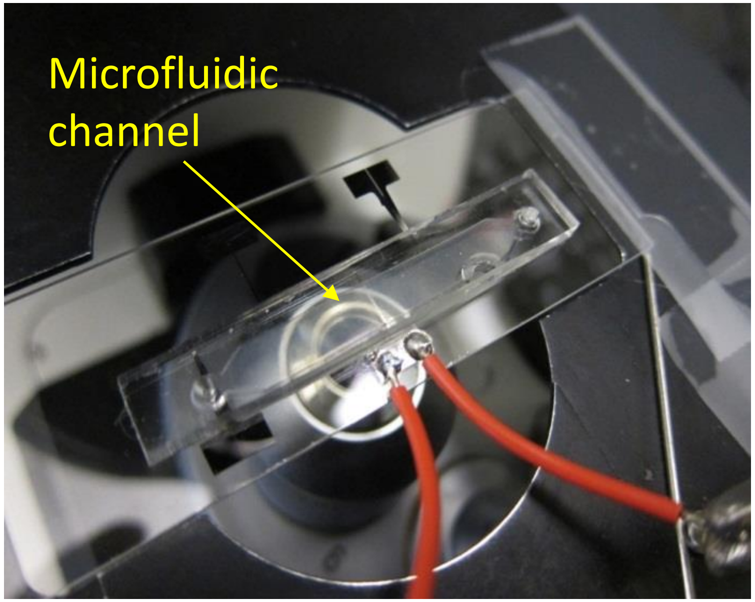

PDMS is relatively lossy but still acceptable, about 0.05 at 0.3 THz.

Cell trapping mechanism

1 MHz, a few volts

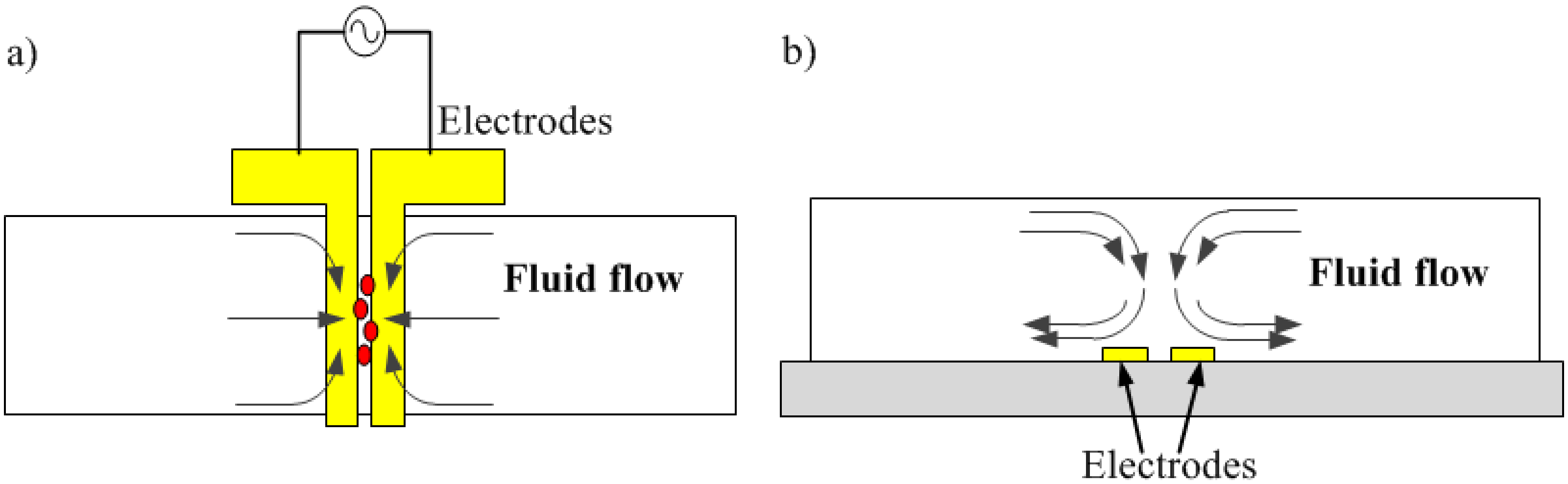

- Appropriate AC frequency and voltage selected
- Cell trapping mechcanism:
  - Electroosmotic forces / heating → cell circulation
  - Dielectrophoresis (DEP) forces → cell concentration

Cell trapping experiment

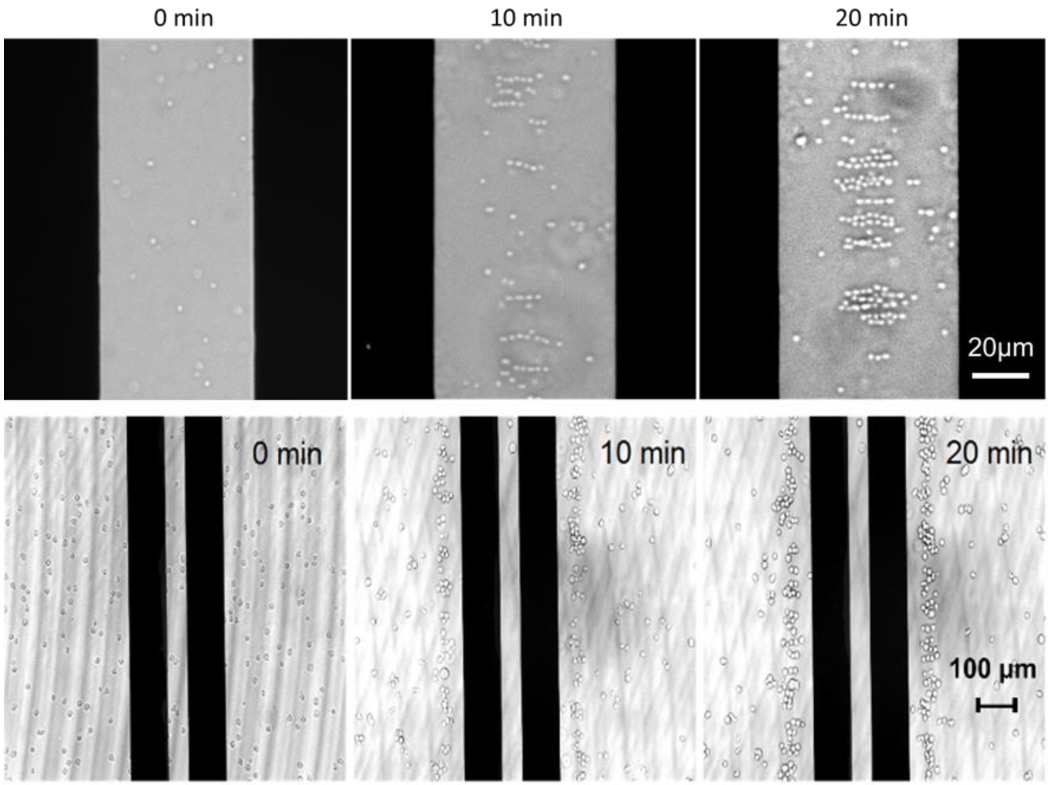

E. coli (~1–2 µm) in Luria Broth medium

Cells higher polarizability than medium
➔ Positive DEP

T-cells (~ 12 µm) in RPMI medium

Cells less polarizability than medium
➔ Negative DEP

- **Positive DEP attracts cells to high field locations.**
- **Negative DEP pushes cells away from the center of electrodes.**

Thermal image of microfluidic chip

Thermal image captured by IR Camera-FLIR 6000
Different bias voltages

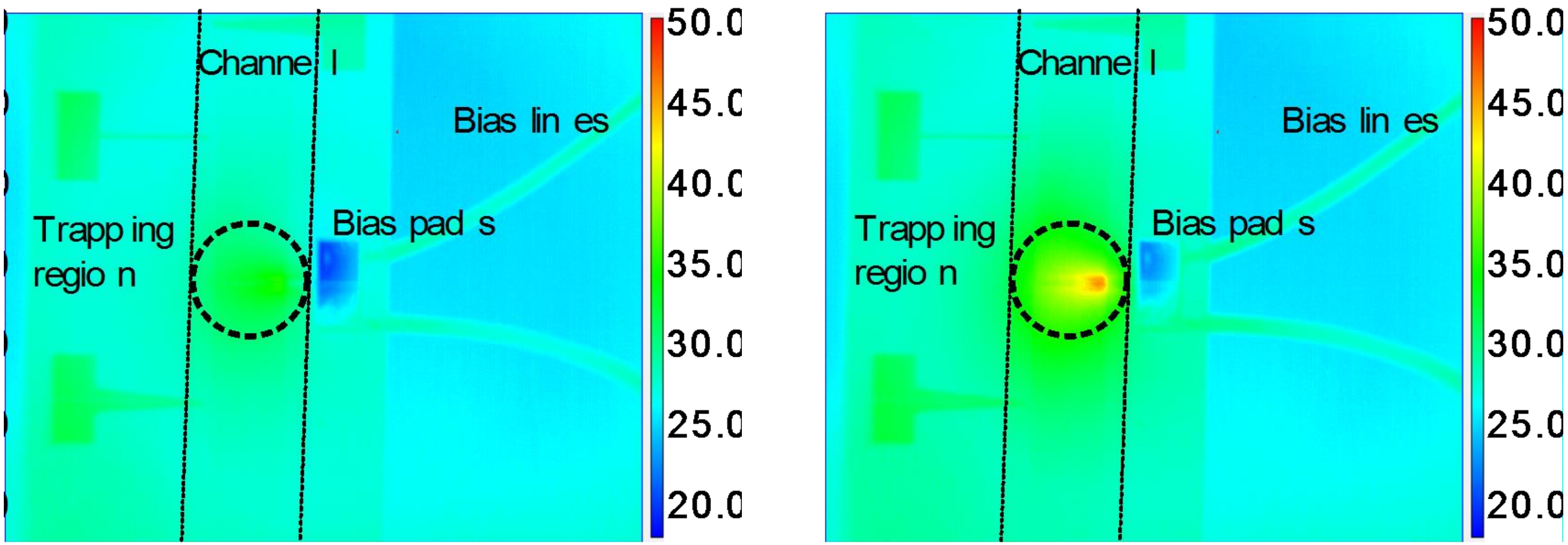

a) 7 V_{pp} at 5 min   b) 10 V_{pp} at 5 min

- **Uniform temperature distribution near 35°C with 7 V bias voltage, which is close to the physiological temperature.**
- **For a 10 V bias case, the temperature at the region of concentration can increase to over 50°C.**

Experimental setup

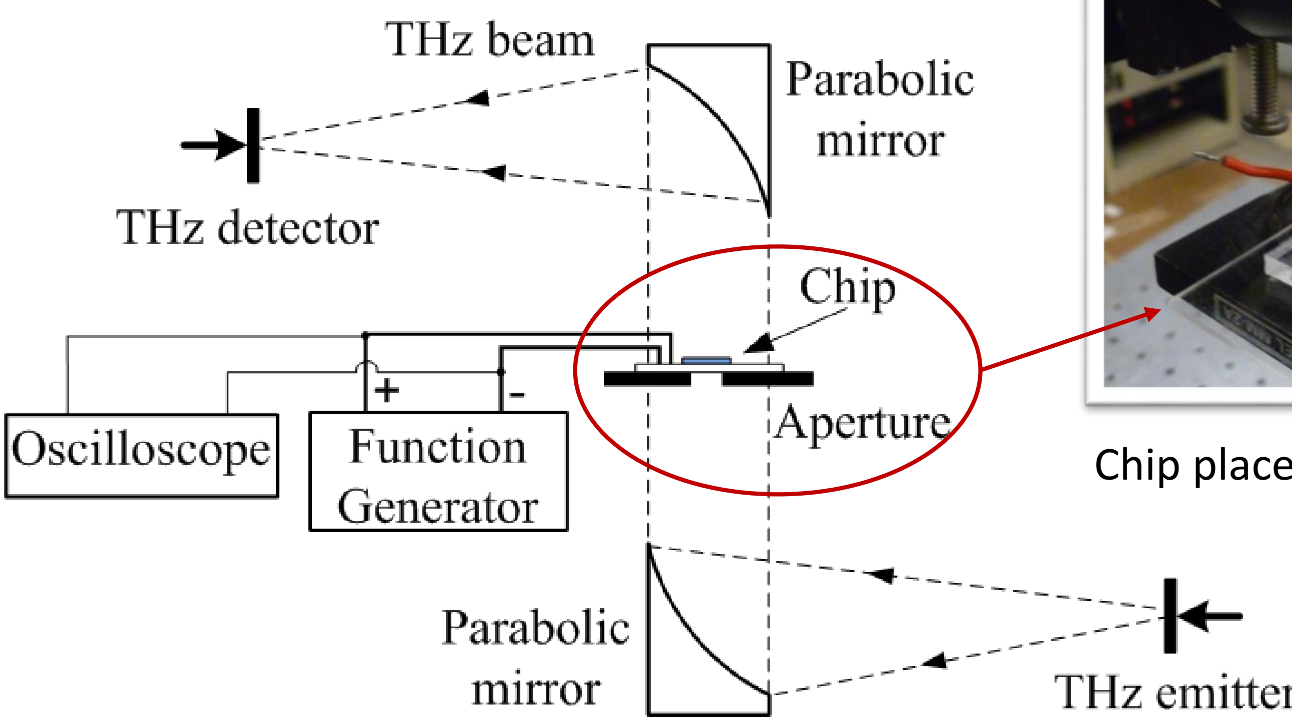

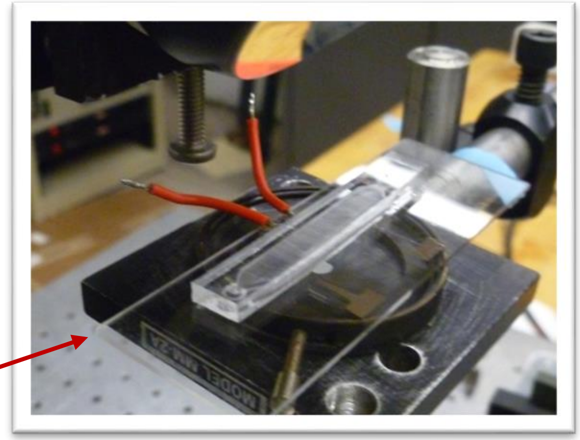

Chip placed on the aperture

The aperture size is 4 mm in diameter, so that THz wave only focuses on the channel.

THz spectroscopy system

THz-TDS system

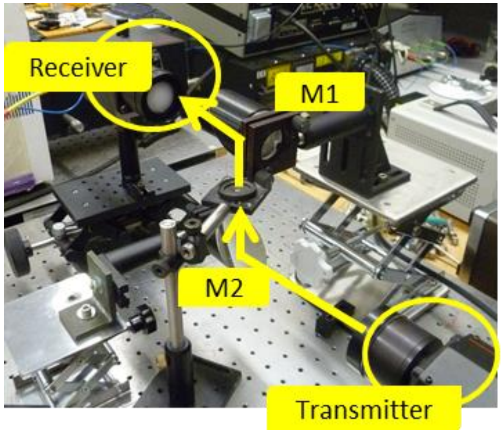

- Model #: T-Ray 2000 by Picometrics
- High temporal resolution (broadband), fast response, and high SNR.
- Limited spectral resolution (usually ~10 GHz)

THz CW system

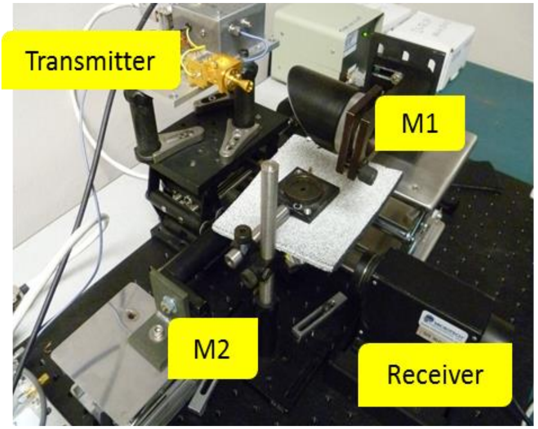

- Model #: VDI-MixAMC-S117
- Spectral resolution: 1 GHz
- Bandwidth: from 0.14 to 0.22 THz
- Output power: 0.5 to 3.5 mW
- Limited bandwidth, time inefficient, only amplitude information.

Test procedure

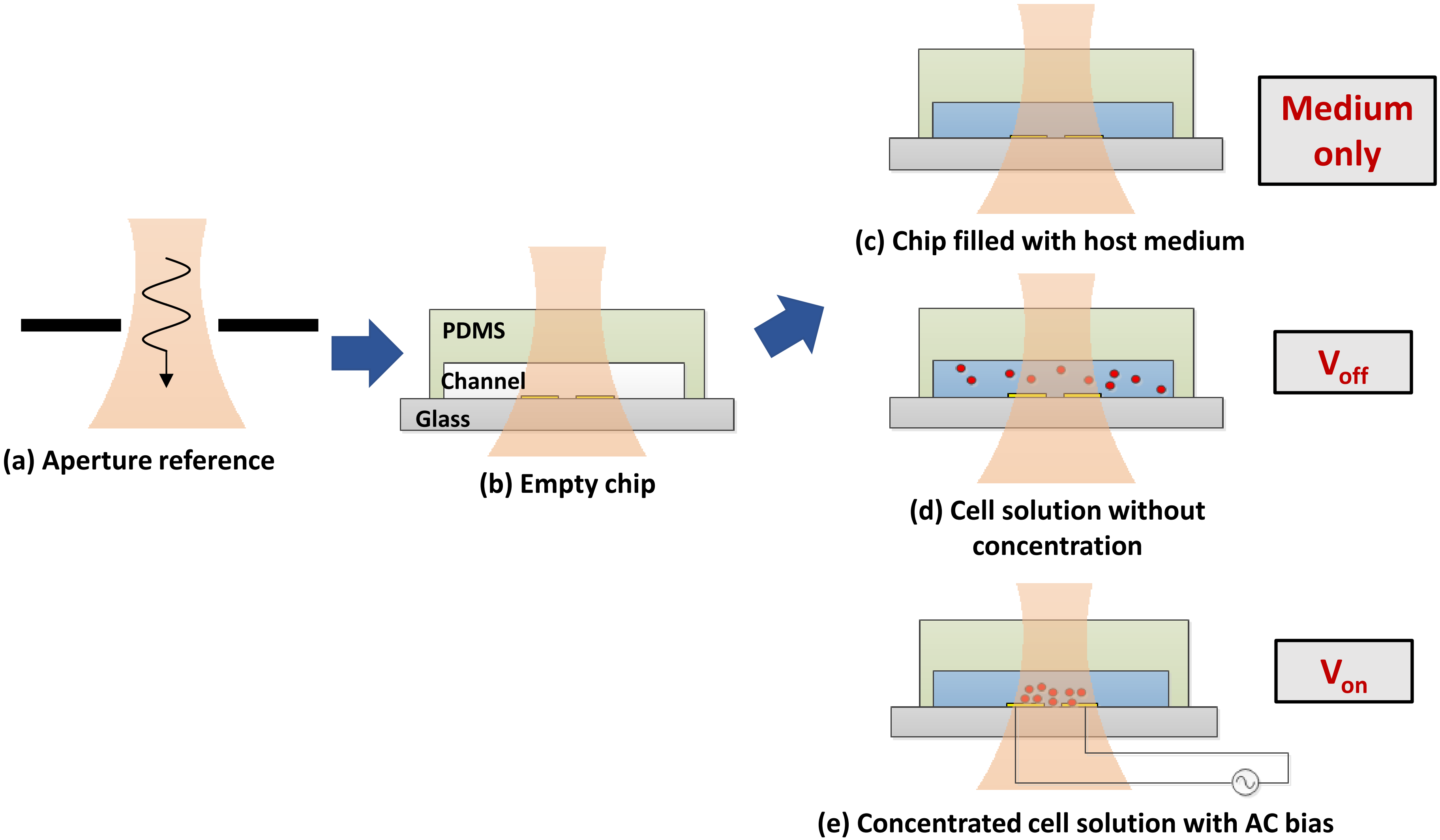

Time-domain signals of E. coli in LB medium by THz-TDS system

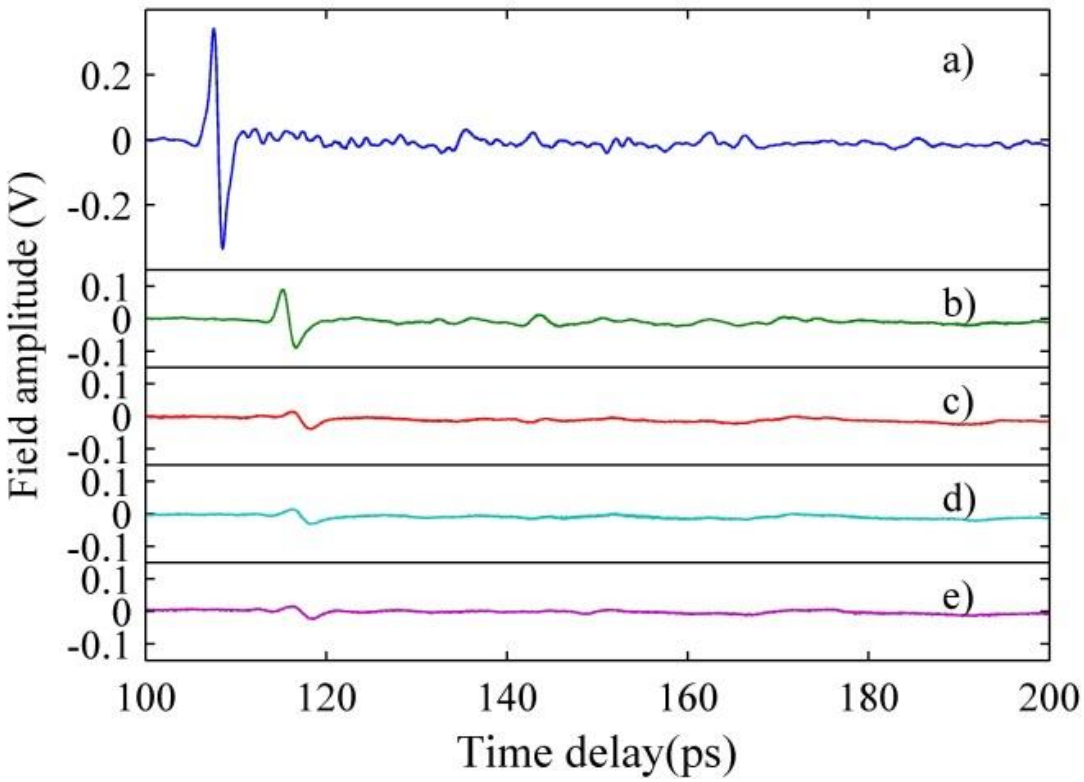

a) Aperture reference
b) Empty chip
c) Chip filled with LB medium
d) Un-concentrated E. coli in LB medium (V_{off})
e) Concentrated E. coli in LB medium (V_{on})

FFT spectra of the THz time-domain signals

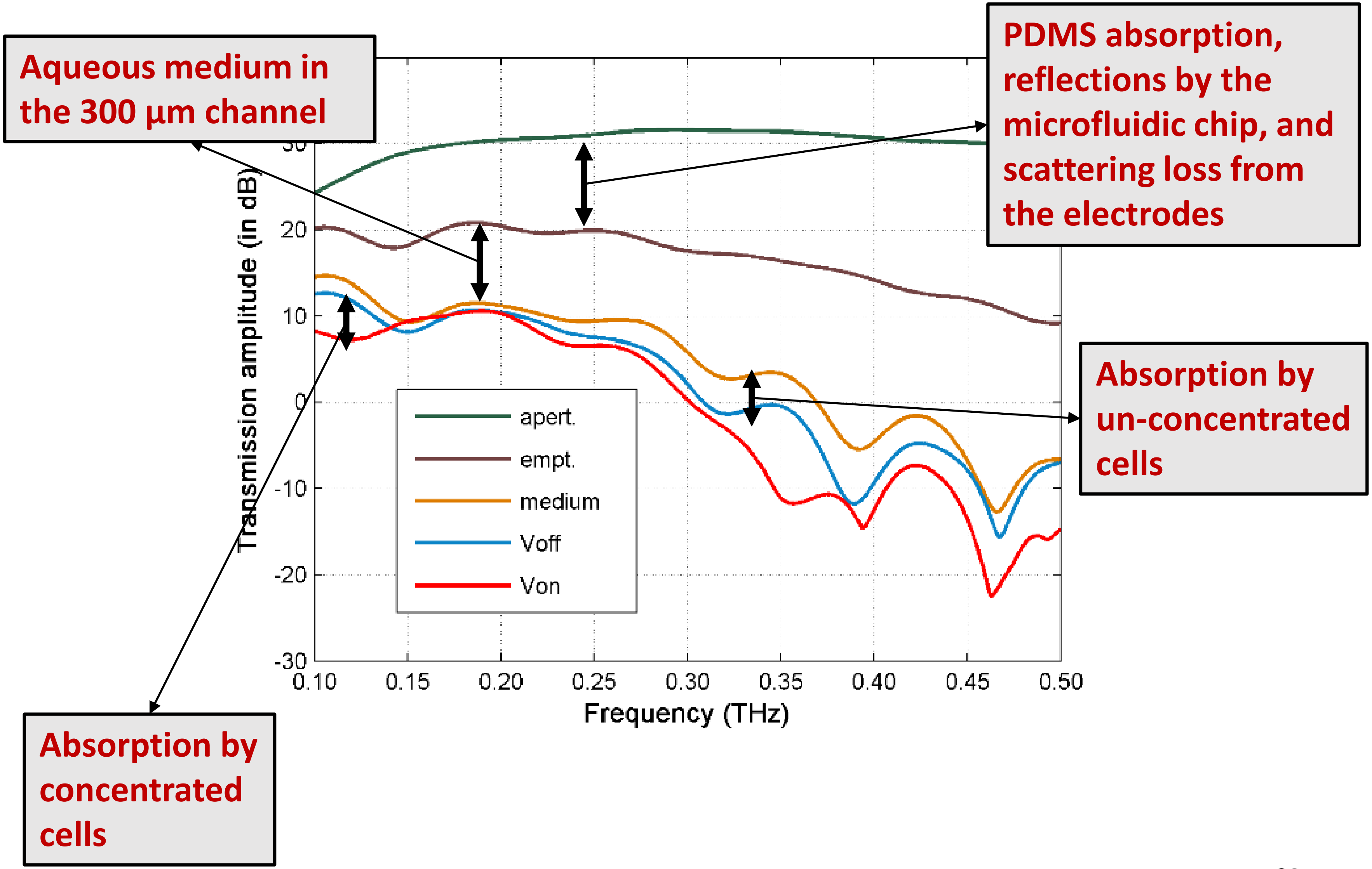

Spectral difference between medium, un-concentrated, and concentrated E. coli samples

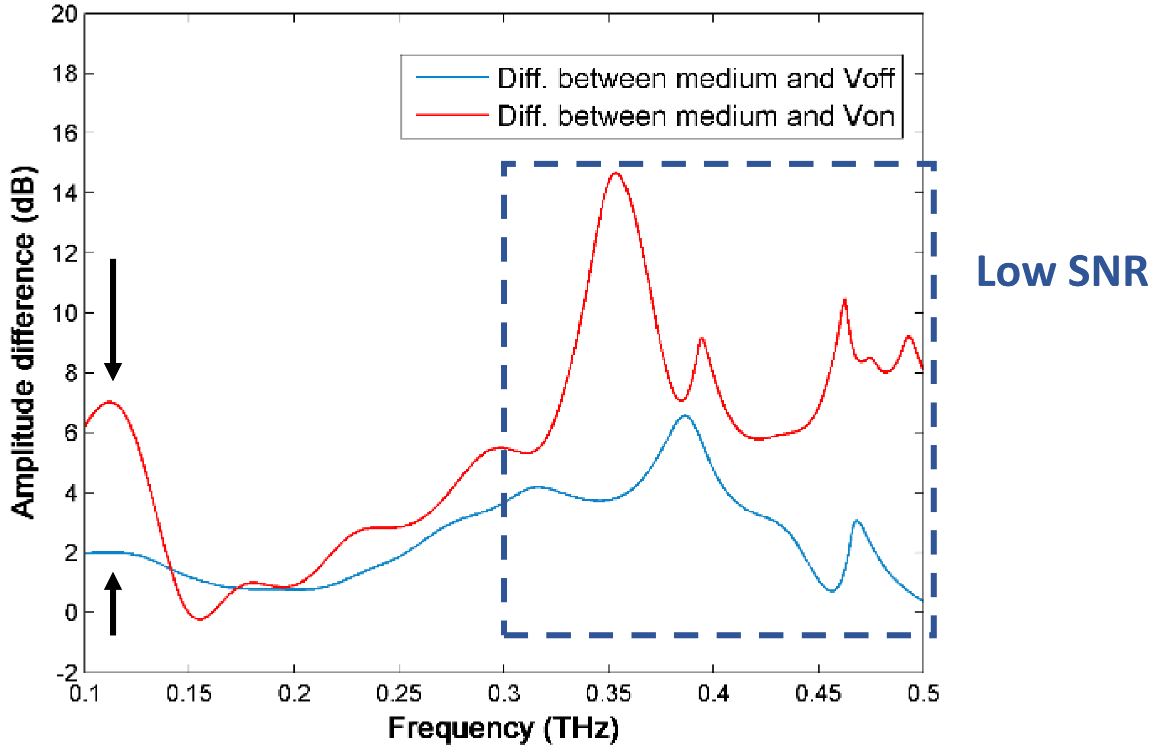

- **Absorption peak near 0.11 THz.**
- **Transmission loss for V_{on} case is mostly higher than that of the V_{off} case, indicating higher THz absorption by the concentrated cells.**

Transmission spectra of T-cells in RPMI medium by THz CW system

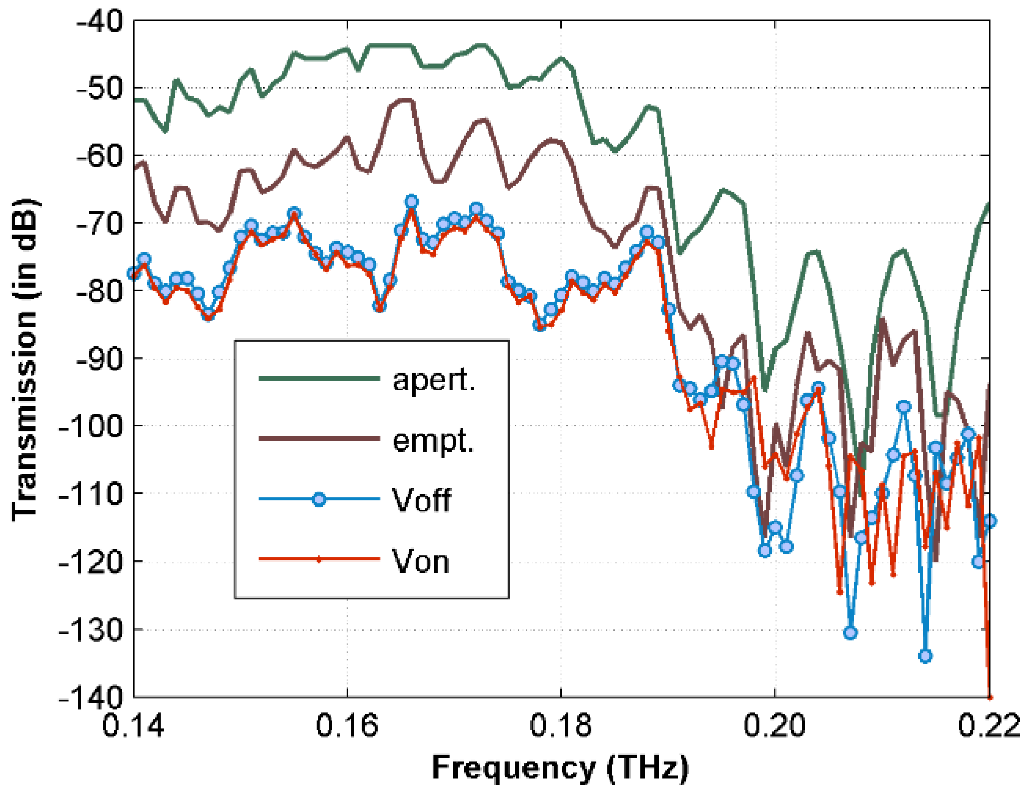

The spectral difference between the un-concentrated and concentrated T-cell samples is much smaller

Spectral difference between the un-concentrated and concentrated T-cell samples

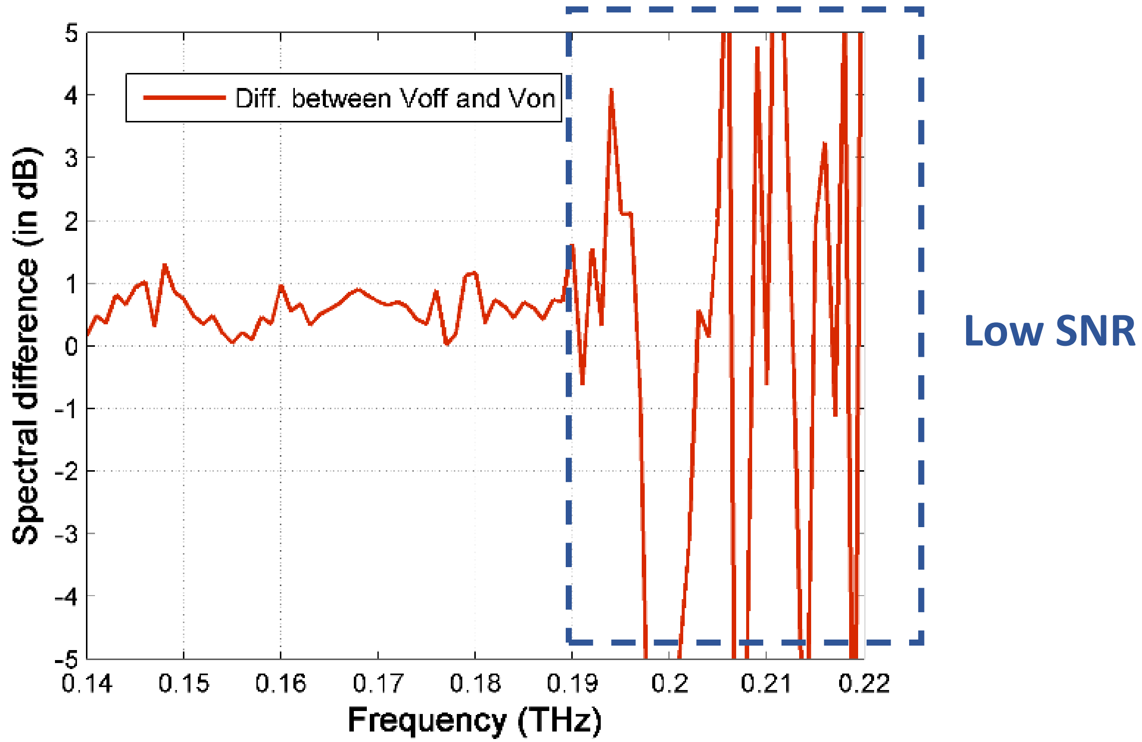

- Cell density of the T-cell sample is much smaller than that of the E. coli sample.
- Trapping position for T-cells is at the outer edges of the electrodes.
- Intrinsic THz properties of T-cells are close to the RPMI medium, further investigation is necessary to be conclusive.

Summary

- An initial proof-of-concept for cell concentration, steady temperature control and THz spectral measurement of live cells.
- Our experimental results on empty channels, channels filled with media only, channels filled with un-concentrated and concentrated cell solutions show different THz transmission responses.
- In general, concentrated cell samples are more absorptive than un-concentrated samples.
- An absorption peak is observed near 0.11 THz for both un-concentrated and concentrated E. coli samples.
- No absorption signatures are observed for T-cell case.

Future works

- **Active gain MTMs**
  - **THz / optical gain MTMs**: scale down the size and build up active gain MTMs at THz or optical frequencies, which have more severe material losses than microwave frequencies.
  - **Potential applications**: active antennas, nanoscale or cavity-free lasers, active imaging, etc.
  - **Nonlinear active MTMs**:
    - Nonlinear effect enhancement, bistability, tuning and switching, nonlinear chirality, frequency conversion and parametric amplification, phase matching and phase conjugation, etc.
- **Non-Foster matching circuit**
  - **Synthesize method, definite design rules.**
  - **In practical communication application**:
    - TX: power capacity and the power efficiency
    - RX: noise figure needs to be optimized.

Future works (cont'd)

- **Microfluidic device for THz cell spectroscopy**
  - Optimize the chip, e.g., by reducing the substrate thickness or utilizing low refraction index material for the substrate.
  - Optimize THz system, to further improve the SNR and to extend the spectral measurement to higher frequencies.

Acknowledgement

I wish to express my gratitude to my advisor, Prof. Hao Xin, for his tutoring and guidance. My gratitude to my committee members, Prof. Steven Dvorak, and Prof. Siyang Cao. Thank my present and past group members and colleagues that I had pleasure to work with Adnan Kantemur, Ahmed Abdelrahman, Alex Wu, Dexin Ye, Kihun Chang, Tao Jiang, Mingguang Tuo, Min Liang, Xiaoju Yu, Xiong Wang, Te-Chuan Chen, Ian Zimmerman, Kokou Gbele, Jitao Zhang, Yi Lu, Tingting Liu, Gitansh Gulati, Yashika Sharma, and others. Last but not the least, I wish to avail myself this opportunity to express my gratitude and love to my friends, my beloved parents and my fiancé, Angela, for their support and help.

Active MTM Appendix

Loss in passive MTMs

The extracted μ in Smith's SRR

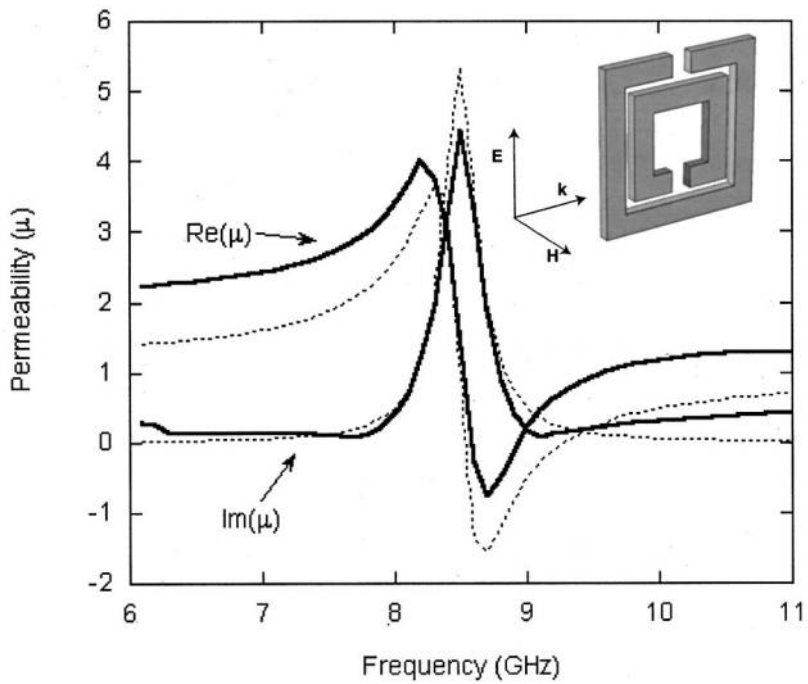

D. R. Smith and S. Schultz, *Phys. Rev. B*, 65, 19, Apr. 2002.

- Material loss or the radiation loss.
- A typical low loss optical NIM reported in experiment has a figure of merit (FOM) of 3.5, where FOM = $|\mathrm{Re}(n)/\mathrm{Im}(n)|$.
- A theoretical reported FOM for optical MTM is of the order of ~25, and maximally ~200 thus far.

Dispersion in passive MTMs

For a passive medium with negligible loss,

Stored field energy: $$u = \frac{1}{2}\left[\frac{d(\omega\epsilon')}{d\omega}|\boldsymbol{E}|^2 + \frac{d(\omega\mu')}{d\omega}|\boldsymbol{H}|^2\right] > 0$$

Larger than in vacuum: $$\frac{d(\omega\epsilon')}{d\omega} > \epsilon_0, \qquad \frac{d(\omega\mu')}{d\omega} > \mu_0.$$

$$\epsilon' + \omega\frac{d\epsilon'}{d\omega} > \epsilon_0, \qquad \mu' + \omega\frac{d\mu'}{d\omega} > \mu_0.$$

Negative Index Medium (NIM) (ε'<0 and μ'<0) with negligible loss has to be dispersive.

Bandwidth limit for passive NIMs

$$\max_{\omega \in B} |\epsilon(\omega) - \epsilon_m| \geq \frac{B}{1+B/2}(\epsilon_\infty - \epsilon_m)\begin{cases} 1/2\,, & \textit{lossy case}, \\ 1, & \textit{lossless case}, \end{cases}$$

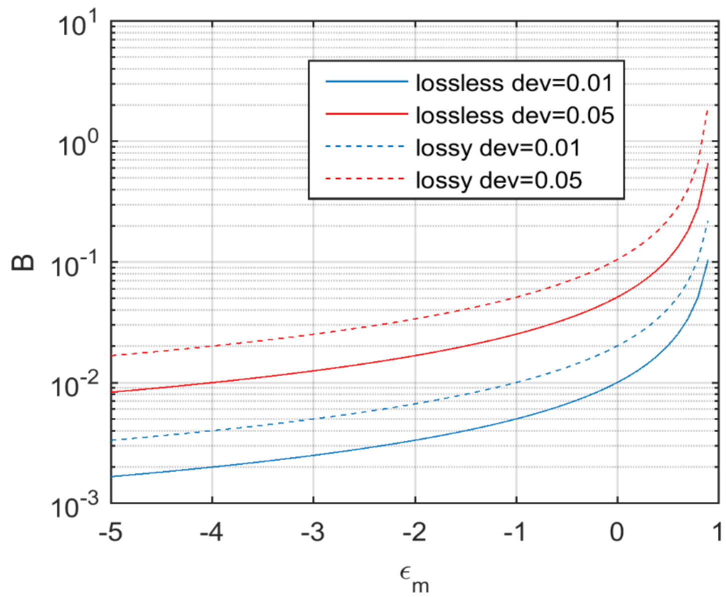

For ε = - 1 with $\pm 1\%$ deviation, the maximum achievable bandwidth is 0.5% for lossless medium.

Active Transmission Line (TL)

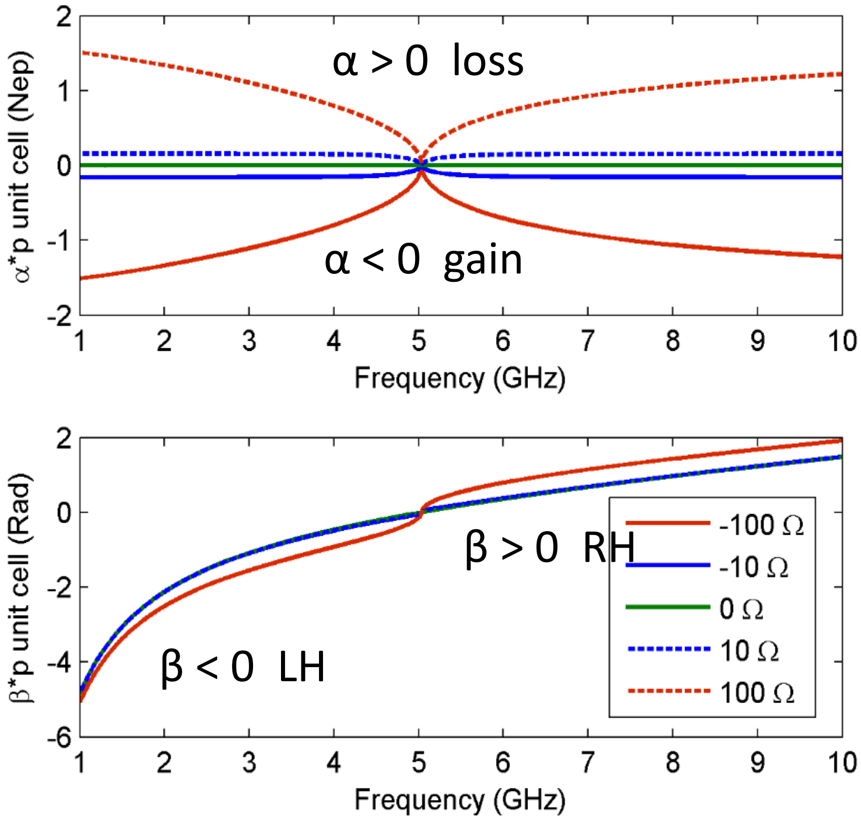

Calculated attenuation constant α<0 and phase constant β<0 simultaneously by incorporating an ideal –R into the unit cell

Non-Foster element for Broadband ε-near-zero MTM

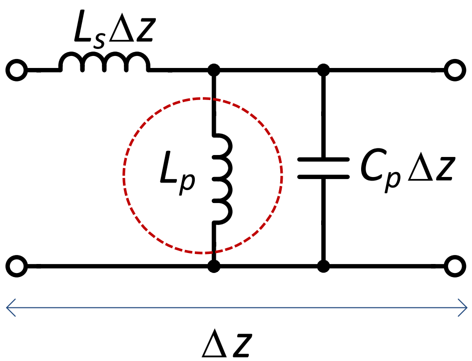

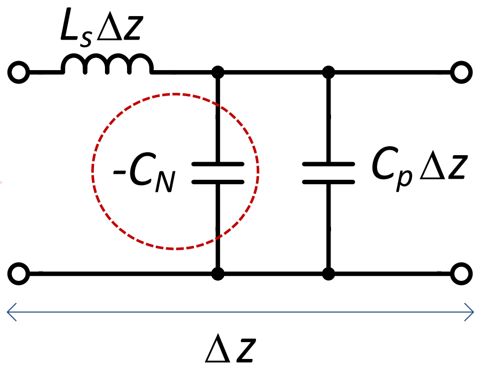

$$\varepsilon_r(\omega) = \frac{1}{\varepsilon_0}(C_p - \frac{1}{\omega^2 L_p \Delta z})$$

$$\varepsilon_r(\omega) = \frac{1}{\varepsilon_0}(C_p - \frac{C_N}{\Delta z})$$

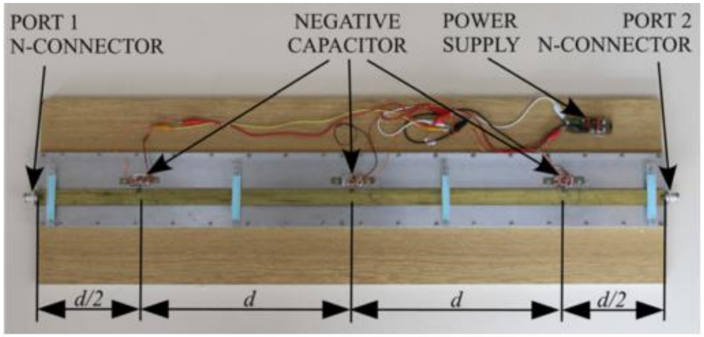

ε ~0.3, 2 – 40 MHz

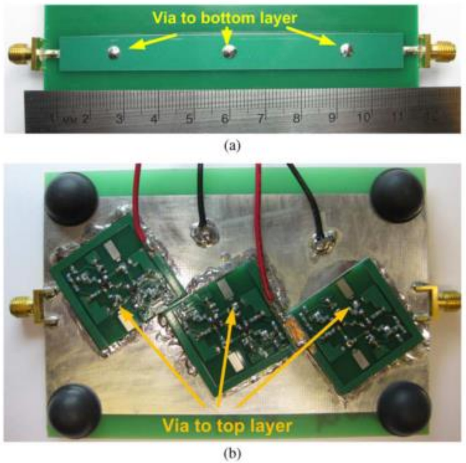

20 – 90 MHz

S. Hrabar, *et. al.*, *Appl. Phys. Lett.*, 99, 2011.

J. Long, *et. al.*, *IEEE MTT trans.*, 62, 2014.

Non-Foster Appendix

Negative-resistor based non-Foster element

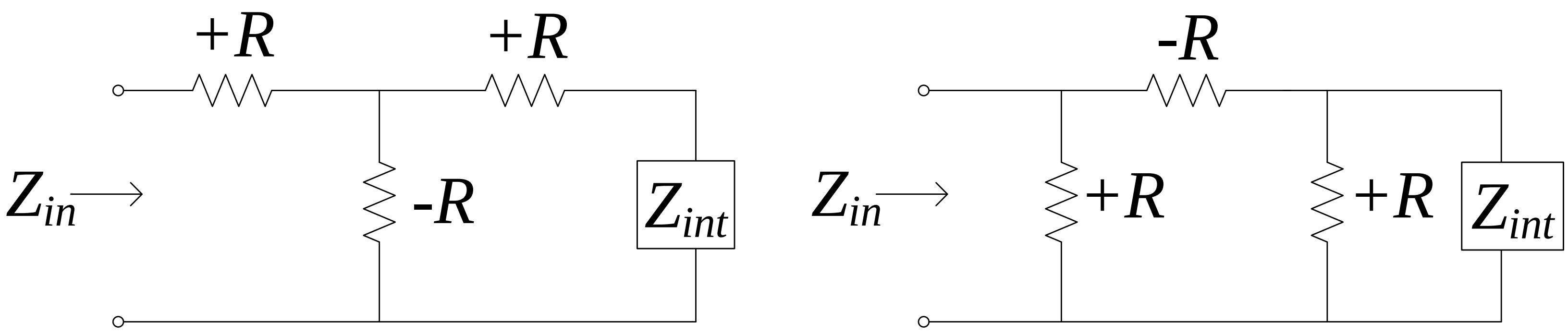

- **Ideally,** $Z_{in} = -\dfrac{R^2}{Z_{int}}$ **, e.g.** $Z_{int} = 1/j\,\omega C$ ➔ $Z_{\text{int}} = -\mathrm{j}\omega(R^2 C)$

- **Practically, the resistors cannot be exactly the same,**

$$Z_{in} \approx -\frac{R^2}{Z_{int} + \delta R}$$

Non-ideal negative capacitor and inductor

Let $\frac{\delta R}{R} = \pm 1\%$, the input impedance of NII goes to

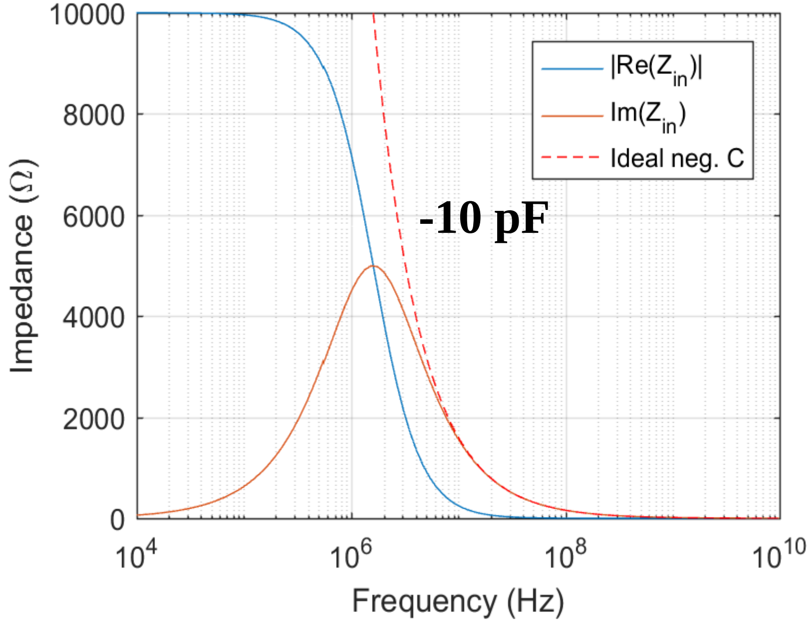

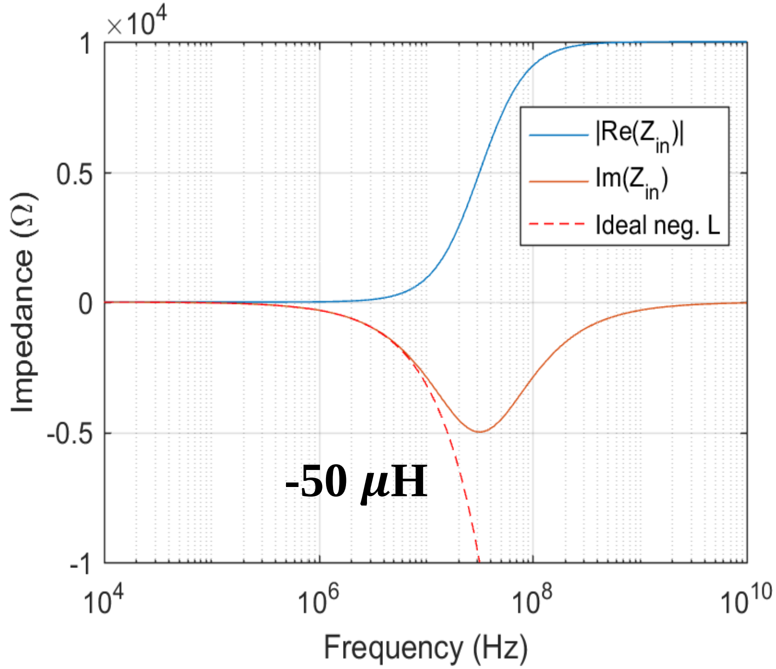

- **Negative capacitor works at high frequency (above 2 MHz)**
- **Negative inductor works at low frequency (below 20 MHz)**
- **Parasitic resistance exists.**
- **non-Foster element achieved by negative R based NII is always bandwidth-limited due to the deviation of circuit parameters**

Transistor-based non-Foster element

Linvill’s negative impedance converter (1953)

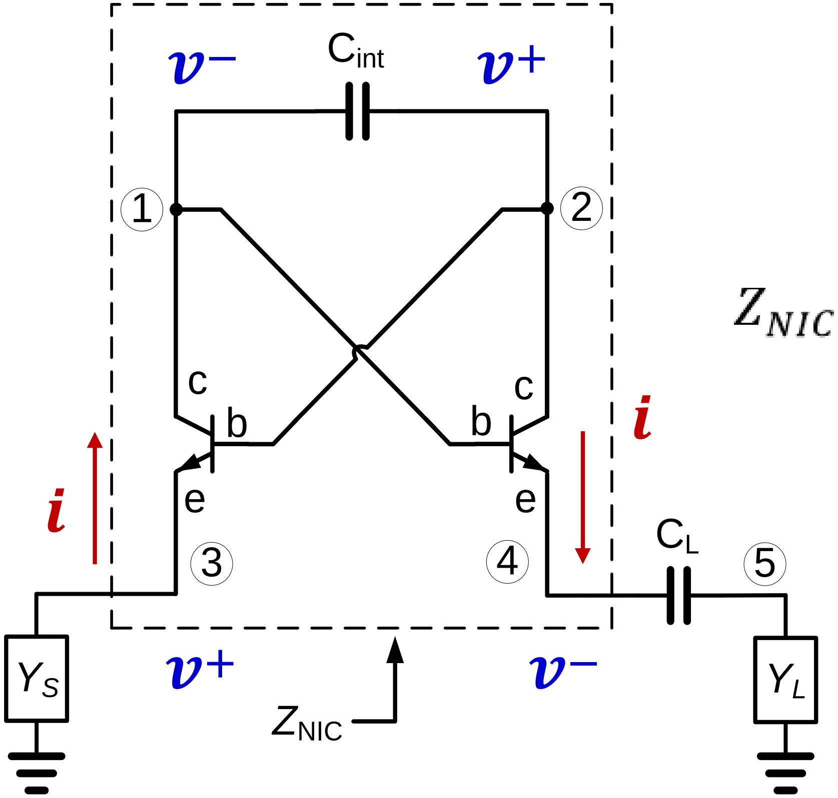

$$Z_{NIC} = \frac{1}{-j\omega(C_{int} + 2C_{bc})} + \frac{2}{g_m}$$

J. G. Linvill, *Proc. IRE*, 41, 6, 725–729, 1953.

Simulated input impedance of NIC

ADS simulation with real BJT model and biasing networks

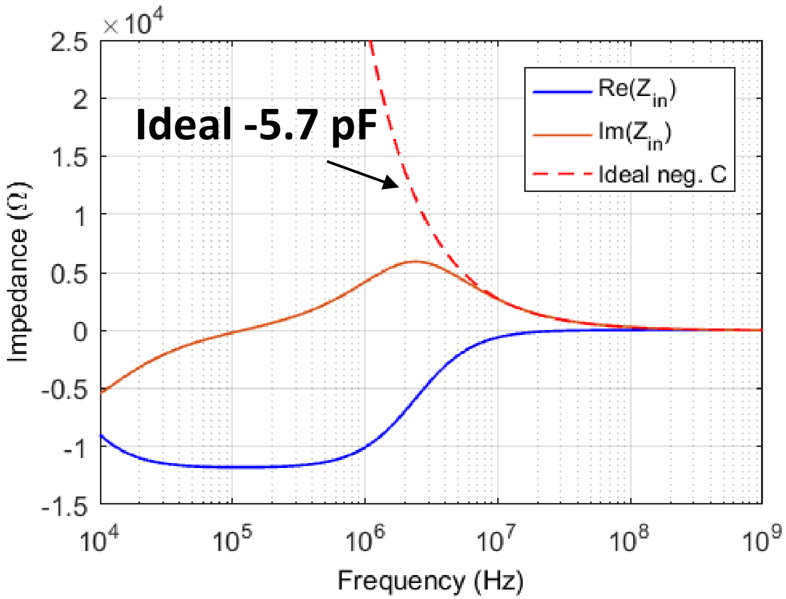

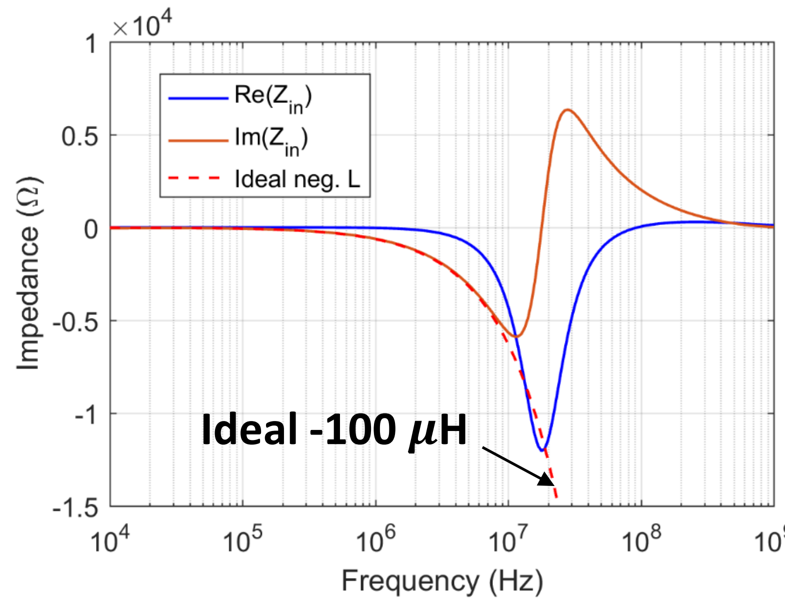

- **Similar to the analysis result of negative resistor NII, the real non-Foster element is always bandwidth limited and with parasitic resistance.**
- **No stability considered yet.**

Measured S-parameters and extraction

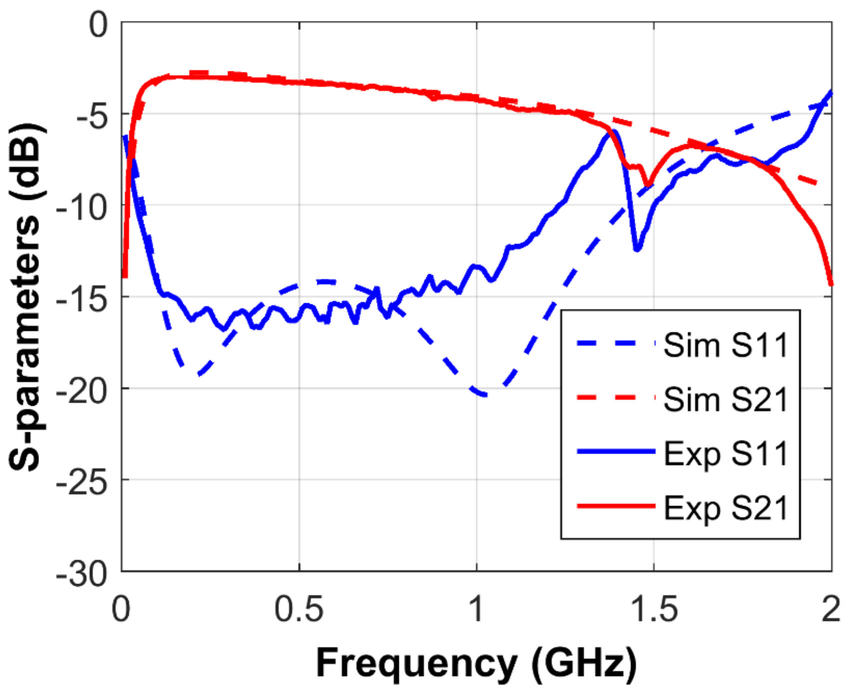

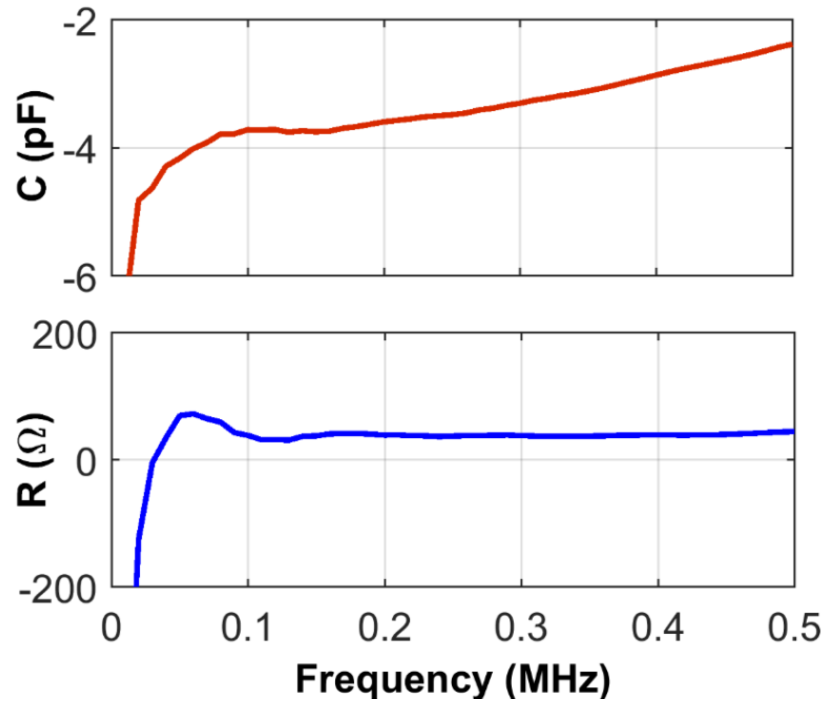

- A good consistency between calculation and measurement
- A -4 pF capacitor achieved at VHF band (30 – 300 MHz)
- Parasitic resistance ~ 30 Ω

The effect of realistic load impedance

Equivalent circuit model & HFSS simulation

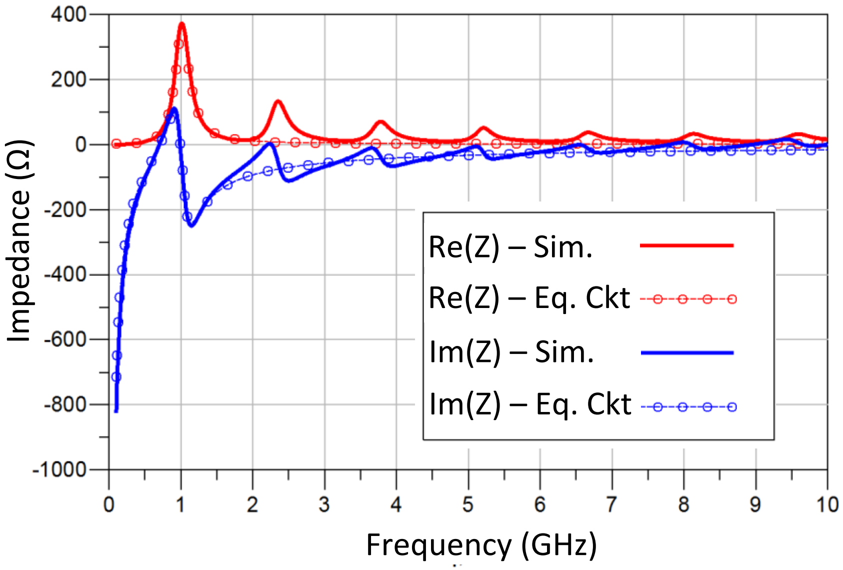

Nyquist plot of NDF of the non-Foster matching network with antenna load impedance

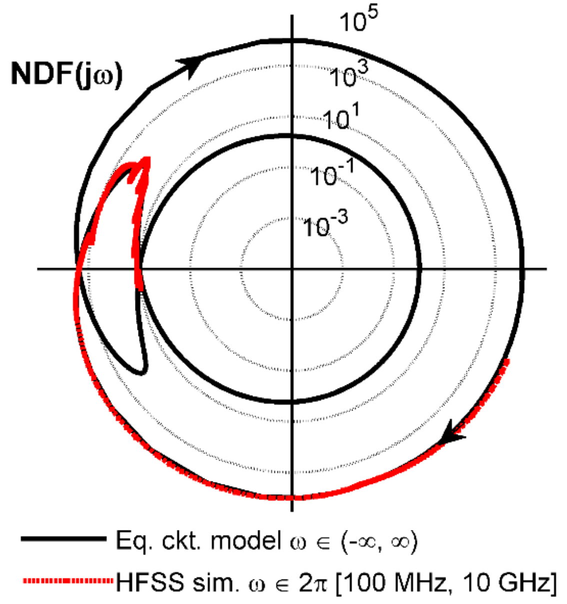

- **Extract an equivalent circuit model of antenna impedance**
- **Nyquist plot of NDF shows the non-Foster antenna matching system can be stable.**

Connect to a 10 cm monopole antenna

Input S11

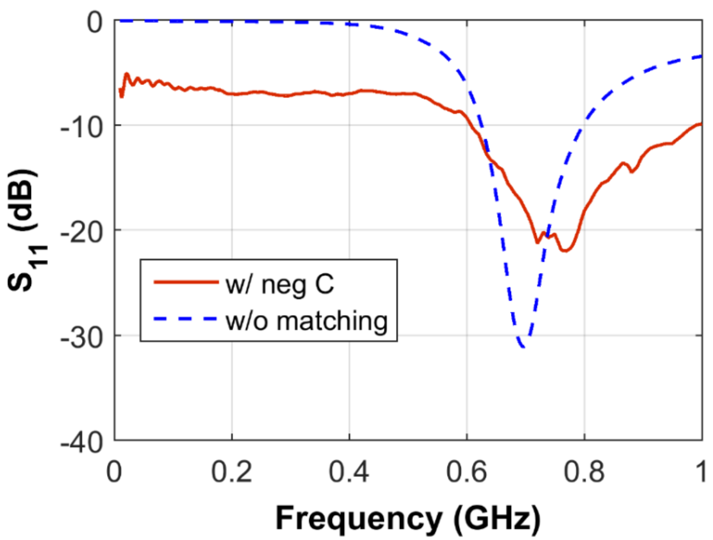

Reactance cancellation

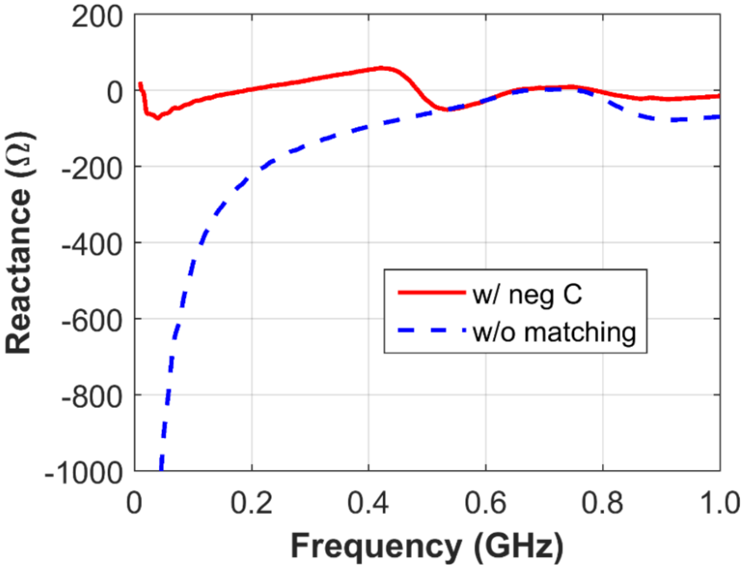

- **The helical antenna has the lowest self-resonant frequency at 24 MHz.**
- **From simulation, we estimate that the overall radiated power increases about 5 – 12 dB from 30 to 300 MHz by the non-Foster matching circuit compared to the without matching case.**

The effect of realistic load impedance

Equivalent circuit model & HFSS simulation

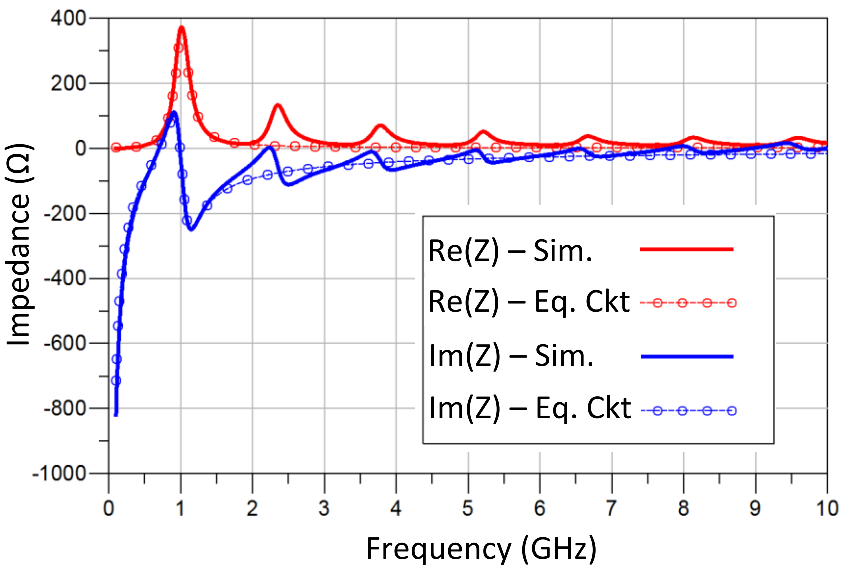

Nyquist plot of NDF of the non-Foster matching network with antenna load impedance

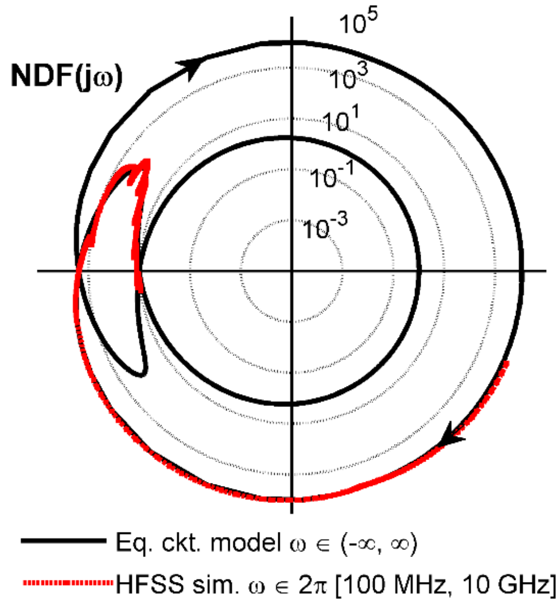

- **Extract an equivalent circuit model of antenna impedance**
- **Nyquist plot of NDF shows the non-Foster antenna matching system can be stable.**

The effect of antenna load impedance

Nyquist plot of NDF w/ and w/o R_{stb}

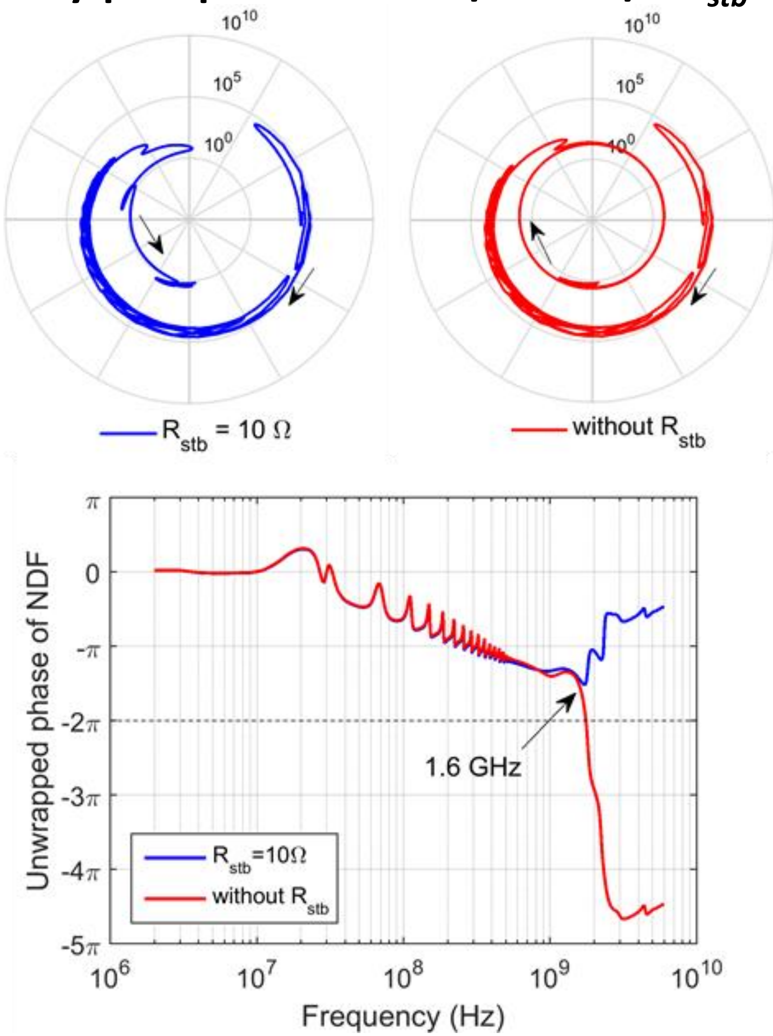

Circuit schematic

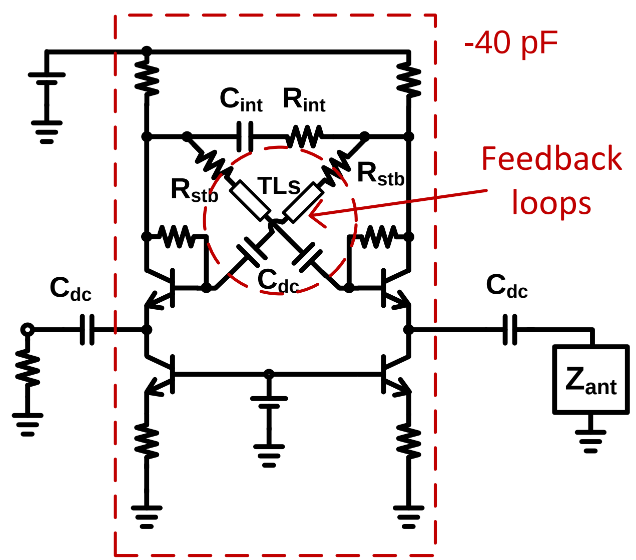

- The same circuit layout is applied.
- The non-Foster antenna system is stable with R_{stb} = 10 Ω, but unstable without R_{stb}.

Sign choice Appendix

Stable region of the system

Loop gain magnitude and phase for $d = 4$ mm

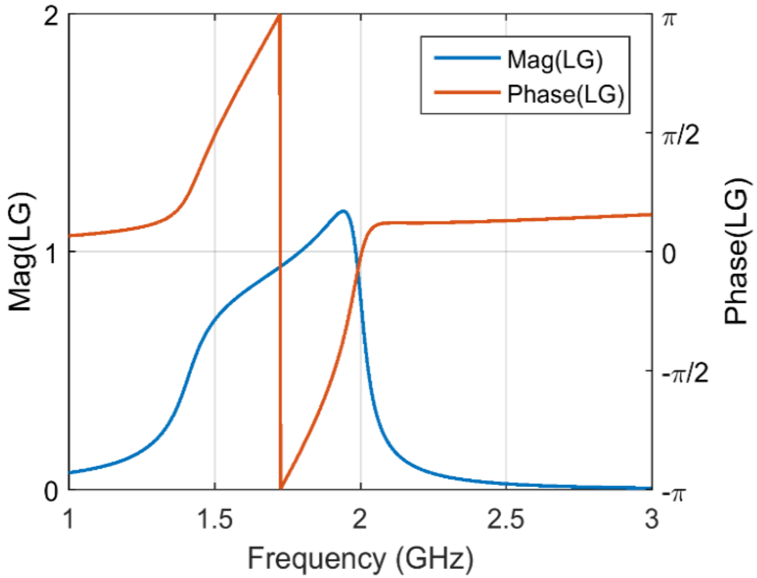

Calculate d_c for all frequencies

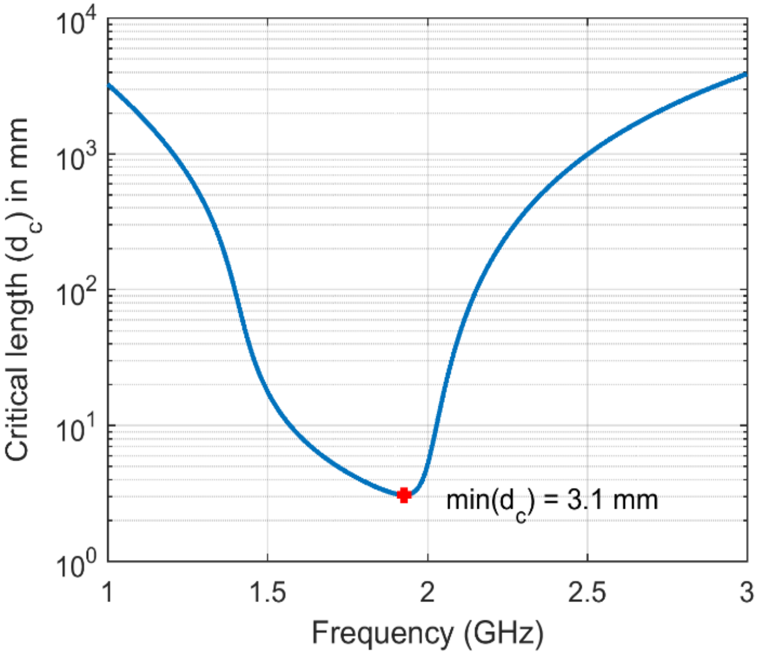

The stable region found by |LG|<1 is d<min(d_c), that is d < 3.1 mm, which is a little smaller than the stable region found by Nyquist criterion (d< 4.785 mm).

$\eta' < 0$ medium doesn't violate causality

P.A. Sturrock 1958, Kinematics of Growing Waves.

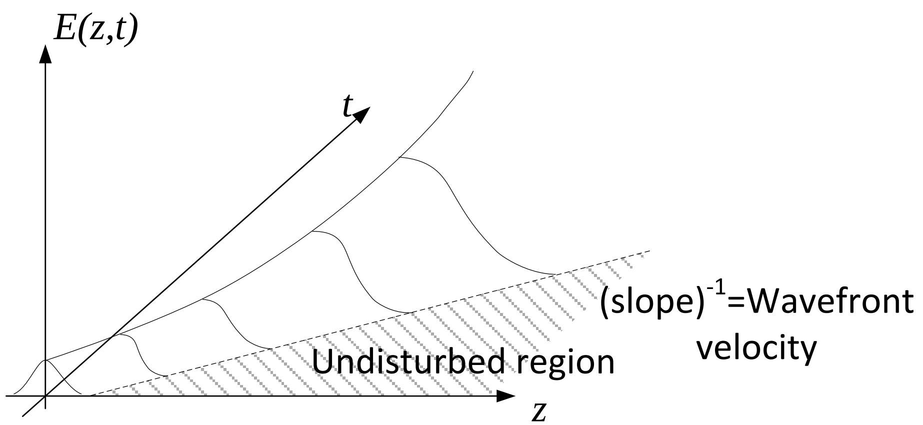

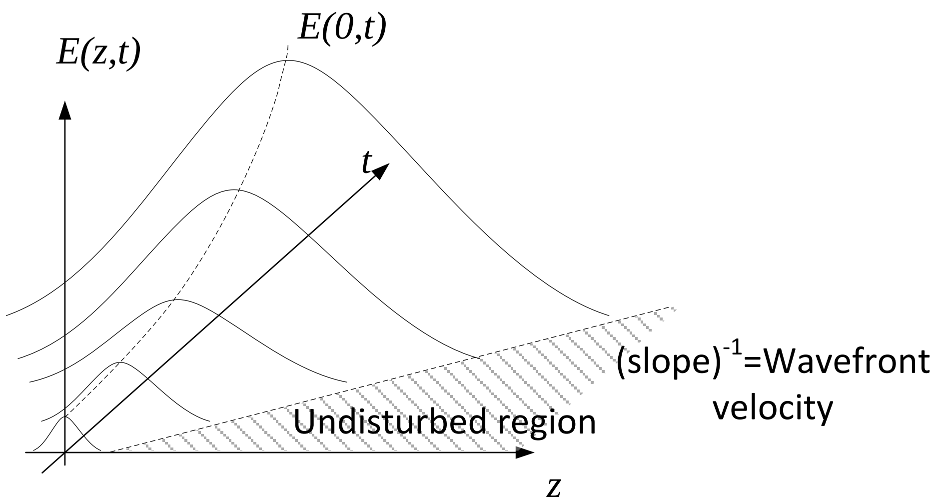

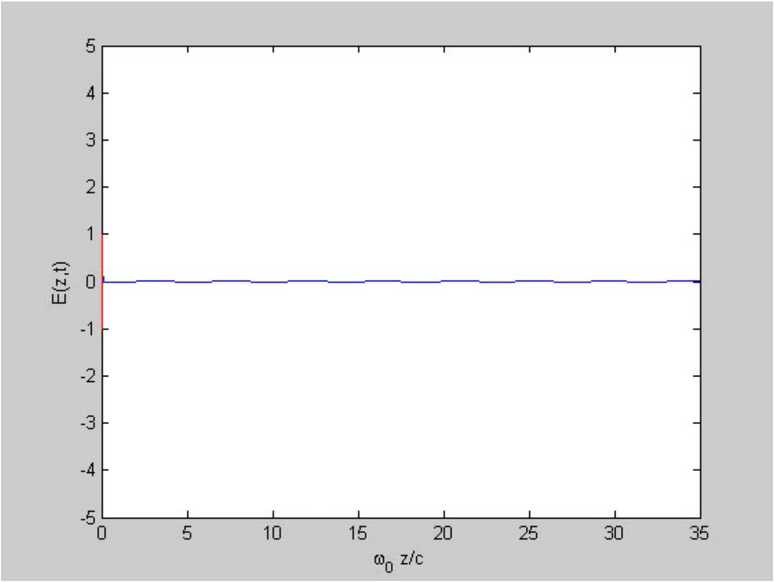

Different sign choice methods

Method 1: η'>0 always holds, so n">0 for lossy medium and n"<0 for gain medium.

$$n = +\sqrt{\epsilon\mu} \cdot \mathrm{sign}[-\mathrm{Im}(\sqrt{\epsilon\mu})] \cdot \mathrm{sign}(\epsilon''/|\epsilon| + \mu''/|\mu|)$$

Method 2: n is an analytical function, therefore the sign choice is selected based on analytical continuation.

$$n(\omega) = +\sqrt{|\epsilon(\omega)||\mu(\omega)|}e^{j\frac{(\phi_\epsilon+\phi_\mu)}{2}}$$

Method 3: n">0 for lossy medium, η'> 0, n"<0 for transparent gain medium, and η'<0, n">0 for non-transparent gain medium.

$$n = \begin{cases} +\sqrt{\epsilon\mu} \cdot \mathrm{sign}[-\mathrm{Im}(\sqrt{\epsilon\mu})] \cdot \mathrm{sign}(\epsilon''/|\epsilon| + \mu''/|\mu|) & if\, \epsilon'\mu' \geq 0 \\ +\sqrt{\epsilon\mu} \cdot \mathrm{sign}[-\mathrm{Im}(\sqrt{\epsilon\mu})] & if\, \epsilon'\mu' < 0 \end{cases}$$

- **Three methods are consistent when η'>0**
- **Method 2 and 3 allows the sign choice of η'<0**
- **Method 1 and 3 can determine the sign at each single frequency**
- **Method 2 cannot determine the sign by only single frequency information**

Different sign choices

Method 1 and 2

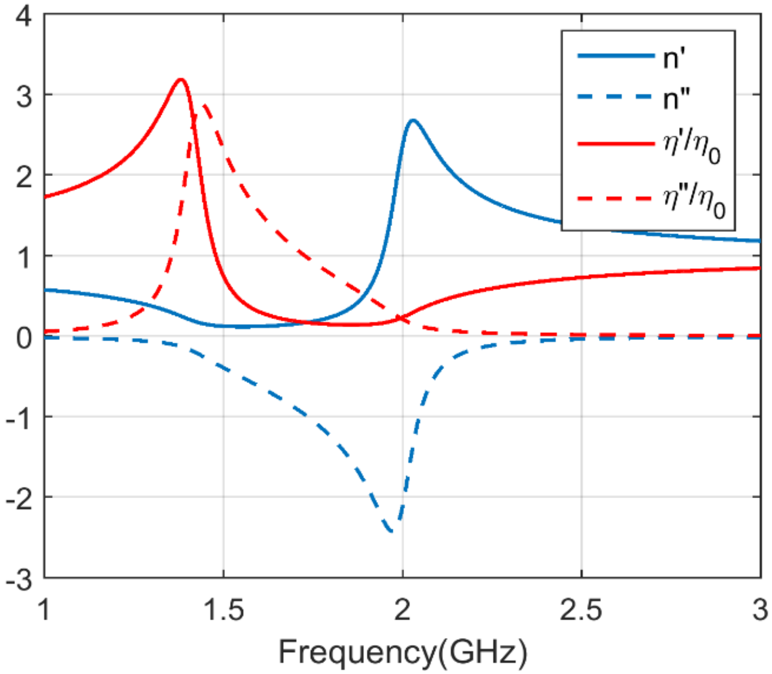

Method 3

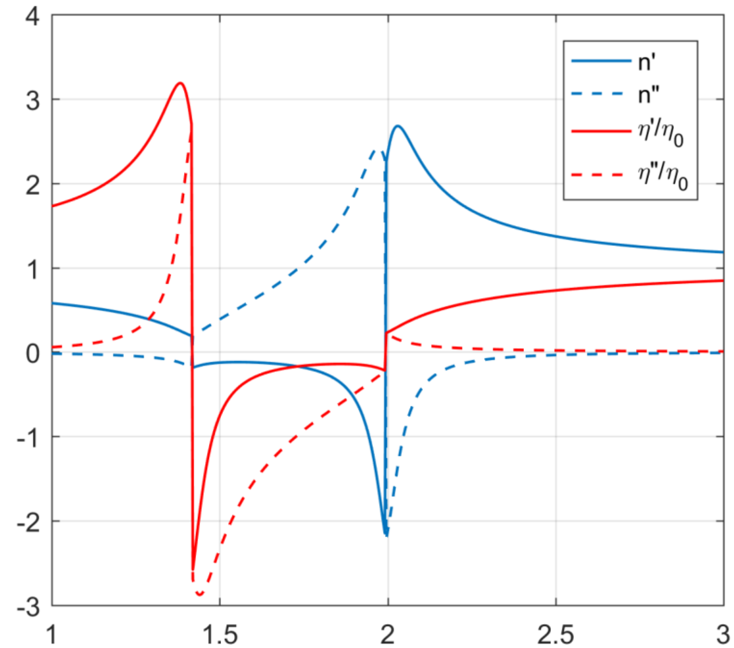

Sign choices with different methods

Refractive index | **Impedance**

Method 1

Method 2

Method 3

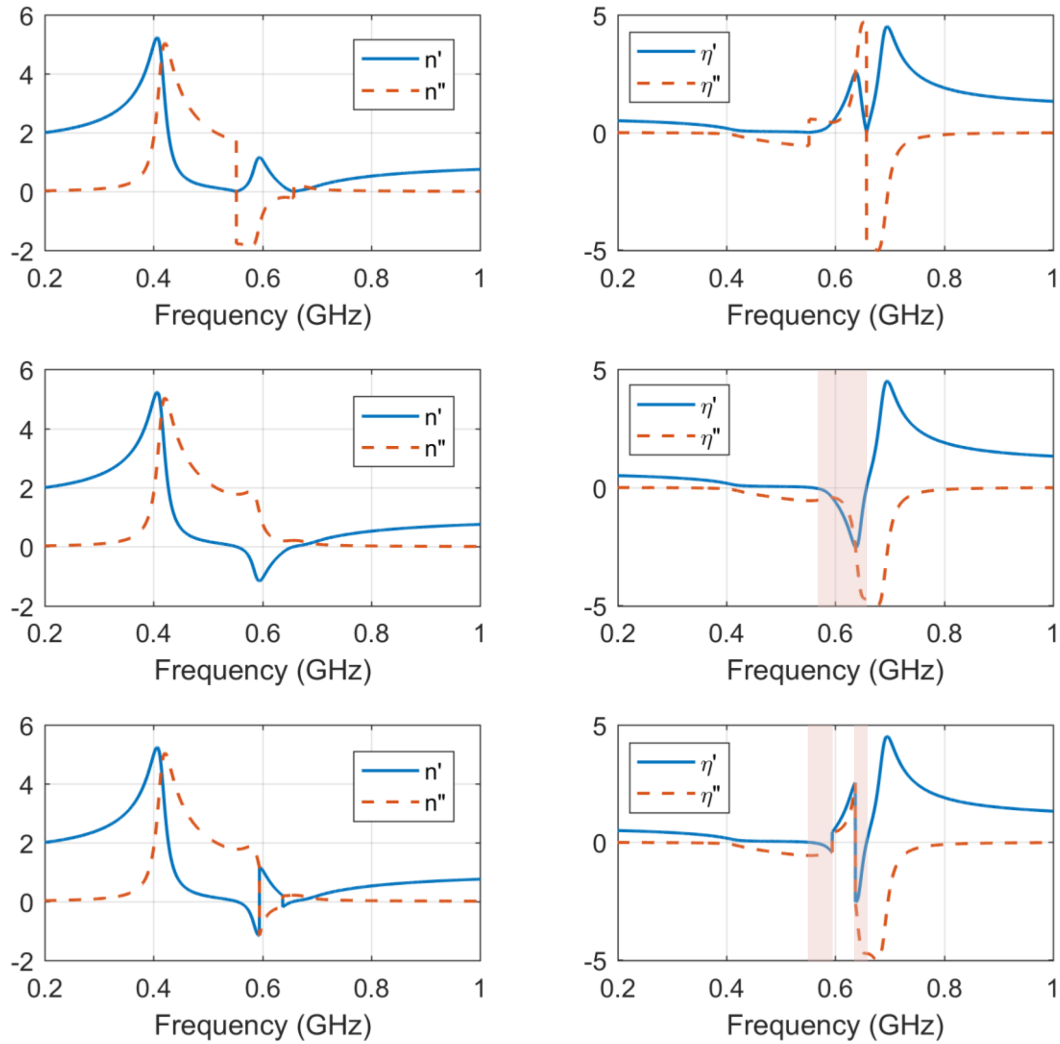

A wedge system

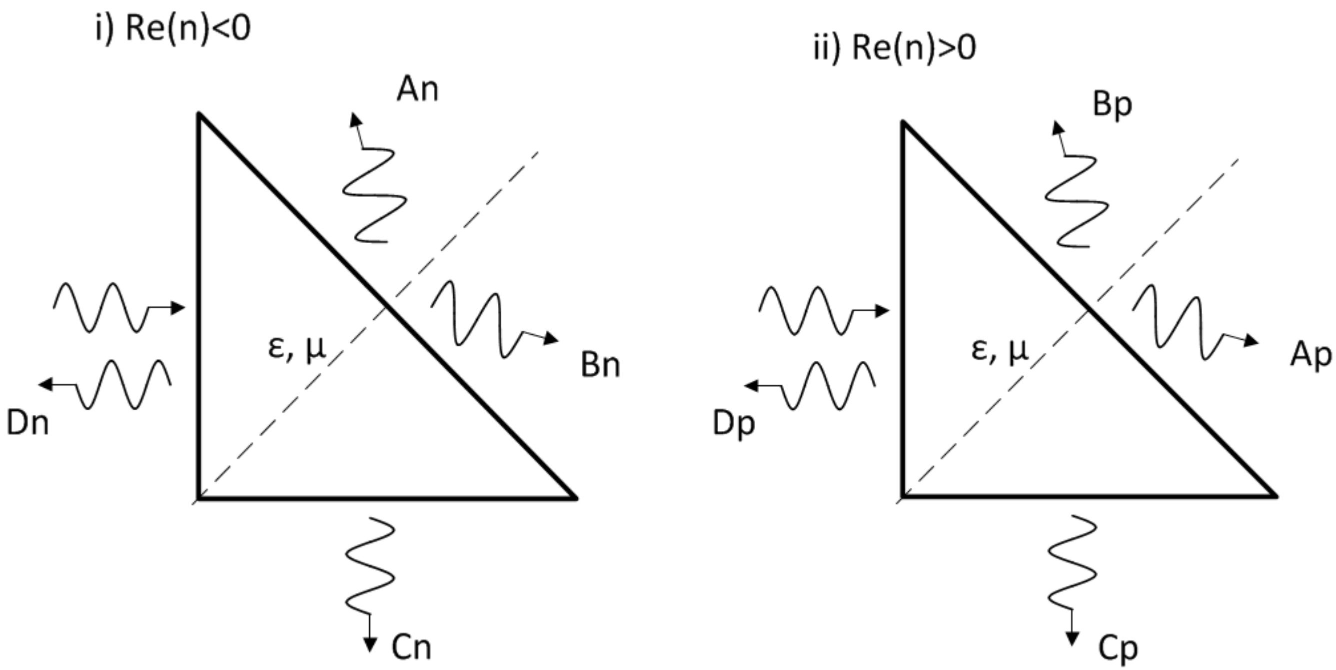

Example I: $\varepsilon = \varepsilon' - j\varepsilon'' = 1.2 \pm j0.05$, $\mu = +1$

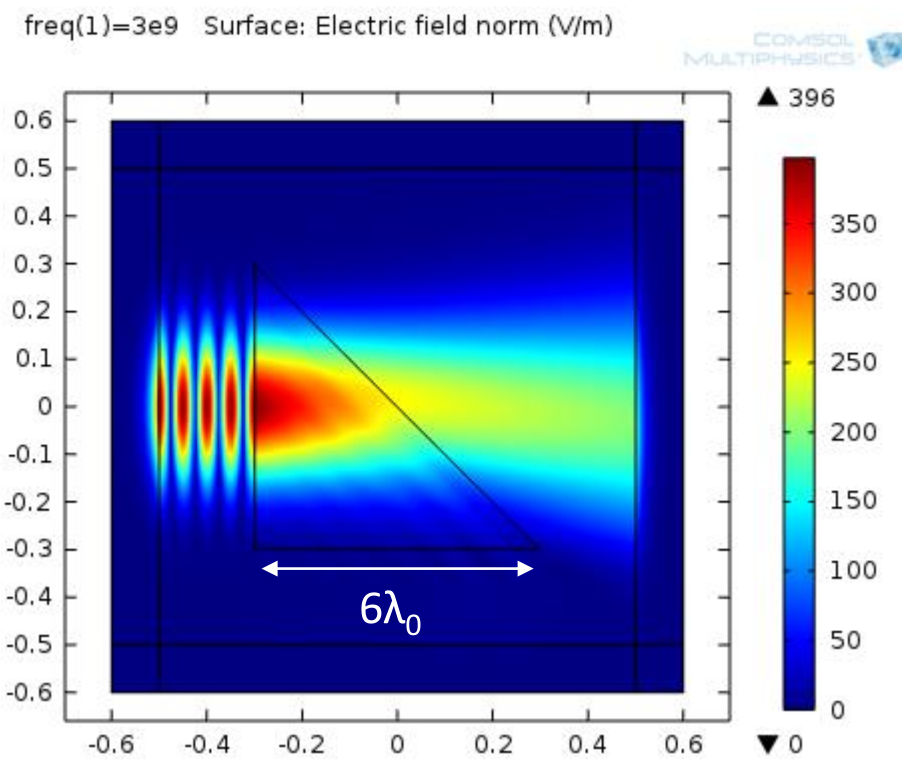

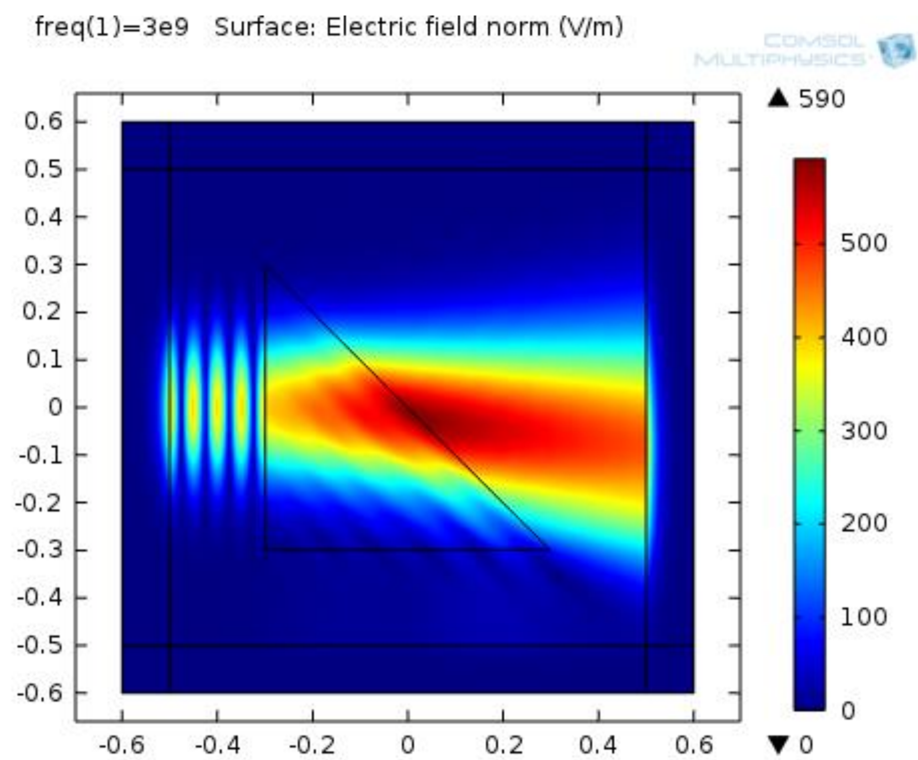

$n = +(1.0957 - 0.0228j)$
positive refraction and lossy

$n = +(1.0957 + 0.0228j)$
positive refraction and gain

Example II: $\varepsilon = \varepsilon' - j\varepsilon'' = -1.2 \pm j0.05$, $\mu = -1$

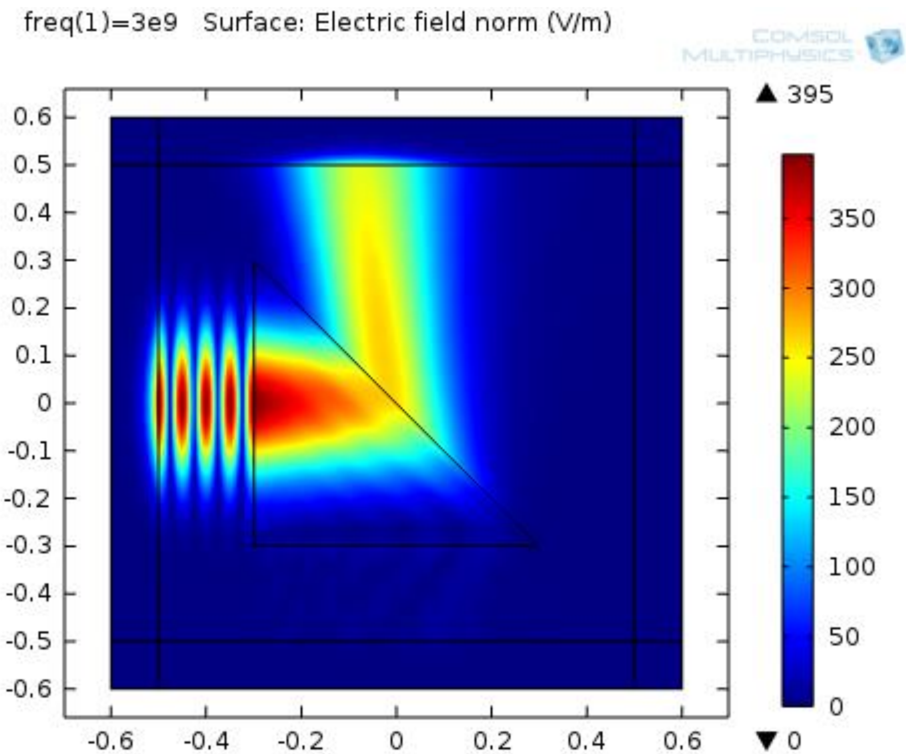

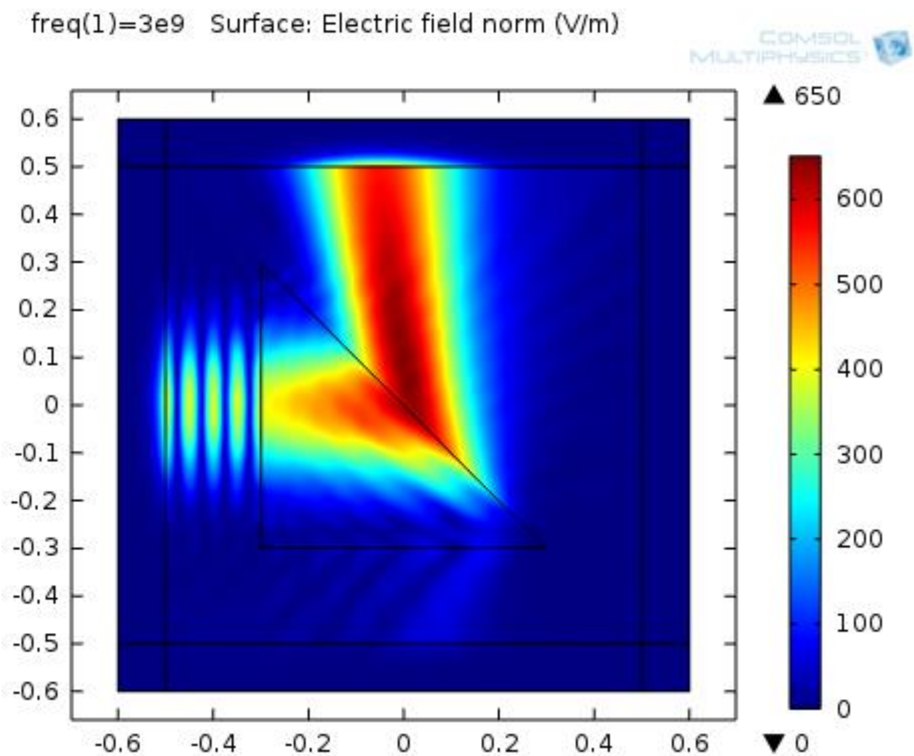

$n = -1.0957 - 0.0228j$
negative refraction and lossy

$n = -1.0957 + 0.0228j$
negative refraction and gain

Frequency domain numerical simulation of gain wedge

	ϵ	μ	n^+	η^+/η_0	d_c/λ_0
Gain	1.32 + 0.16j	1.08 - 0.11j	1.2 + 0.01j	0.9 - 0.1j	33.5

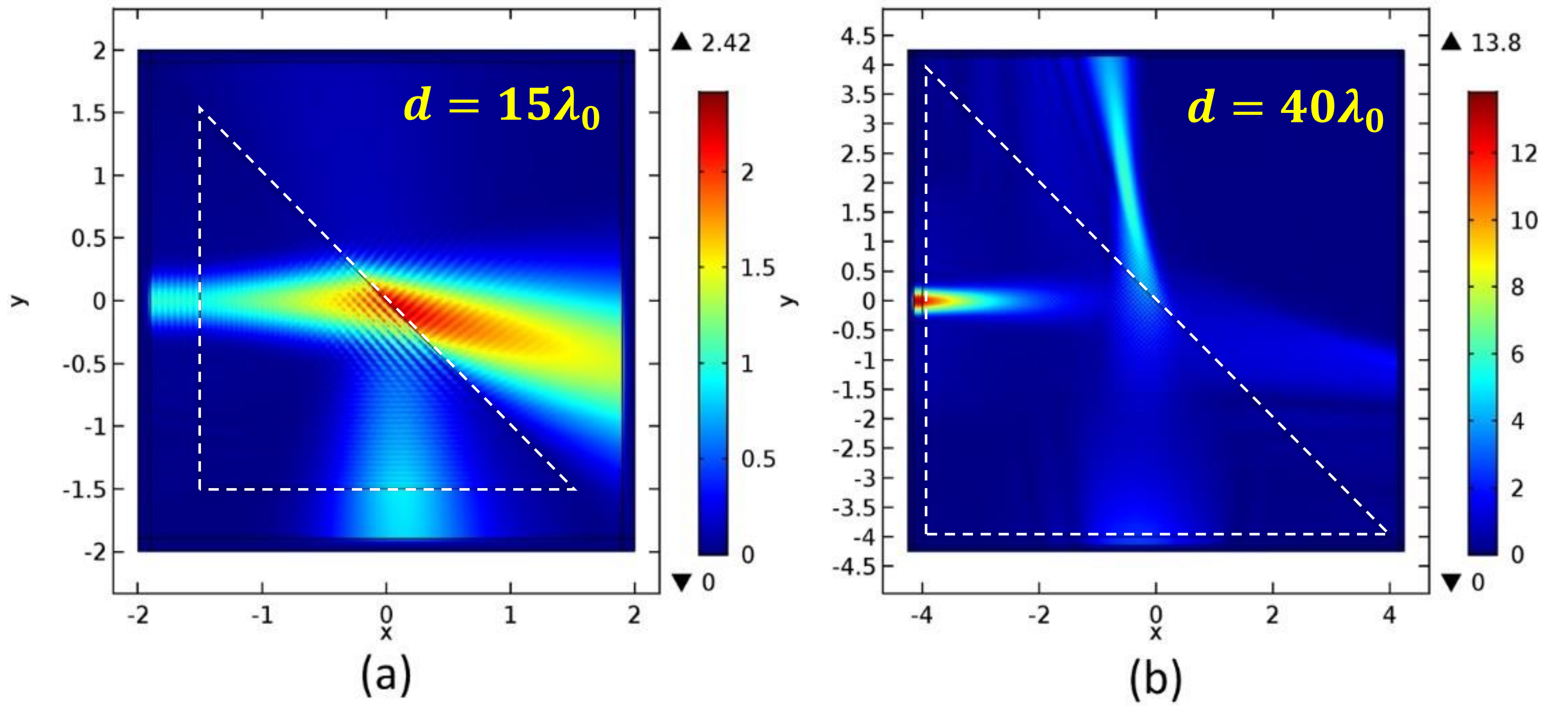

positive refraction with gain

negative refraction with “loss”

Frequency domain simulation of gain wedge: Example 2

	ϵ	μ	n^+	η^+/η_0	d_c/λ_0
Gain	-1.32 - 0.14j	-1.08 + 0.13j	-1.2 + 0.1j	0.9 - 0.1j	33.5

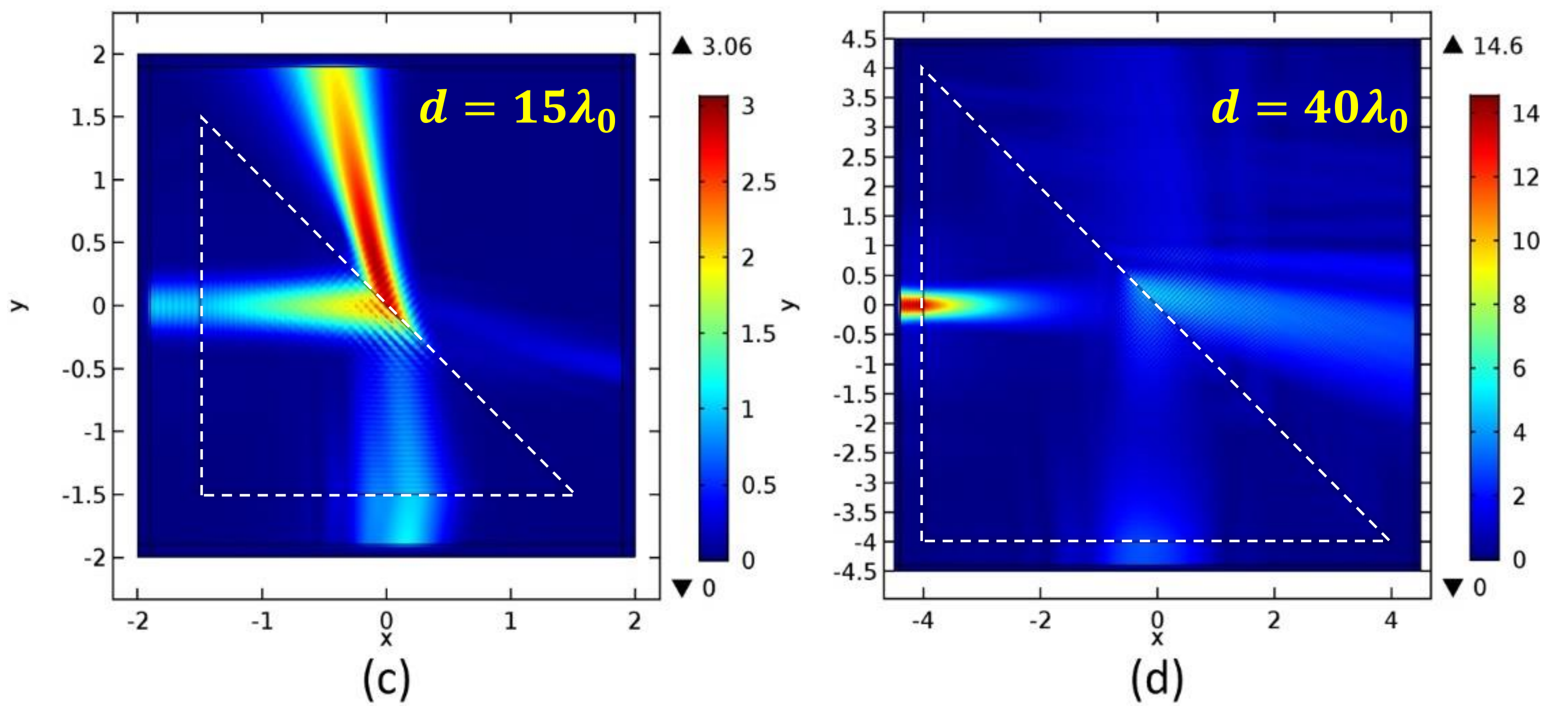

(c) negative refraction with gain

(d) positive refraction with loss

The result shows the strong output beam direction changes as the size of the wedge changes, which indicates the result come from different sign media.

THz Appendix

Reported THz Microfluidics

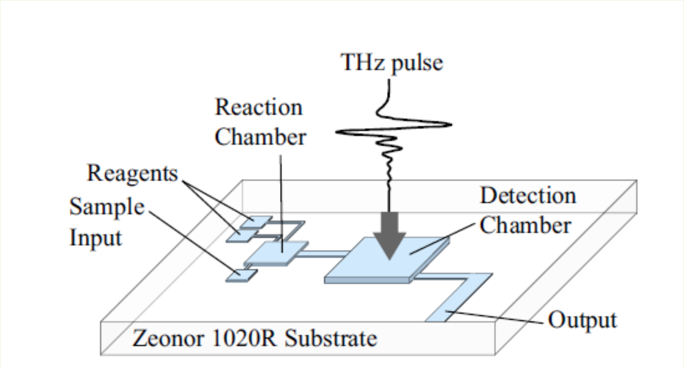

- George, P. A. *et al.*[1]
- Measure the absorption spectra of vibrational modes of bovine serum albumin from 0.5 - 2.5 THz
- Detect molecular quantities as small as 10 picomoles without integrated probes

[1] George, P. A. *et al.* Microfluidic devices for terahertz spectroscopy of biomolecules. *Optics Express* **16**, 1577 (2008).

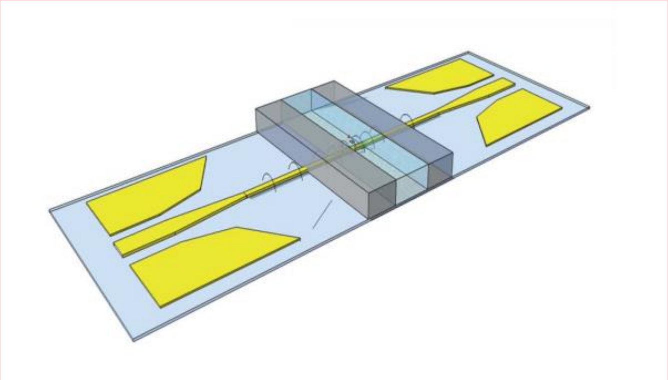

- Laurette, S. *et al.*[2]
- Measure the absorption spectra of BSA, lysozyme and chymotrypsine proteins
- By combining THz waveguides, the sensitivity can be down to 0.6 picomoles (5mg/mL BSA solution)

[2] **Laurette, S. *et al.*** Highly sensitive terahertz spectroscopy in microsystem. *RSC Advances* **2**, 10064 (2012).

THz-TDS system setup

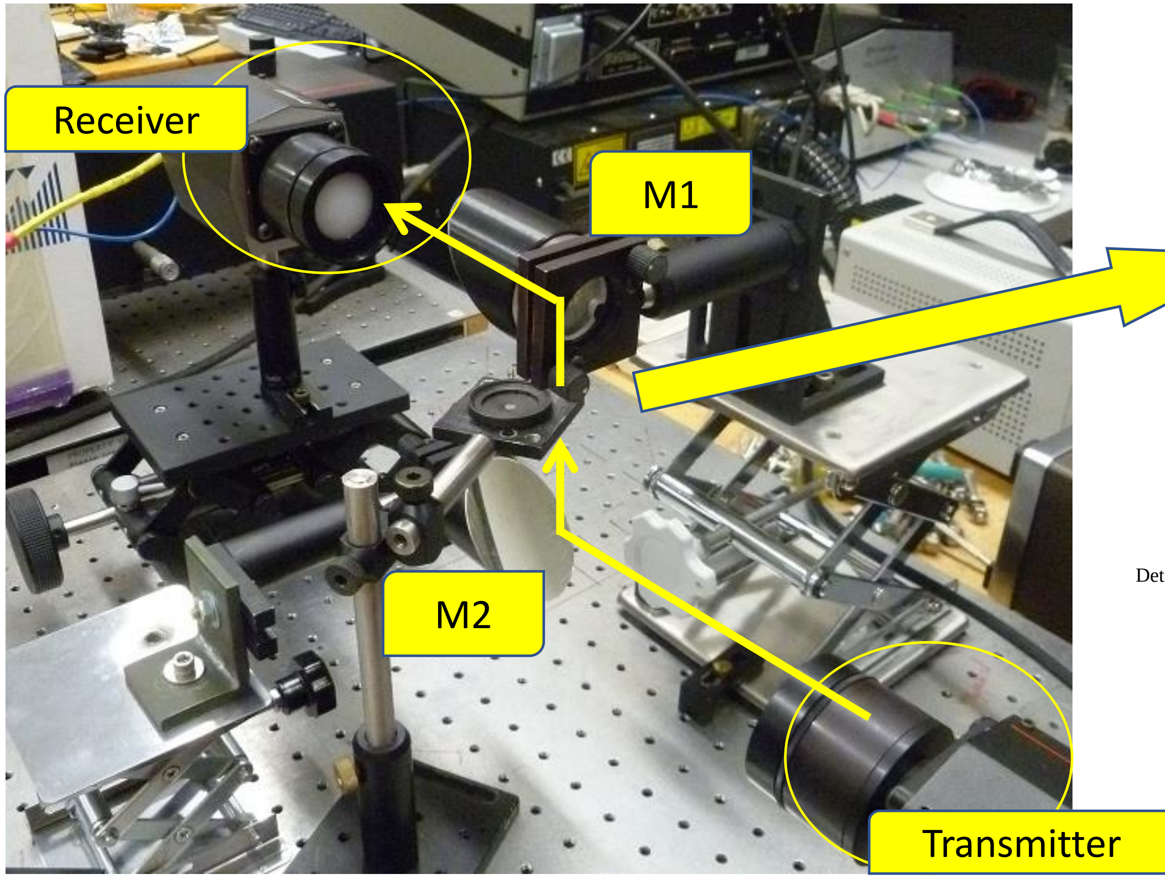

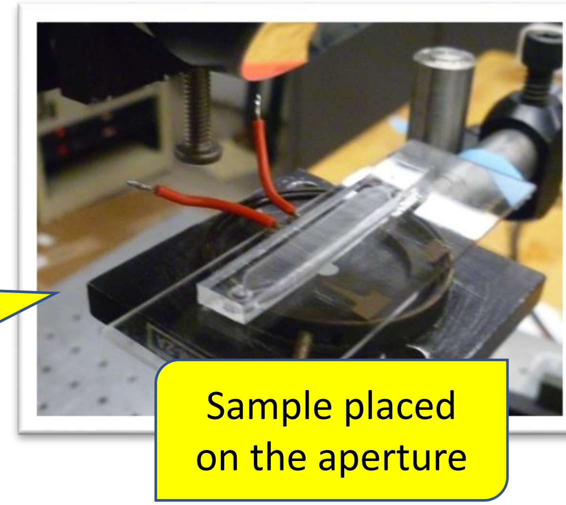

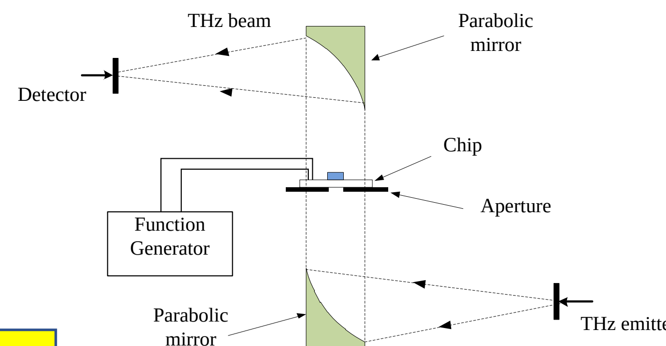

T-Ray 2000® made by Picometrics. 100 ps time-domain window

PDMS Dielectric Properties

Relative permittivity

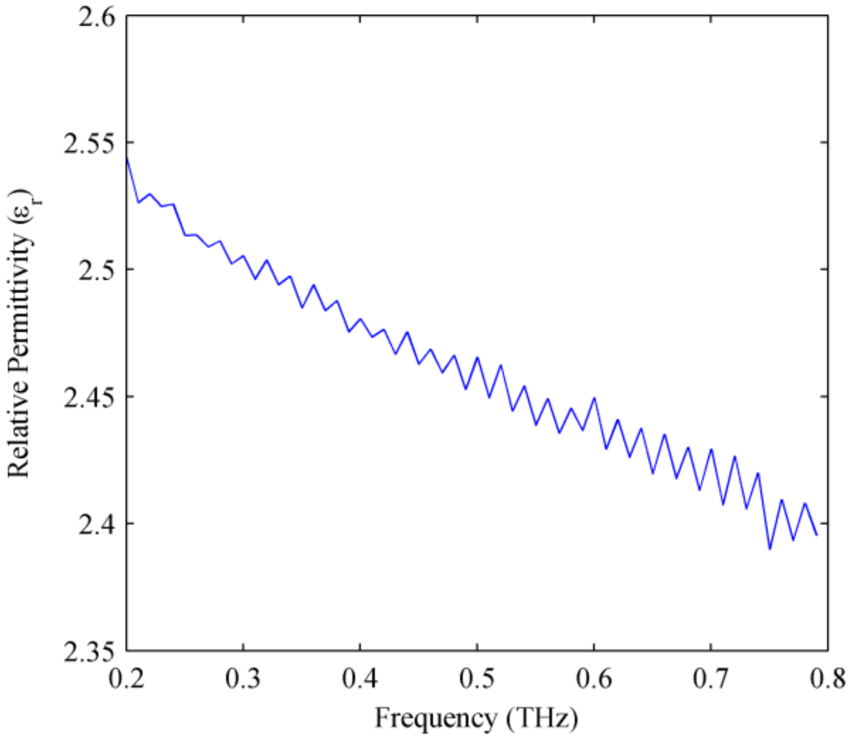

Loss tangent

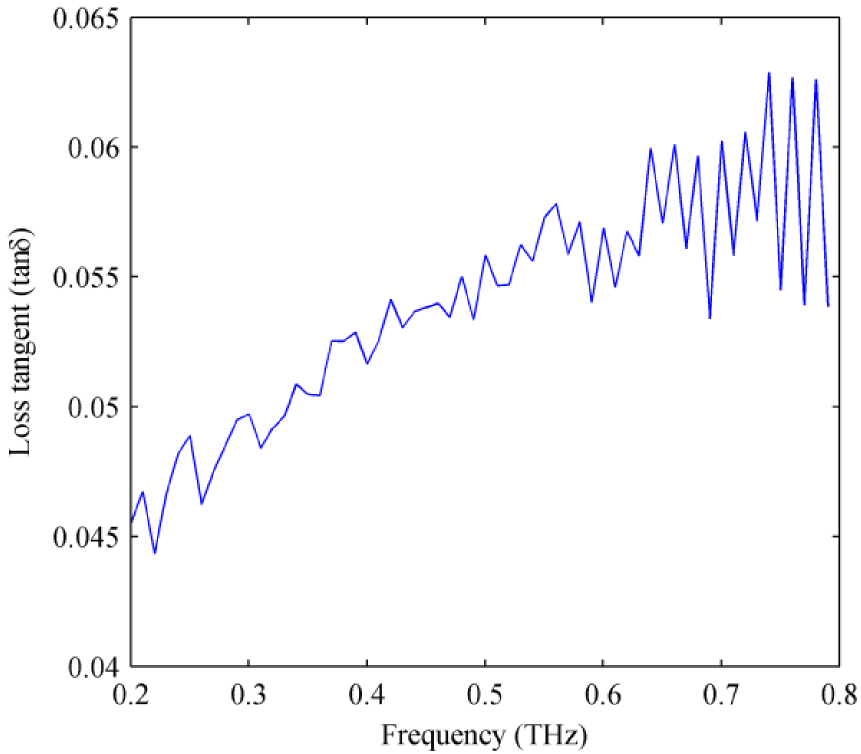

- **Relatively lossy but still acceptable at low frequency range - about 0.05 at 0.3 THz.**

Maximum temperature vs. bias voltage

The maximum temperature near the electrodes within the microfluidic channel as a function of the AC bias voltage Vpp.